A journal about nanoscience

Open Journal of Nano

Open Journal of Nano

Editorial Assistants

Mücahid SARI, Sakarya University of Applied Sciences, Sakarya, Turkey.
https://dergipark.org.tr/en/pub/@mucahidsari

Dr. Hamza ŞİMŞİR, Karabuk University, Turkey.
hamzasimsir@karabuk.edu.tr

Engin Deniz PARLAR, Sakarya University of Applied Sciences, Sakarya, Turkey. denizparlar-97@hotmail.com

Nadir ATMACA, The Istanbul Metropolitan Municipality, Istanbul, Turkey.
nadiratmaca@gmail.com

Halid ÖZGÜR, FreshForty Media, Turkey
halid@freshforty.media

Enis AKSOY, Areya illüstrasyon, Sakarya, Turkey
enisaksoy@gmail.com

OPEN JOURNAL OF NANO
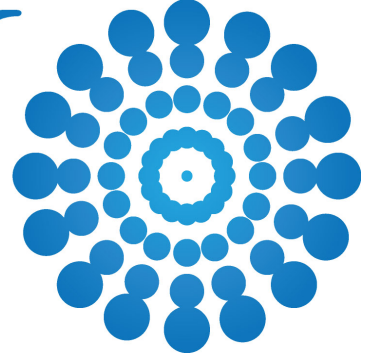
Contents (İçindekiler)
Volume: 9, Issue: 2, Year: 2024

OPEN JOURNAL OF
NANO

Nano Transdermal Delivery Systems of Herbal Extracts for Dermatological Therapeutics and Skin Care

*[1,2]Elçin Tören ID, [2] Adnan Ahmed Mazari ID

[1] Technical University of Liberec, Textile Faculty, Department of Clothing, 1402/2, 461 17, Liberec, Czech Republic.

[2] RESPILON Membranes s.r.o., Nové sady 988/2, 602 00, Brno-střed, Czech Republic.
* Corresponding author, e-mail: elcin.toren@tul.cz, https://orcid.org/0000-0002-1491-5389

Abstract
This article discusses the use of nanotechnology in the development of transdermal delivery systems for herbal extracts for dermatological therapeutics and skin care. Nanotechnology involves manipulating nanoscale materials to create nanoparticles that can penetrate the skin and deliver active ingredients more effectively. Natural products are commonly used in cosmetics because of their therapeutic properties and minimal side effects; however, the safety of nanoparticles in cosmetic products is a concern that requires further research. Chronic and nonhealing wounds pose a significant threat to patients' lives, and there is a pressing need for novel materials and approaches to wound healing. Nanomaterials exhibit unique physicochemical properties owing to their distinct structures, resulting in small size, surface, and macroscopic quantum tunnelling effects, making them ideal for use in wound dressings. Herbal transdermal patches offer advantages such as better patient tolerance, minimal side effects, renewable sources of medication, extensive availability, and cost-effectiveness; however, they also have disadvantages such as slower growth in demand, testing difficulties, and limited availability. This article concludes that by following a regimen that includes both natural ingredients and over-the-counter treatments, consumers can improve their skin health and appearance.

Keywords: herbal extracts, nanotechnology, skin care, transdermal delivery systems

1. Introduction

Nanotechnology is a rapidly growing field in the cosmetics industry that involves manipulating nanoscale materials to create nanoparticles that can penetrate the skin and deliver active ingredients more effectively [1]. Nanotechnology involves studying substances at the molecular and atomic levels, focusing on objects and structures calibrated on a nanometer scale, which is one billionth of a meter (10^{-9} m) [2]. For comparison, the diameter of the influenza virus is 100 nm, whereas that of human hair is approximately 100 µm [3].

Nanotechnology in cosmetic products has led to innovative products with improved performances [4]. Natural products are commonly used in cosmetics because of their therapeutic properties and minimal side effects [5]. Despite this, the safety of nanoparticles in cosmetic products is a concern, and further research is needed to fully understand their impact on human health and the environment [6].

Recently, there has been a significant increase in the prevalence of persistent medical conditions, including vascular dysfunction, obesity, and diabetes, which has led to an increase in the number of individuals afflicted with chronic wounds. It is estimated that patients with diabetes have a 15-25% risk of developing chronic diabetic abscesses [7]. Certainly, some skin conditions that can be transmitted, such as malignant skin tumours, sporotrichosis, autoimmune skin diseases, dermatomyositis, and physical skin diseases, can render individuals susceptible to persistent sore [8].

Chronic and nonhealing wounds expose hypodermic tissue to the external environment for a prolonged duration, resulting in an increased risk of bleeding and osteomyelitis in patients, particularly those in severe conditions. Such conditions pose a significant threat to patients' lives. In addition, the recurrence of chronic infections diminishes patients' quality of life, heightens their

77

financial burden, and triggers severe mental and psychosocial complications. The complexity of wound healing presents a continuous challenge for clinicians, and there is a pressing need for novel materials and approaches. Considerable advancements in nanotechnology, particularly in nanochemistry and nanomanufacturing, have significantly impacted the pharmaceutical and biotechnology sectors. Nanomaterials, characterized by at least one dimension below 100 nm, exhibit unique physicochemical properties owing to their distinct structures, resulting in small size, surface, and macroscopic quantum tunnelling effects.

Nanomaterials have also been extensively employed in wound healing owing to their superior adsorption capacity, antimicrobial properties, and drug-loading capabilities [9]. Wound dressings act as impermanent skin that alternates and plays an essential role in hemostasis, infection control, and wound closure. Several dressing materials have been investigated for many years. Traditionally, wound dressings such as gauze and bandages have been used to treat skin defects [10]. The development of nanomaterial dressings requires a simulation of the extracellular matrix (ECM) in a wet environment, as well as the inclusion of antimicrobial properties and the promotion of cell proliferation and angiogenesis. The significant demand for these resources in the market has contributed to the growth of nanomaterial dressings [11].

Herbal transdermal patches offer advantages such as better patient tolerance [12], minimal side effects [13], renewable sources of medication[12], extensive availability[14], and cost-effectiveness [15]. Nevertheless, it also has disadvantages such as slower growth in demand, testing difficulties and limited availability, strict manufacturing procedures, and a lack of standardization in ingredients and techniques [16]. The skin is the primary barrier that shields the body from various free radicals [17]. Various sources produce free radicals such as UV rays, dust, chemicals, and air pollution [18].

People of all ages seek premium skincare products for flawless, youthful skin. The quality and density of extracellular matrices and the provision of cells to connective tissues influence the concept of an ideal skin [19]. Skin conditions, such as acne, abnormal pigmentation, and xerosis, can indicate skin pathology [20]. Nutritional deficiencies can cause skin lesions; however, combining cosmetic skin care products and over-the-counter (OTC) treatments can help improve skin health and appearance[21]. By following a regimen that includes both products, consumers can rebuild their skin and achieve a more beautiful complexion [22]. Natural ingredients are substances derived from natural sources, such as plants or minerals, without synthetic or artificial additives, such as coconut oil, shea butter, or lavender essential oil [15]. Incorporating natural ingredients into skin care products improves skin conditions [23]. Nanotechnology is used in various ways in skincare products to provide benefits, such as UV protection [24], anti-ageing effects [25], improved moisturization [26], and wound healing [15].

Nanomaterials are increasingly used in various industries, including cosmetics [27], pharmaceuticals [28], and dermatology [29]. In cosmetics, nanomaterials are used as hair conditioners [30], serums [31], moisturizers [32], and shampoos [33] for damaged hair, skin-lightening creams, and anti-ageing creams [4].

Nanofibrous technology allows for the encapsulation of nanoparticles, which then act as a drug delivery substrate, allowing the active components to reach deeper layers of the skin where they can have the most effect [15]. Therefore, nanofibrous technology is gaining popularity in cosmetics and medicine.

In this review, we examined the recent applications of nanomaterials in skin wound healing, focusing on their potential mechanisms and the various aspects involved. By filling the existing research gap, this study aimed to elucidate the effective utilization of nanotechnology in seamlessly integrating natural ingredients into cosmetic formulations. This study offers novel insights into the application of nanotechnology and presents a fresh perspective on harnessing the potential of natural ingredients in skincare. The findings of this study hold promise for advancing our understanding of

how nanotechnology can revolutionize the use of natural ingredients in skincare and pave the way for innovative approaches to cosmetic and pharmaceutical product development **(Fig.1)**.
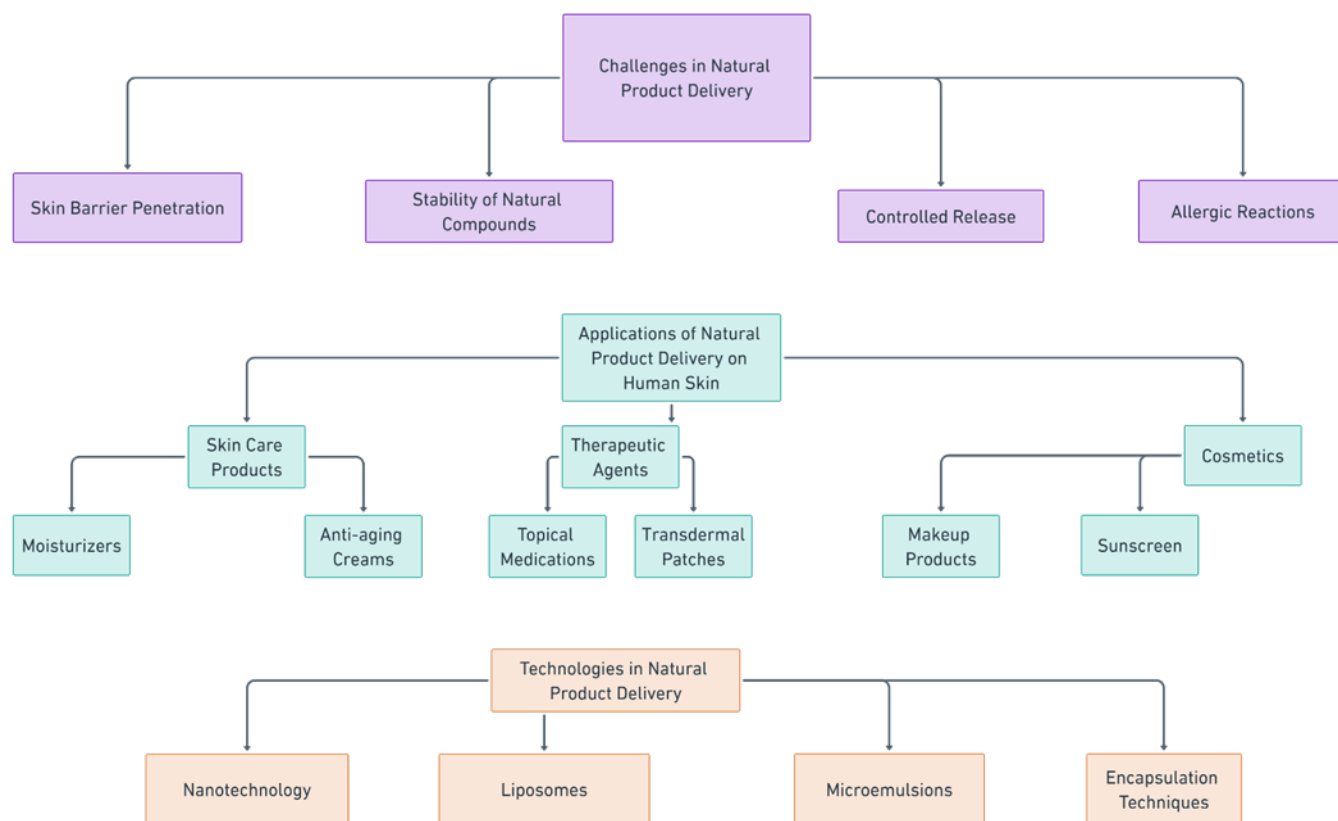
Figure 1. Applications, challenges, and technologies associated with the delivery of natural products to human skin.

2. Transdermal Patches

A transdermal patch is a medical device consisting of an adhesive layer impregnated with a specific medication. This patch is placed on the skin, where it delivers the medication through the skin and into the bloodstream [34]. One advantage of transdermal drug delivery over other routes, such as oral, topical, intravenous, or intramuscular, is that it provides a controlled release of the medication [35]. This is typically achieved through either a porous membrane covering a reservoir of medication or through body heat melting of thin layers of medication embedded in the adhesive **(Fig.2)** [36]. However, the main disadvantage of transdermal delivery systems is that the skin is a highly effective barrier, which limits the types of medications that can be delivered using this method. Only medications with molecules small enough to penetrate the skin can be administered using a transdermal patch [37]. The first prescription patch was approved by the US. In December 1979, the Food and Drug Administration administered scopolamine for motion sickness [36].

Transdermal delivery systems are self-contained and discrete dosage forms that, when applied to the skin, deliver the drug through the pores at a controlled rate to the systemic circulation. These dosage forms maintain drug absorption and concentration within the therapeutic window for an extended period, thereby ensuring that drug levels fall below the minimum effective dose (MED) or exceed the maximum tolerated dose (MTD) [38]. A drug to be used as a model for formulating transdermal drug delivery should acquire several physiochemical properties, such as short half-life and smaller molecular size for easy penetration, small dose, and minimal oral bioavailability. [39].

OPEN JOURNAL OF
NANO
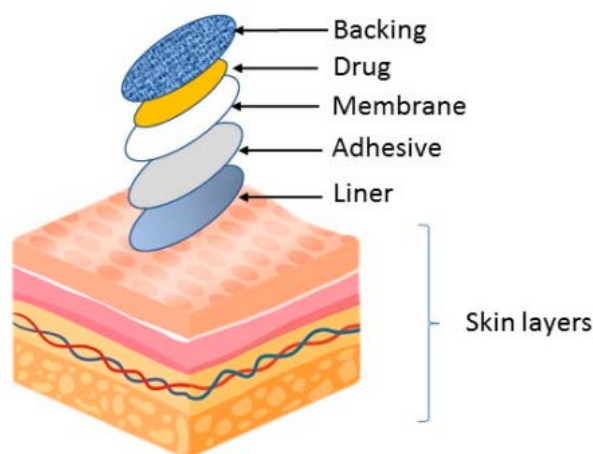
Figure 2. Basic components of a transdermal medical patch [35].

2.1. Types of Transdermal Patches

Transdermal delivery systems are self-contained and discrete dosage forms that, when applied to the skin, deliver the drug through the pores at a controlled rate to the systemic circulation. These dosage forms maintain drug absorption and concentration within the therapeutic window for an extended period, thereby ensuring that drug levels fall below the minimum effective dose (MED) or exceed the maximum tolerated dose (MTD) [38]. A drug to be used as a model for formulating transdermal drug delivery should acquire several physiochemical properties, such as short half-life and smaller molecular size for easy penetration, small dose, and minimal oral bioavailability. [39].

Transportation of active pharmaceutical ingredients across the skin is affected by various factors such as skin permeability, area, and duration of application, as well as the metabolic activity of the skin (i.e., first-pass metabolism) [40]. Every drug has unique properties that can affect transdermal delivery. In order to achieve adequate skin absorption and penetration, the drug should be nonionic and relatively lipophilic to cross the skin barrier [41]. Molecules larger than 500 Da make it difficult to cross the stratum corneum, and ideally, the therapeutic dose of the drug should be less than 10 mg/day [42].

Transdermal patches typically consist of several layers designed to deliver medication through the skin and into the bloodstream [35]. Figure 2 illustrates the basic components of the medicated patch. The specific composition and structure of the patch may vary depending on the drug being delivered and the desired rate of drug release [43].

The outermost layer of the patch, known as the backing layer, protects other layers from external influences. It is commonly composed of flexible waterproof materials, such as polyethene or polypropylene. The adhesive layer was responsible for securely affixing the patch to the skin and ensuring its retention. It is typically comprised of a potent hypoallergenic adhesive that is gentle on the skin. The drug layer contains medication that is delivered through the skin and formulated to release the medication at a consistent rate over a predetermined period. The rate-controlling membrane regulates the release of drugs from the patch and is typically constructed of a semipermeable material that allows the medication to pass through at a controlled rate. The protector and adhesive layer act as barriers for the patch. It is necessary to remove the patch before its application to the skin.

80

2.1.1. Single-layer Drug-in-adhesive

The present system incorporated an adhesive or gummy layer that served the dual purpose of securing the transdermal patch onto the porous membrane and facilitating the release and penetration of the drug into the skin. The patch comprises a single-layer film, which houses the active pharmaceutical ingredient (API) along with all other excipients blended within a single layer [44].

2.1.2. Multilayer Drug-in-Adhesive

The Multilayer Drug in the gummy layer functions in a manner similar to that of the single/solo layer patch. However, it employs the unique feature of utilizing multiple layers of adhesive to achieve controlled and predetermined drug release. Specifically, one layer is designed for immediate release, whereas the other layer regulates the controlled and predetermined release of the drug [45]. The Multilayer Drug in Adhesive possesses the ability to accommodate two distinct classes of pharmaceuticals.

2.1.2.1. Reservoir system: The Reservoir transdermal system incorporates a unique layer specifically designed for the Active Pharmaceutical Ingredient (API). This layer consists of a solution or suspension of the medication in a separate liquid compartment, which is separated from the outer layer by a semipermeable membrane and an adhesive layer. The adhesive layer functions as a continuous coating, establishing a connection between the skin and the release liner [46].

2.1.2.2. Matrix system: The matrix system is characterized by a semi-solid matrix, which incorporates a drug suspension and solution. This matrix is encased in an adhesive layer that affixes the system to the skin and forms a semi-solid matrix [37]. This particular type of system is commonly known as a "monolithic system."

2.1.2.3. Micro-Reservoir System: This system combines reservoir and matrix dispersion technologies. The drug is formulated by suspending drug solids in an aqueous solution of a water-soluble liquid polymer, which is then uniformly dispersed in a lipophilic polymer to generate a vast array of non-leaching microscopic drug reservoirs [47].

3. Mechanism of Actions Transdermal Patches

A transdermal patch serves as the primary means of delivering the drug that it holds in place. Upon application, the adhesive secures the patch on the skin, enabling it to adhere to the surface and facilitate drug release [48,49].

81

OPEN JOURNAL OF
NANO
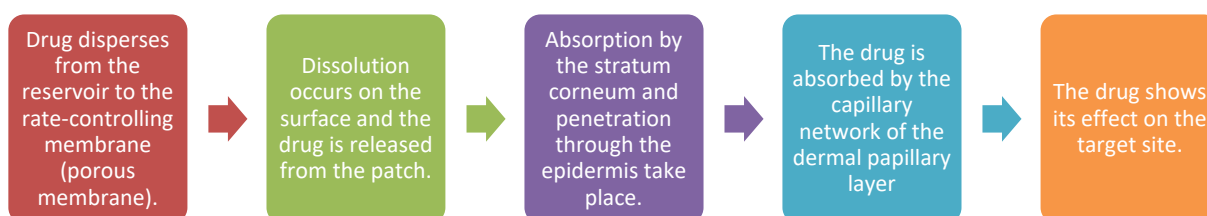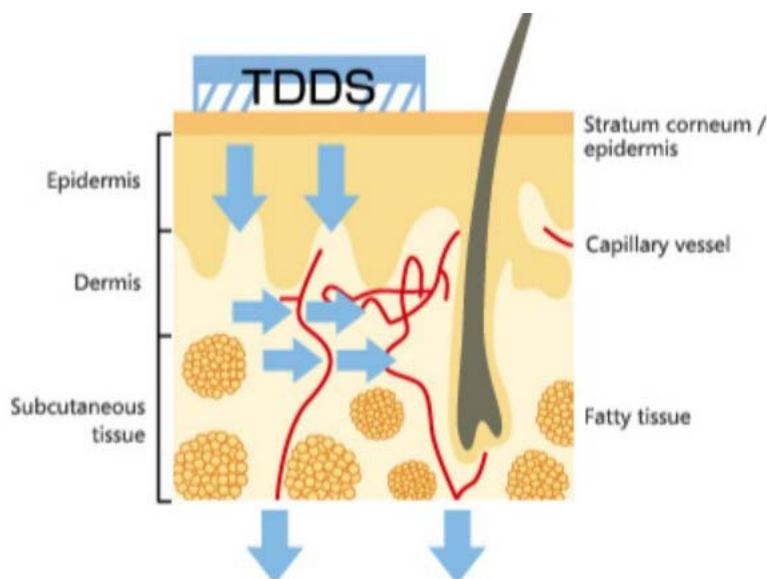
Figure 3. Mechanism of action transdermal patches [50]

Understanding the dynamics of skin permeation is of the utmost importance for the development of effective topical drug delivery (TDD) systems. To evaluate any TDD, assessing the percutaneous absorption of molecules is a vital step, as it pertains to the penetration of substances into the various layers of the skin and their subsequent permeation through the skin into the systemic circulation [51]. Percutaneous absorption of molecules is a multistep process that includes **(Fig.3)** [52]:

i. Penetration: entry of a substance into a specific layer of the skin.
ii. Partitioning: redistribution of the substance from the stratum corneum to the aqueous viable epidermis.
iii. Diffusion: Movement of the substance through the viable epidermis and into the upper dermis.
iv. Permeation: The passage of molecules from one layer to another is distinct in terms of both structure and function from the initial layer.
v. Absorption: uptake of the substance into the systemic circulation.

The release of drugs from the transdermal patches can be evaluated by determining the maximum flux of the drug compound across the skin, which is typically expressed in units of µg/cm²/h (Equation 1). This flux is governed by Fick's law of diffusion, which states that the transport of therapeutic molecules across the skin continues until the concentration gradient no longer exists. Transdermal patches can be classified into two types: those that use a solid polymer as a rate-controlling membrane (reservoir type) and those that use a liquid or gel-based reservoir (matrix type) [53].

$$J = -D\frac{dc}{dl} \qquad (1)$$

where J is the molecular flux, D is the diffusion coefficient, L is the cross-sectional thickness of the diffusion, and dc/dt is the concentration gradient. The equation indicates Fick's law of diffusion [53].

3.1. Brief of Skin Structure

The skin is the body's largest and most accessible organ, spanning an area of 1.7 m^2 and accounting for approximately 16% of the average individual's total body mass [53]. The primary role of the skin is to act as a barrier that protects the body against external threats such as microorganisms, penetration of ultraviolet (UV) radiation, chemicals, allergens, and dehydration [54]. The skin can be

82

OPEN JOURNAL OF
NANO

classified into three primary regions: the outermost layer, the epidermis, which comprises the stratum corneum; the middle layer, the dermis; and the innermost layer, the hypodermis [55–57]. **Figure 4** shows the structure of the skin.
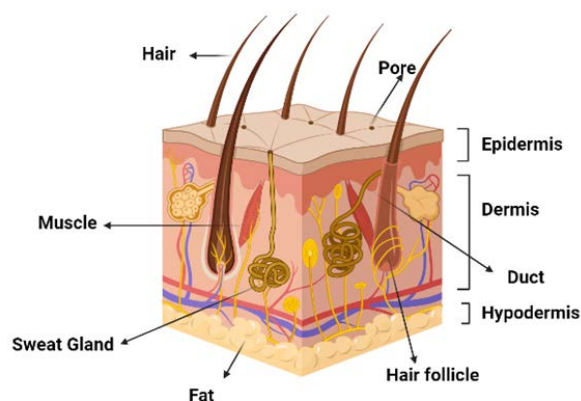

Figure 4. Skin anatomy [58].

3.1.1. Epidermis

The epidermis constitutes the outermost layer of the skin, and its thickness is not uniform, measuring approximately 0.8 millimetres on the palms of the hands and soles of the feet [59]. The epidermis is composed of multiple layers of epithelial cells, with the living tissue below the outermost layer, the stratum corneum, commonly referred to as the epidermal layer [60,61]. The cellular composition of the epidermis primarily comprises keratinocytes, which account for nearly all (95%) of the cells. In addition, other cell types present in the epidermis include melanocytes, Langerhans cells, and Merkel cells [62]. The stratum corneum is the most superficial layer of the stratum corneum [53,63,64]. The stratum corneum is in direct contact with the external environment, and its barrier properties may be partly related to its high density ($1.4 \ g/cm^3$ in the dry state) and low hydration level (15%-20%) [53]. The stratum corneum cells are primarily composed of insoluble keratins (70%) and lipids (20%). Water in the stratum corneum is associated with keratin in corneocytes [65].

3.1.2. Dermis

The dermis measures approximately 2-3 millimetres in thickness and is composed of collagenous (70%) and elastin fibres, which endow the skin with strength and flexibility. The presence of blood vessels within the dermis ensures the provision of essential nutrients to both the dermis and epidermis [66].

3.1.3. Hypodermis

The hypodermis, also known as the subcutaneous layer, is the deepest layer of skin and is characterized by a network of fat cells. It serves as the interface between the skin and underlying tissues of the body, such as muscles and bones [67]. The primary functions of the hypodermis include protection against physical impact, insulation against heat, and facilitation of vascular and neural signal transmission. Approximately 50% of the body's fat is stored in hypodermis-resident fat cells, while the remaining predominant cells in this layer include fibroblasts and macrophages [68].

4. Natural Bioactive Ingredients in Transdermal Applications

The absorption of percutaneous drugs or active ingredients is a complex phenomenon that is influenced by several factors, such as molecular size, hydrophile/lipophilic balance, melting point, and water solubility of the drug. Natural product compounds are commonly used in the clinical setting. **Table 1** presents a compilation of scientifically supported active ingredients derived from natural sources, curated for their potential effectiveness in addressing various skin types. Specifically, for individuals with dry skin, the following ingredients are recommended: aloe vera *(Aloe*

83

barbadensis), chamomile *(Matricaria chamomilla)*, calendula *(Calendula officinalis)*, lavender *(Lavandula angustifolia)*, coconut oil *(Cocos nucifera)*, jojoba oil *(Simmondsia Chinensis)*, shea butter *(Butyrospermum parkii)*, olive oil *(Olea europaea)*, rosehip oil *(Rosa canina)*, and witch hazel *(Hamamelis virginiana)*. These ingredients have been identified for their potential soothing, moisturizing, and hydrating effects, offering a natural approach to alleviate dryness and improve skin health [69]. Furthermore, cosmeceuticals can regulate the distribution of their active ingredients by forming thin films on the skin, facilitating targeted and precise delivery [13]. This controlled release mechanism enables the recommended ingredients for normal, oily, and combination skin types, such as niacinamide, vitamin C, hyaluronic acid, green tea extract, salicylic acid, tea tree oil, zinc, witch hazel, alpha hydroxy acids, jojoba oil, to exert their beneficial effects in specific areas as needed. By incorporating such advanced delivery systems, cosmeceuticals can optimize the efficacy of these ingredients, ensuring their effective penetration into the skin and enhancing desired outcomes [30].

Monton et al. developed controlled-release herbal transdermal patches using a microwave-assisted extraction of *Lysiphyllum strychnifolium* stem extract, which, when incorporated into a polyvinyl alcohol matrix, displayed potent antioxidant properties and efficacious skin permeation of astilbin, fitting Korsmeyer–Peppas and zero-order kinetic models, showing promise for herbal medicinal applications [70]. Kanjani et al. explored the transdermal delivery of *Azadirachta indica*, formulating a transdermal patch via solvent casting and assessing its properties, including SEM analysis and in-vitro release kinetics, with the patch showing 74.89% cumulative drug release over 24 hours and indicating a novel herbal application in transdermal delivery technologies [71]

Traditional topical skin care formulations may have limitations that affect their safety and efficacy [72]. Researchers have developed various nanomaterials to overcome these limitations and facilitate drug delivery [73]. Using nanomaterials to develop skin care products is an ongoing process in the healthcare and cosmetics industries, potentially creating new opportunities and positive impacts on society and various industries [74].

Nano-sized drug delivery systems are being studied to improve the delivery of active pharmaceutical ingredients (APIs) in nano-products such as cosmetics and pharmaceuticals [75]. The skin is a barrier, and the administration of APIs can be challenging because of the complex physiological layers with different polarities [76]. Various active ingredients in cosmetic products can prevent, delay, and treat skin ageing [77]. Nanofibers have been studied as potential solutions to address the challenges of transdermal drug delivery [78]. Skin care products that use nanotechnology, including nano-products, have demonstrated promising results in delivering active ingredients to the skin [12,14,79,80].

OPEN JOURNAL OF
NANO

Table 1. Active Ingredients from Natural Sources for Different Skin Types

Skin Type	Active Ingredient	Benefits	References
Dry skin	Aloe vera	Moisturises and soothes dry skin and helps restore the natural skin moisture barrier.	[81]
	Chamomile	It has anti-inflammatory properties and soothes dry, irritated skin.	[82]
	Calendula	Helps to hydrate and heal dry, damaged skin.	[83]
	Lavender	Has calming properties and soothes dry, itchy skin.	[84]
	Coconut oil	Has moisturizing properties and helps to soothe and hydrate dry skin.	[85]
	Jojoba oil	Helps to moisturize dry skin without leaving a greasy residue	[86]
	Shea butter	Has deeply moisturizing properties, helps to soothe and nourish dry skin	[87]
	Olive oil	Contains antioxidants and moisturizing properties, helps to hydrate and protect dry skin	[88]
	Rosehip oil	Contains essential fatty acids and vitamin A, helps to hydrate and rejuvenate dry skin	[89]
	Witch hazel	Has astringent properties, helps to tighten and tone dry, ageing skin	[90]
Normal skin	Niacinamide	Helps improve skin texture and tone, reduces the appearance of fine lines and wrinkles, and strengthens the skin barrier	[91]
	Vitamin C	Helps brighten and even out skin tone, promotes collagen synthesis, and protects against environmental damage	[92]
	Hyaluronic acid	Provides deep hydration and helps retain moisture in the skin, improving skin elasticity and firmness.	[93]
	Green tea extract	Has anti-inflammatory and antioxidant properties, helps protect against UV damage, and promotes healthy skin ageing	[79]
	Retinoids	Helps stimulate collagen production, improves skin texture and tone, and reduces the appearance of fine lines and wrinkles	[94]
Oily skin	Salicylic acid	Helps unclog pores, reduces oiliness, and prevents breakouts	[95]
	Tea tree oil	Has anti-inflammatory and antimicrobial properties, helps reduce acne and oiliness	[96]
	Zinc	Helps regulate sebum production, has anti-inflammatory and antimicrobial properties, and promotes wound healing.	[97]
	Witch hazel	Has astringent properties that can help tighten and tone oily skin, reduce inflammation and irritation	[90]
Combination	Niacinamide	Helps regulate sebum production, improves skin texture and tone, and strengthens the skin barrier.	[91]
	Hyaluronic acid	Provides deep hydration to dry areas while being lightweight enough not to exacerbate oiliness in the T-zone	[93]
	Vitamin C	Helps brighten and even out skin tone, promotes collagen synthesis, and protects against environmental damage	[92]
	Alpha-hydroxy acids (AHAs)	Help exfoliate dead skin cells, improve skin texture and tone, and reduce the appearance of fine lines and wrinkles.	[91]
	Jojoba oil	A similar structure to the natural skin sebum helps regulate oil production and hydrates dry areas.	[86]

Traditional topical skin care formulations may have limitations that affect their safety and efficacy [72]. Researchers have developed various nanomaterials to overcome these limitations and facilitate drug delivery [73]. Using nanomaterials to develop skin care products is an ongoing process in the healthcare and cosmetics industries, potentially creating new opportunities and positive impacts on society and various industries [74]. Nano-sized drug delivery systems are being studied to improve the delivery of active pharmaceutical ingredients (APIs) in nano-products such as cosmetics and pharmaceuticals [75]. The skin is a barrier, and the administration of APIs can be challenging because of the complex physiological layers with different polarities [76]. Various active ingredients in cosmetic products can prevent, delay, and treat skin ageing [77]. Nanofibers have been studied as potential solutions to address the challenges of transdermal drug delivery [78]. Skin care products that use nanotechnology, including nano-products, have demonstrated promising results in delivering active ingredients to the skin [12,14,79,80].

The transdermal drug delivery system (TDDS) represents a cutting-edge approach to drug delivery that transcends the limitations of traditional methods. Our country is fortunate to possess an extensive repository of Ayurvedic knowledge, which has been increasingly recognized and utilized in recent times. Nevertheless, the conventional means of administering herbal remedies to patients is antiquated and ineffective, which restricts the therapeutic potential of the drug. Given its application in herbal medicine, TDDS offers a promising solution to improve efficacy and reduce the adverse effects associated with various herbal remedies and plant-based treatments [98]. The problem of the ineffectiveness of oral medications, which account for 90% of medications taken in comparison to their high cost, can be addressed by exploring the use of a transdermal drug delivery system (TDDS). TDDS has several benefits, such as increased bioavailability, controlled absorption, higher plasma levels and half-life, ease of use without causing pain or side effects, and the convenience of discontinuing drug administration by simply removing the patch from the skin [72,99,100].

Recently, the use of herbal remedies has gained popularity worldwide owing to their remarkable healing properties and minimal side effects. Nevertheless, the creation of herbal medications requires adjustments to ensure the effective and sustained release of active pharmaceutical ingredients (APIs).

The oral administration of medication presents various concerns, such as unpleasant taste and colour. In contrast, the transdermal patch offers a non-irritating and non-invasive means of delivering medication with a precise time of action, making it a more appealing option for systematic drug administration than traditional approaches. However, patients may still become noncompliant during recovery, and the use of pills can cause additional complications [101]. The transdermal drug delivery system involves the application of medication through the skin to elicit a systemic response rather than employing conventional topical methods [81]. To deliver therapeutic agents across the human dermal layer for systemic effects, it is imperative to consider the detailed morphological, biophysical, and physiochemical properties of the dermal layer. Among the various drug delivery methods, transdermal drug delivery systems offer the most significant advantage over oral and injectable routes, particularly in terms of circumventing first-pass metabolism and promoting patient compliance [102]. Transdermal drug delivery systems are self-contained discrete dosage forms that deliver medication to the systemic circulation at a regulated and controlled rate when applied to healthy skin [59]. This mode of delivery offers several advantages, including controlled and consistent drug administration, continuous input of medications with limited biological half-lives, and prevention of pulsed entry into the systemic circulation, which may result in unwanted side effects [103]. Consequently, various novel and innovative drug delivery systems have been developed, including transdermal, controlled and predetermined release, and transmucosal delivery systems. Table 2 encompasses a range of herbal remedies for the treatment of diverse ailments through the administration of herbal medications.

Table 2. Transdermal Delivery of Herbal Bioactive Compounds for the Treatment of Various Ailments[104–109].

Active Constituent	Biological Source	Method of Preparation of Patch	Pharmacological Activity
Zingiber, Podina (Mentha arvensis), and Sirka (Vinegar) were envisaged	Brassica nigra, Zingiber officinale, Mentha arvensis and Vinegar	Solvent evaporation technique	Antiemetic Therapy
Extract of Hibiscus	Hibiscus sassiness	Two different polymers in the ratio of (1:4) are used for its preparation	Antidiabetic activity
Ginger, Turmeric, Lavender, Clove oil, Wintergreen, Camphor, Menthol, aloe Vera, Turpentine	rhizomes of Zingiber officinale, Curcuma longa, Lavandula angustifolia, Aloe barbadense	Matrix diffusion-controlled systems, Solvent casting Technique	Anti-inflammatory
Neem oil	Azedarach indica	Solvent casting method	Antimicrobial

5. Nanofiber-Based Transdermal Drug Delivery: Prospects and Challenges
5.1. Methods of production of nanofibers

Nanofibers are nanostructured vehicles with an individual diameter below 100 nm [17]. Developed fibres with diameters in the range of 100–1000 nm are also designated as nanofibers and are generally manufactured using a technique known as electrospinning [18].

5.1.1. Self-assembly method

In this method, there is a spontaneous arrangement of atomic/molecular aggregates into structurally defective nanofibrous forms. The Tis method leads to the production of nanofibers with sizes of up to 100 nm. The Tis method requires a longer time to generate nanofibers; therefore, it is less commonly used. However, nanofibers manufactured through self-assembly can very closely mimic natural materials such as chitin (polysaccharide), which has been explored in tissue engineering [19].

5.1.2. Template synthesis method

Template synthesis involves the use of nanoporous membranes that are available in the form of templates to extrude available fibres of different sizes into the nanoscale size range. The size of the nanofibers produced was in the range of 200–400 nm [20].

5.1.3. Phase-separation method

This method involves lyophilization of the polymeric blend, resulting in the formation of a nanofibrous mat. However, this method is very time-consuming, and the nanofibers obtained using this method are shorter in length, with a size range of 50–500 nm [21].

5.1.4. Melt-blown technology

The melt-blowing method involves the extrusion of the polymer blend across a minute orifice followed by passage through a heated air stream with a very high velocity. The Te size of the nanofibers produced using this method was 150– 1000 nm [22].

5.1.5. Electrospinning methods

Electrospinning is a scientifically established process that uses an electric field to induce the transformation of a charged polymer solution or melt into finely spun fibres [110]. The process commences with the preparation of a polymer solution that is subsequently loaded into a syringe or spinneret apparatus [111]. The polymer solution was carefully extruded through a needle or spinneret orifice, subsequently experiencing the influence of a high-voltage electric field [110]. This causes the solution to become charged and form a Taylor cone at the tip of the needle [112]. As the electric field strength increases, the surface tension of the solution is overcome, and a charged jet is ejected from the cone [113]. The jet undergoes a whipping motion as it travels towards a grounded collector, and

as it dries, it solidifies into a continuous nanofiber [114]. The diameter of the fibres can be controlled by adjusting the concentration of the polymer solution [115], flow rate [116], and the strength of the electric field [111]. Electrospinning is versatile and can be used with various polymers, including synthetic and natural materials. They have numerous applications in tissue engineering [117], drug delivery [118], filtration [119], energy storage [120], and sensors [3]. Several electrospinning approaches that can be used to encapsulate active ingredients and produce nanofibers are shown in **Figure 5**.
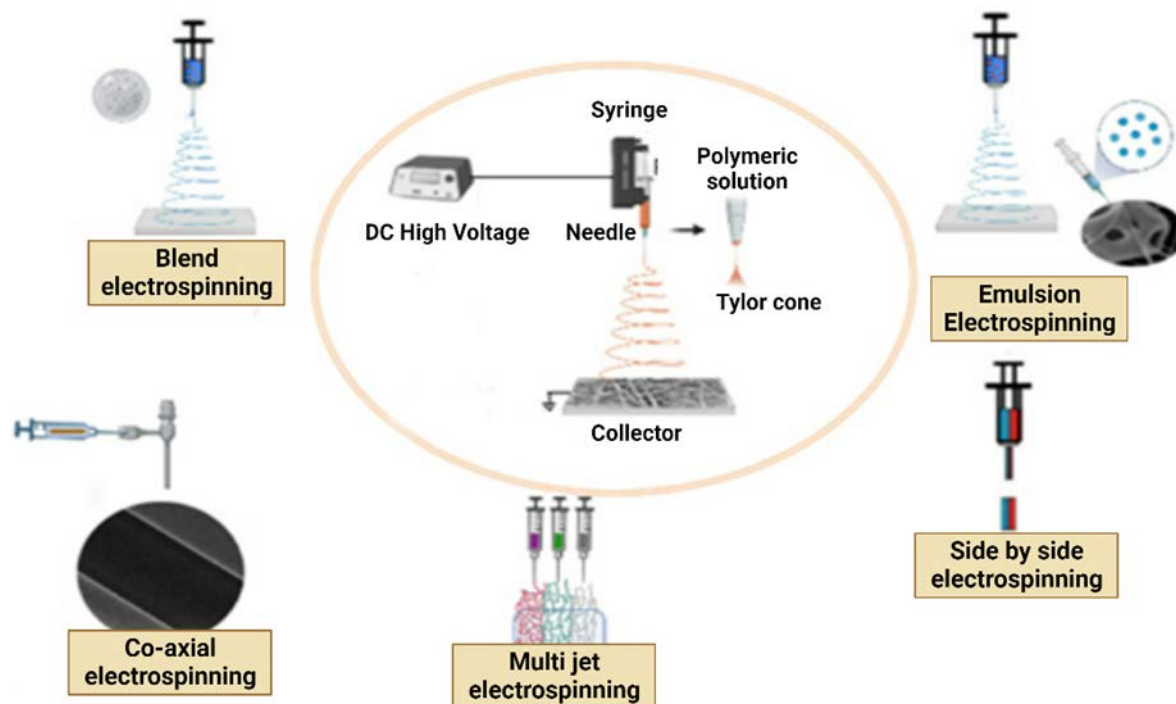

Figure 5. Schematic representation of various methods for incorporating drugs into polymer-carriers using electrospinning.

5.1.5.1. Single Fluid Electrospinning_Blend Electrospinning: This approach involves dissolving the drug and the polymer carrier in a suitable solvent to create a homogenous spinning solution. Electrospinning this solution can achieve a wide range of drug release profiles, ranging from rapid (within seconds) to sustained release over weeks or even months. The choice of solvent, polymer, and processing conditions can be optimized to achieve the desired release profile for a particular drug and delivery application [47]. The main weakness of this approach is the commonly observed burst release phenomenon [30].

5.1.5.2. Emulsion Electrospinning: Emulsion electrospinning is a scientifically established technique for fabricating core-shell nanofibers, enabling the encapsulation of growth factors, proteins, and drugs within the core region to enhance drug stability and improve bioavailability [121]. Forming a stable emulsion requires three crucial components: an oil phase, a water phase, and surfactants/emulsifiers, all of which influence the drug-release properties of the resulting fibres based on their respective compositions [122]. Typically, a hydrophobic polymer is dispersed in an organic solvent (oil phase), whereas hydrophilic compounds are dispersed in water, ensuring the desired characteristics of the emulsion for successful electrospinning. [20]. Tao et al. successfully manufactured polycaprolactone/carboxymethyl chitosan/sodium alginate fibres by emulsion electrospinning with minimal organic solvents. The resulting fibres positively affected osteoblast viability and osteogenesis [41].

5.1.5.3. Multifluid Electrospinning Multijet Electrospinning: Multijet electrospinning can be implemented using two distinct methods: needleless and needle-based configurations [123]. This technique offers substantial advantages for large-scale nanofiber fabrication because it considerably enhances the throughput. The production rate can be significantly increased by enabling simultaneous electrospinning of multiple jets, thereby facilitating the efficient manufacturing of nanofibers on a larger scale [124]. Moreover, it enables the preparation of multi-component fibre mats, wherein diverse populations of fibres fabricated from distinct materials are seamlessly integrated into a unified scaffold. This capability facilitates the development of complex and versatile structures with tailored properties, opening up possibilities for a wide range of applications in tissue engineering, filtration systems, and other fields [125]. This feature is valuable in cases where the inclusion of multiple polymers in a formulation is necessary; however, they cannot be dissolved within the same solution because of their incompatible solubilities. By employing multi-component fibre mats produced through this technique, the simultaneous incorporation of diverse polymers can be achieved, offering enhanced flexibility in designing materials with desired characteristics and functionalities [126]. The resulting fibre mat can deliver multiple drugs at varying rates, and different fibre populations can also influence the mechanical and cell adhesion properties [127]. However, there are some drawbacks to multijet spinning in the needle modality. The electric fields around different needles can interact with each other, which can cause spinning to be erratic [128]. Determining the optimal needle arrangement is a significant challenge in the electrospinning process. However, this obstacle can be overcome by using needleless or auxiliary electrodes. These approaches contribute to the enhanced stability of the spinning process, thereby improving the overall quality and consistency of the resulting fibre mats [78].

5.1.5.4. Side-by-Side Electrospinning: The side-by-side electrospinning technique involves the extrusion of multiple spinning solutions through adjacent spinnerets. This method offers a notable advantage in the form of side-by-side Janus morphology, enabling both compartments to establish physical contact with the biological microenvironment. The efficacy of this approach relies on the precise design of the spinneret and meticulous optimization of the electrospinning parameters [129,130]. Zheng et al., in 2021, tamoxifen, a chemotherapeutic drug, was incorporated into polymer matrices of PVP and Ethyl cellulose (EC). The research findings highlight the significance of shape, structure, and composition in the design of functional nanomaterials. By precisely manipulating these factors, novel materials with enhanced drug release profiles and other desirable properties can be developed for biomedical applications [131].

5.1.5.5. Coaxial/Multiaxial Electrospinning: Coaxial or multiaxial electrospinning enables the fabrication of nanofibers with core-shell or multilayered structures. This technique involves simultaneous electrospinning of two or more spinning solutions through concentric or parallel spinnerets [132]. The outer layer of the fibre is formed by the polymer solution dispensed from the outer spinneret, whereas the inner layer (core) is formed by the solution dispensed from the inner spinneret [133]. Core-shell nanofibers offer the incorporation of various drugs and biomolecules, enabling precise modulation of drug release rates and durations for advanced drug delivery [132]. Their structure enhances their mechanical properties and biocompatibility, making them suitable for biomedical applications such as drug delivery, tissue engineering, and wound healing [134]. Coaxial electrospinning allows for the precise control of small drug molecule release rates from a hydrophobic matrix and enables the encapsulation of liquids within the nanofiber cores [135]. Baykara and Taylan fabricated core-shell fibres using a polyvinyl alcohol (PVA) shell and a core containing Nigella sativa seed oil, renowned for its antimicrobial properties. This core-shell structure effectively regulated the release of oil, preventing sudden bursts of release [93]. This approach can be extended to various drugs or biomolecules that require controlled release rates or encounter compatibility issues with the matrix material, offering a versatile solution for tailored drug delivery systems and overcoming formulation limitations [136]. Triaxial spinning, which involves three fluids, allows the production of multilayer nanofibers [137]. Liu et al. demonstrated the application of triaxial electrospinning to

89

encapsulate ferulic acid within cellulose acetate nanofibers, resulting in a multilayer structure. The in vitro drug release from these fibres exhibited nearly zero-order kinetics, indicating a controlled and steady release rate. This technique can be used to encapsulate various drugs with varying properties, and the number of layers can be adjusted to achieve the desired release profile. Triaxial electrospinning holds promise for the development of drug delivery systems with improved efficacy and reduced toxicity [138]. Quad-axial electrospinning fabricates nanofibers using four simultaneous fluids, enabling precise control over their composition and functionality [139]. Quad-axial electrospinning enables the fabrication of intricate, multilayered structures with improved properties and customized release profiles, thereby revolutionizing drug delivery, tissue engineering, and biomedical applications [140]. Zhang et al. [141] utilized this approach to encapsulate the antimicrobial moxifloxacin in polycaprolactone and gelatine nanofibers with a quad-axial structure. By incorporating moxifloxacin into the nanofibers, quad-axial electrospinning facilitated controlled release kinetics over an extended duration, highlighting the adaptability of this technique in the design of drug delivery strategies. With its precise control over nanofiber composition and structure, quad-axial electrospinning presents a promising avenue for developing advanced drug delivery systems with tailored release profiles [141].

5.2. Applications of Nanofibers in Transdermal Delivery of Various Therapeutic Agents

Electrospinning has opened new avenues for investigating the efficacy of nanofibers in enhancing the properties of matrix materials used in cosmetic applications [153]. The integration of composites offers a distinct advantage by combining the strength of the reinforcement with the toughness of the matrix, resulting in exceptional properties that surpass those of conventional single materials [103]. The emergence of electrospinning techniques employing biopolymers has led to innovative nano-biocomposites distinguished by their multifaceted nature, superior functionality, and commendable environmental sustainability, making them highly promising for future applications [154]. Table 3 summarizes the active ingredients electrospun into nanofibrous scaffolds for a specific skin care product, outlining their benefits for the skin. This information can aid in the selection of skincare products tailored to address specific skin concerns. Enzymes are commonly used in the cosmetic industry because of their ability to improve skin texture, reduce wrinkles, and enhance skin hydration [142]. Enzyme immobilization is a well-established technique used in various fields because of its ability to improve the stability, activity, and reusability of enzymes [143]. However, using free enzymes in cosmetic formulations can be challenging because of their instability and susceptibility to degradation [144].

The utilization of nanofibers for transdermal drug delivery has gained attention because of several advantages, such as high drug loading capacity, high surface-to-volume ratio, and resemblance to the extracellular matrix. The successful production of nanofibrous mats depends on the appropriate selection of polymers and solvents for electrospinning. Nanofibers suitable for transdermal drug delivery can be produced using multiple polymer blends for electrospinning. A polymeric nanofibrous mat loaded with a therapeutic agent has the capacity to control and prolong its transdermal release. Transdermal nanofibers have demonstrated therapeutic potential in preclinical studies conducted by pharmaceutical scientists. However, their entry into the pharmaceutical market is governed by the development of effective scale-up technologies and comprehensive clinical evaluation.

OPEN JOURNAL OF

NANO

Table 3. The sum of bioactive ingredients and their benefits to skin.

Electrospun polymers	Ingredients	Benefits for skin	Personal Care Category	References
Silk fibroin	Lanolin	Occlusive, emollient	Lipophilic	[145–147]
Chitosan, PVA	Glycerine	Anti-inflammatory, barrier recovery	Humectant, moisturizer	[148–150]
Chitosan, Gelatin, and PVA	Hyaluronic Acid	Humectant, anti-aging	Humectant, moisturizer	[93,151]
Silk fibroin	Vitamin B5 (Pantothenic Acid/Dexpanthenol)	Hydration, barrier protection, reduction of trans-epidermal water loss (TEWL), fibroblast stimulation, and re-epithelialization.	Humectant, emollient, antiinflammatory	[152–155]
Chitosan,Gelatin, and PVA	Aloesin	Tyrosinase inhibition, antioxidant, anti-inflammatory	Depigmenting, sun protective (UVB)	[156,157]
PVA, PCL, Chitosan	Mulberry Extract	Antityrosinase, antihyperglycemic, antitumorigenic, anti-inflammatory, antipyretic, antioxidant, anti-atherogenic, antimicrobial chemo-preventive, neuro-protective	Depigmenting	[158–160]
PVA	Niacinamide	PAR-2 inhibition, anti-inflammatory, antioxidant, anti-ageing, photoprotective	Depigmenting, exfoliant	[158,161,162]
PVA, Chitosan	Green Tea	Antioxidant, anti-ageing, antiacne, antiangiogenic, anticarcinogenic, anticarcinogenic, anti-inflammatory, antimicrobial, chemo-preventive, immunomodulatory,2photoprotective	Anti-ageing, moisturizing, antiacne, anogenital wart treatment	[79,163,164]
PVA, PLGA.Chitosan	Flaxseed Oil	Antioxidant, anti-ageing, anti-inflammatory, and antiapoptotic	Antioxidant, anti-ageing	[165–167]
PVA, PLGA	Caffeic Acid	Antioxidant, anticarcinogenic, anti-inflammatory, antimicrobial, immunostimulatory, neuroprotective, photoprotective	Antioxidant, anti-ageing	[168–171]
PLGA.PEO	Ferulic Acid	Antioxidant, anticancer, anti-inflammatory, antimicrobial, cardioprotective, neuroprotective, hepatoprotective, photoprotective, skin-lightening	Antioxidant, anti-ageing, photoprotection	[170,172,173]
Cellulose acetate	Tocopherol (Vitamin E)	Antioxidant, photoprotection, wound healing	Antioxidant, moisturizing, anti-ageing	[174–176]
Hyaluronic acid, PEO	Honey/Propolis/Royal Jelly	Analgesic, antioxidant, antiinflammatory, antimicrobial, antitumor, antiseptic, antipyretic, antiulcer, hepatoprotective, immunomodulatory	Antioxidant, anti-ageing, photoprotection, antiseptic, wound healing	[177–180]
Chitosan, Polycaprolactone,PVA	Melatonin	Antioxidant, anticarcinogenic, anti-ageing, anti-inflammatory, anxiolytic, immunomodulatory	Antioxidant, anti-ageing	[181–183]
Pullulan	Aloe Vera	Anti-inflammatory, antioxidant, antimicrobial, immunomodulatory, laxative, wound healing	Moisturizing, soothing, cooling, burning, healing	[81,184,185]

6. Conclusions and Future Challenges

Transdermal patches represent a strategic advancement in medicinal treatment, offering enhanced safety and efficiency. These patches, equipped with a drug reservoir, penetration enhancer, and various layers integral to their function, facilitate a crucial drug release mechanism. Diffusion from the patch through the skin to the underlying blood capillaries is pivotal for its efficacy. The advantages of transdermal patches include their ability to control drug release, their non-invasive nature, diminished side effects, bypassing of hepatic first-pass metabolism, and a quicker and more potent onset of action. Nevertheless, challenges such as the risk of self-toxicity, adhesion issues, suboptimal drug penetration, skin irritation, and patch malfunction necessitate further innovation and exploration to refine these delivery systems. Notably, transdermal applications present an opportunity to enhance the delivery of natural products, although the complexity of herbal medicine constituents and dosage discrepancies between traditional uses and nanotechnological limitations pose significant research areas. Addressing these complexities, particularly the authentic effects of natural products via nanocarriers and systemic mechanisms underlying their efficacy, is critical. Future studies should focus on developing suitable transdermal methods and proper evaluation techniques for natural products to fully harness their potential in this domain. The current work encapsulates these aspects and has published research in this field.

Abbreviations

MED: Minimum Effective Dose
MTD: Maximum Tolerated Dose
FDA: US Food and Drug Administration
API: Active Pharmaceutical Ingredient
TDD: Topical Drug Delivery
J: Molecular Flux (mol/s·m²)
D: Diffusion Coefficient (m²/s)
L: Cross-Sectional Thickness of Diffusion (m)
dc/dl: Concentration Gradient (mol/m⁴)

Peer-review: Externally peer - reviewed.

Author contributions: -

Conflict of Interest: No conflict of interest was declared by the authors.

Financial Disclosure: The authors declared that this study has received no financial support.

References

[1]   Gupta V, Mohapatra S, Mishra H, Farooq U, Kumar K, Ansari MJ, et al. Nanotechnology in Cosmetics and Cosmeceuticals—A Review of Latest Advancements. Gels 2022;8:173. https://doi.org/10.3390/gels8030173.

[2]   Bayda S, Adeel M, Tuccinardi T, Cordani M, Rizzolio F. The History of Nanoscience and Nanotechnology: From Chemical–Physical Applications to Nanomedicine. Molecules 2019;25:112. https://doi.org/10.3390/molecules25010112.

[3]   Qiao L, Han M, Gao S, Shao X, Wang X, Sun L, et al. Research progress on nanotechnology for delivery of active ingredients from traditional Chinese medicines. J Mater Chem B 2020;8:6333–51. https://doi.org/10.1039/d0tb01260b.

[4]   Salvioni L, Morelli L, Ochoa E, Labra M, Fiandra L, Palugan L, et al. The emerging role of nanotechnology in skin care. Advances in Colloid and Interface Science 2021;293:102437. https://doi.org/10.1016/j.cis.2021.102437.

[5]   Liu J-K. Natural products in cosmetics. Nat Prod Bioprospect 2022;12:40. https://doi.org/10.1007/s13659-022-00363-y.

[6]   Chauhan A, Chauhan C. Emerging trends of nanotechnology in beauty solutions: A review. Materials Today: Proceedings 2021. https://doi.org/10.1016/j.matpr.2021.04.378.

[7]   Spampinato SF, Caruso GI, De Pasquale R, Sortino MA, Merlo S. The Treatment of Impaired Wound Healing in Diabetes: Looking among Old Drugs. Pharmaceuticals (Basel) 2020;13:60. https://doi.org/10.3390/ph13040060.

[8]   Wang M, Huang X, Zheng H, Tang Y, Zeng K, Shao L, et al. Nanomaterials applied in wound healing: Mechanisms, limitations and perspectives. Journal of Controlled Release 2021;337:236–47. https://doi.org/10.1016/j.jconrel.2021.07.017.

[9]   Berthet M, Gauthier Y, Lacroix C, Verrier B, Monge C. Nanoparticle-Based Dressing: The Future of Wound Treatment? Trends Biotechnol 2017;35:770–84. https://doi.org/10.1016/j.tibtech.2017.05.005.

[10]   Kushwaha A, Goswami L, Kim BS. Nanomaterial-Based Therapy for Wound Healing. Nanomaterials 2022;12:618. https://doi.org/10.3390/nano12040618.

[11]   Mihai MM, Dima MB, Dima B, Holban AM. Nanomaterials for Wound Healing and Infection Control. Materials 2019;12:2176. https://doi.org/10.3390/ma12132176.

[12]   Kaur A, Singh TG, Dhiman S, Arora S, Babbar R. NOVEL HERBS USED IN COSMETICS FOR SKIN AND HAIR CARE : A REVIEW n.d.

[13]   Mohd-Setapar SH, John CP, Mohd-Nasir H, Azim MM, Ahmad A, Alshammari MB. Application of Nanotechnology Incorporated with Natural Ingredients in Natural Cosmetics. Cosmetics 2022;9:110. https://doi.org/10.3390/cosmetics9060110.

[14]   Bowe WP, Pugliese S. Cosmetic benefits of natural ingredients. J Drugs Dermatol 2014;13:1021–5; quiz 26–7.

[15]   Dini I, Laneri S. The New Challenge of Green Cosmetics: Natural Food Ingredients for Cosmetic Formulations. Molecules 2021;26:3921. https://doi.org/10.3390/molecules26133921.

[16]   Costa EF, Magalhães WV, Di Stasi LC. Recent Advances in Herbal-Derived Products with Skin Anti-Aging Properties and Cosmetic Applications. Molecules 2022;27:7518. https://doi.org/10.3390/molecules27217518.

[17]   Nguyen AV, Soulika AM. The Dynamics of the Skin's Immune System. Int J Mol Sci 2019;20:1811. https://doi.org/10.3390/ijms20081811.

[18]   Juliano C, Magrini GA. Cosmetic Functional Ingredients from Botanical Sources for Anti-Pollution Skincare Products. Cosmetics 2018;5:19. https://doi.org/10.3390/cosmetics5010019.

[19]   Rodan K, Fields K, Majewski G, Falla T. Skincare Bootcamp: The Evolving Role of Skincare. Plast Reconstr Surg Glob Open 2016;4:e1152. https://doi.org/10.1097/GOX.0000000000001152.

[20]   Thibane VS, Ndhlala AR, Abdelgadir HA, Finnie JF, Staden JV. The cosmetic potential of plants from the Eastern Cape Province traditionally used for skincare and beauty. South African Journal of Botany 2019;122:475–83. https://doi.org/10.1016/j.sajb.2018.05.003.

[21]   Hoang HT, Moon J-Y, Lee Y-C. Natural Antioxidants from Plant Extracts in Skincare Cosmetics: Recent Applications, Challenges and Perspectives. Cosmetics 2021;8:106. https://doi.org/10.3390/cosmetics8040106.

[22]   Dlova NC, Hamed SH, Tsoka-Gwegweni J, Grobler A. Skin lightening practices: an epidemiological study of South African women of African and Indian ancestries. British Journal of Dermatology 2015;173:2–9. https://doi.org/10.1111/bjd.13556.

[23]   Kumar V. Perspective of Natural Products in Skincare. PPIJ 2016;4. https://doi.org/10.15406/ppij.2016.04.00072.

[24]   He H, Li A, Li S, Tang J, Li L, Xiong L. Natural components in sunscreens: Topical formulations with sun protection factor (SPF). Biomed Pharmacother 2021;134:111161. https://doi.org/10.1016/j.biopha.2020.111161.

[25]   Ahmed IA, Mikail MA, Zamakshshari N, Abdullah A-SH. Natural anti-aging skincare: role and potential. Biogerontology 2020;21:293–310. https://doi.org/10.1007/s10522-020-09865-z.

[26]   Verdier-Sévrain S, Bonté F. Skin hydration: a review on its molecular mechanisms. J Cosmet Dermatol 2007;6:75–82. https://doi.org/10.1111/j.1473-2165.2007.00300.x.

[27]   Hu X, He H. A review of cosmetic skin delivery. J Cosmet Dermatol 2021;20:2020–30. https://doi.org/10.1111/jocd.14037.

[28]   Zeng Q, Qi X, Shi G, Zhang M, Haick H. Wound Dressing: From Nanomaterials to Diagnostic Dressings and Healing Evaluations. ACS Nano 2022;16:1708–33. https://doi.org/10.1021/acsnano.1c08411.

[29]   Antonio JR, Antônio CR, Cardeal ILS, Ballavenuto JMA, Oliveira JR. Nanotechnology in dermatology. An Bras Dermatol 2014;89:126–36. https://doi.org/10.1590/abd1806-4841.20142228.

[30]   Pereira-Silva M, Martins AM, Sousa-Oliveira I, Ribeiro HM, Veiga F, Marto J, et al. Nanomaterials in hair care and treatment. Acta Biomater 2022;142:14–35. https://doi.org/10.1016/j.actbio.2022.02.025.

[31]   He M, Zhang W, Liu Z, Zhou L, Cai X, Li R, et al. The interfacial interactions of nanomaterials with human serum albumin. Anal Bioanal Chem 2022;414:4677–84. https://doi.org/10.1007/s00216-022-04089-1.

[32]   Puglia C, Santonocito D. Cosmeceuticals: Nanotechnology-Based Strategies for the Delivery of Phytocompounds. Curr Pharm Des 2019;25:2314–22. https://doi.org/10.2174/1381612825666190709211101.

[33]   Santos AC, Panchal A, Rahman N, Pereira-Silva M, Pereira I, Veiga F, et al. Evolution of Hair Treatment and Care: Prospects of Nanotube-Based Formulations. Nanomaterials (Basel) 2019;9:903. https://doi.org/10.3390/nano9060903.

[34]   Veerabadran NG, Price RR, Lvov YM. Clay nanotubes for encapsulation and sustained release of drugs. NANO 2007;02:115–20. https://doi.org/10.1142/S1793292007000441.

[35]   Wong WF, Ang KP, Sethi G, Looi CY. Recent Advancement of Medical Patch for Transdermal Drug Delivery. Medicina (Kaunas) 2023;59:778. https://doi.org/10.3390/medicina59040778.

[36]   Pastore MN, Kalia YN, Horstmann M, Roberts MS. Transdermal patches: history, development and pharmacology. Br J Pharmacol 2015;172:2179–209. https://doi.org/10.1111/bph.13059.

[37]   Jeong WY, Kwon M, Choi HE, Kim KS. Recent advances in transdermal drug delivery systems: a review. Biomaterials Research 2021;25:24. https://doi.org/10.1186/s40824-021-00226-6.

[38]   Benson HAE. Transdermal drug delivery: penetration enhancement techniques. Curr Drug Deliv 2005;2:23–33. https://doi.org/10.2174/1567201052772915.

[39]   Mumtaz N, Imran M, Javaid A, Latif S, Hussain N, Mitu L. Nanomaterials for Targeted Drug Delivery through Skin to Treat Various Diseases: Recent Trends and Future Perspective. Journal of Chemistry 2023;2023:e3861758. https://doi.org/10.1155/2023/3861758.

[40]   Souto EB, Macedo AS, Dias-Ferreira J, Cano A, Zielińska A, Matos CM. Elastic and Ultradeformable Liposomes for Transdermal Delivery of Active Pharmaceutical Ingredients (APIs). Int J Mol Sci 2021;22:9743. https://doi.org/10.3390/ijms22189743.

[41]   Bird D, Ravindra NM. Transdermal drug delivery and patches—An overview. MEDICAL DEVICES & SENSORS 2020;3:e10069. https://doi.org/10.1002/mds3.10069.

[42]   Bos J, Meinardi M. The 500 Dalton rule for the skin penetration of chemical compounds and drugs. Experimental Dermatology 2000;9:165–9. https://doi.org/10.1034/j.1600-0625.2000.009003165.x.

[43]   Mitchell MJ, Billingsley MM, Haley RM, Wechsler ME, Peppas NA, Langer R. Engineering precision nanoparticles for drug delivery. Nat Rev Drug Discov 2021;20:101–24. https://doi.org/10.1038/s41573-020-0090-8.

[44]   Patel NA, Patel NJ, Patel RP. Design and evaluation of transdermal drug delivery system for curcumin as an anti-inflammatory drug. Drug Dev Ind Pharm 2009;35:234–42. https://doi.org/10.1080/03639040802266782.

[45]   Gu Y, Yang M, Tang X, Wang T, Yang D, Zhai G, et al. Lipid nanoparticles loading triptolide for transdermal delivery: mechanisms of penetration enhancement and transport properties. J Nanobiotechnology 2018;16:68. https://doi.org/10.1186/s12951-018-0389-3.

[46]   Thacharodi D, Rao KP. Development and in vitro evaluation of chitosan-based transdermal drug delivery systems for the controlled delivery of propranolol hydrochloride. Biomaterials 1995;16:145–8. https://doi.org/10.1016/0142-9612(95)98278-m.

[47]   S AS. Transdermal Drug Delivery Systems. Research & Reviews: Journal of Pharmaceutics and Nanotechnology 2016;4:1–7.

[48]   Qindeel M, Ullah MH, Fakhar-Ud-Din null, Ahmed N, Rehman AU. Recent trends, challenges and future outlook of transdermal drug delivery systems for rheumatoid arthritis therapy. J Control Release 2020;327:595–615. https://doi.org/10.1016/j.jconrel.2020.09.016.

[49]   Akram MR, Ahmad M, Abrar A, Sarfraz RM, Mahmood A. Formulation design and development of matrix diffusion controlled transdermal drug delivery of glimepiride. Drug Des Devel Ther 2018;12:349–64. https://doi.org/10.2147/DDDT.S147082.

[50]   TDDS (Transdermal Drug Delivery System) │ OperationsResearch & Development Organization │ About Us │ Hisamitsu Pharmaceutical co.,inc. n.d. https://global.hisamitsu/operations/tdds.html (accessed December 22, 2023).

[51]   Bhowmick M, Sengodan T. Mechanisms, kinetics and mathematical modelling of transdermal permeation-an updated review. Pharmacie Globale 2013;4:1.

[52]   Dhote V, Bhatnagar P, Mishra PK, Mahajan SC, Mishra DK. Iontophoresis: A Potential Emergence of a Transdermal Drug Delivery System. Sci Pharm 2012;80:1–28. https://doi.org/10.3797/scipharm.1108-20.

[53]   Zaid Alkilani A, McCrudden MTC, Donnelly RF. Transdermal Drug Delivery: Innovative Pharmaceutical Developments Based on Disruption of the Barrier Properties of the stratum corneum. Pharmaceutics 2015;7:438–70. https://doi.org/10.3390/pharmaceutics7040438.

[54]   Kong Y-H, Xu S-P. Juglanin administration protects skin against UVB-induced injury by reducing Nrf2-dependent ROS generation. International Journal of Molecular Medicine 2020;46:67. https://doi.org/10.3892/ijmm.2020.4589.

[55]   Schoellhammer CM, Blankschtein D, Langer R. Skin Permeabilization for Transdermal Drug Delivery: Recent Advances and Future Prospects. Expert Opin Drug Deliv 2014;11:393–407. https://doi.org/10.1517/17425247.2014.875528.

[56]   Gratieri T, Alberti I, Lapteva M, Kalia YN. Next generation intra- and transdermal therapeutic systems: using non- and minimally-invasive technologies to increase drug delivery into and across the skin. Eur J Pharm Sci 2013;50:609–22. https://doi.org/10.1016/j.ejps.2013.03.019.

[57]   Lambert PH, Laurent PE. Intradermal vaccine delivery: will new delivery systems transform vaccine administration? Vaccine 2008;26:3197–208. https://doi.org/10.1016/j.vaccine.2008.03.095.

[58]   Fernandez-Carro E, Angenent M, Gracia-Cazaña T, Gilaberte Y, Alcaine C, Ciriza J. Modeling an Optimal 3D Skin-on-Chip within Microfluidic Devices for Pharmacological Studies. Pharmaceutics 2022;14:1417. https://doi.org/10.3390/pharmaceutics14071417.

[59]   Ghosh BRJ William Abraham, Tapash K. Transdermal and Topical Drug Delivery Systems. Theory and Practice of Contemporary Pharmaceutics, CRC Press; 2004.

[60]   Tuan-Mahmood T-M, McCrudden MTC, Torrisi BM, McAlister E, Garland MJ, Singh TRR, et al. Microneedles for intradermal and transdermal delivery. Eur J Pharm Sci 2013;50:623–37. https://doi.org/10.1016/j.ejps.2013.05.005.

[61]   Benson HAE, Grice JE, Mohammed Y, Namjoshi S, Roberts MS. Topical and Transdermal Drug Delivery: From Simple Potions to Smart Technologies. Curr Drug Deliv 2019;16:444–60. https://doi.org/10.2174/1567201816666190201143457.

[62]   Suh H, Shin J, Kim Y-C. Microneedle patches for vaccine delivery. Clin Exp Vaccine Res 2014;3:42–9. https://doi.org/10.7774/cevr.2014.3.1.42.

[63]   Domínguez-Delgado C, Rodríguez Cruz I, López-Cervantes M. The Skin: A Valuable Route for Administration of Drugs. Current Technologies to Increase the Transdermal Delivery of Drugs, 2010, p. 01–22. https://doi.org/10.2174/978160805191511001010001.

[64]   El Maghraby GM, Barry BW, Williams AC. Liposomes and skin: from drug delivery to model membranes. Eur J Pharm Sci 2008;34:203–22. https://doi.org/10.1016/j.ejps.2008.05.002.

[65]   Del Rosso JQ, Levin J. The Clinical Relevance of Maintaining the Functional Integrity of the Stratum Corneum in both Healthy and Disease-affected Skin. J Clin Aesthet Dermatol 2011;4:22–42.

[66]   Wang Y, Xu R, He W, Yao Z, Li H, Zhou J, et al. Three-Dimensional Histological Structures of the Human Dermis. Tissue Eng Part C Methods 2015;21:932–44. https://doi.org/10.1089/ten.TEC.2014.0578.

[67]   Abdo JM, Sopko NA, Milner SM. The applied anatomy of human skin: A model for regeneration. Wound Medicine 2020;28:100179. https://doi.org/10.1016/j.wndm.2020.100179.

[68]   Khavkin J, Ellis DAF. Aging skin: histology, physiology, and pathology. Facial Plast Surg Clin North Am 2011;19:229–34. https://doi.org/10.1016/j.fsc.2011.04.003.

[69]   Ratz-Łyko A, Arct J, Pytkowska K. Moisturizing and Anti-inflammatory Properties of Cosmetic Formulations Containing Centella asiatica Extract. Indian J Pharm Sci 2016;78:27–33.

[70]   Monton C, Sampaopan Y, Pichayakorn W, Panrat K, Suksaeree J. Herbal transdermal patches made from optimized polyvinyl alcohol blended film: Herbal extraction process, film properties, and in vitro study. Journal of Drug Delivery Science and Technology 2022;69:103170. https://doi.org/10.1016/j.jddst.2022.103170.

[71]   Kanjani B, Rai G, Gilhotra R, Kohli S, Pandey V. Formulation Design, Optimization and Characterization of Herbal Bioactive Loaded Transdermal Patch: The State of The Art 2018.

[72]   Mohammed YH, Moghimi HR, Yousef SA, Chandrasekaran NC, Bibi CR, Sukumar SC, et al. Efficacy, Safety and Targets in Topical and Transdermal Active and Excipient Delivery. Percutaneous Penetration Enhancers Drug Penetration Into/Through the Skin 2017:369–91. https://doi.org/10.1007/978-3-662-53270-6_23.

[73]   Patra JK, Das G, Fraceto LF, Campos EVR, Rodriguez-Torres M del P, Acosta-Torres LS, et al. Nano based drug delivery systems: recent developments and future prospects. J Nanobiotechnology 2018;16:71. https://doi.org/10.1186/s12951-018-0392-8.

[74]   Souto EB, Fernandes AR, Martins-Gomes C, Coutinho TE, Durazzo A, Lucarini M, et al. Nanomaterials for Skin Delivery of Cosmeceuticals and Pharmaceuticals. Applied Sciences 2020;10:1594. https://doi.org/10.3390/app10051594.

[75]   Mukherjee B. Nanosize drug delivery system. Curr Pharm Biotechnol 2013;14:1221. https://doi.org/10.2174/13892010415140804121008.

[76]   Souto EB, Fangueiro JF, Fernandes AR, Cano A, Sanchez-Lopez E, Garcia ML, et al. Physicochemical and biopharmaceutical aspects influencing skin permeation and role of SLN and NLC for skin drug delivery. Heliyon 2022;8:e08938. https://doi.org/10.1016/j.heliyon.2022.e08938.

[77]   Ganceviciene R, Liakou AI, Theodoridis A, Makrantonaki E, Zouboulis CC. Skin anti-aging strategies. Dermatoendocrinol 2012;4:308–19. https://doi.org/10.4161/derm.22804.

[78]   Rajpoot K. Solid Lipid Nanoparticles: A Promising Nanomaterial in Drug Delivery. Curr Pharm Des 2019;25:3943–59. https://doi.org/10.2174/1381612825666190903155321.

[79]   Silverberg JI, Jagdeo J, Patel M, Siegel D, Brody N. Green tea extract protects human skin fibroblasts from reactive oxygen species induced necrosis. J Drugs Dermatol 2011;10:1096–101.

[80]   Department of Pharmaceutical Technology, Faculty of Pharmacy, Istanbul Altınbaş University, Istanbul, Turkey, Otlatici G, Yegen G, Department of Pharmaceutical Technology, Faculty of Pharmacy, Istanbul Altınbaş University, Istanbul, Turkey, Gungor S, Department of Pharmaceutical Technology, Faculty of Pharmacy, Istanbul University, 34116, Istanbul, Turkey, et al. Overview on nanotechnology based cosmeceuticals to prevent skin aging. Istanbul J Pharm 2019;48:55–62. https://doi.org/10.5152/IstanbulJPharm.2018.424278.

[81]   Surjushe A, Vasani R, Saple DG. Aloe vera: a short review. Indian J Dermatol 2008;53:163–6. https://doi.org/10.4103/0019-5154.44785.

[82]   Srivastava JK, Shankar E, Gupta S. Chamomile: A herbal medicine of the past with bright future. Mol Med Rep 2010;3:895–901. https://doi.org/10.3892/mmr.2010.377.

[83]   Preethi KC, Kuttan R. Wound healing activity of flower extract of Calendula officinalis. J Basic Clin Physiol Pharmacol 2009;20:73–9. https://doi.org/10.1515/jbcpp.2009.20.1.73.

[84]   Kim HM, Cho SH. Lavender oil inhibits immediate-type allergic reaction in mice and rats. J Pharm Pharmacol 1999;51:221–6. https://doi.org/10.1211/0022357991772178.

[85]   Evangelista MTP, Abad-Casintahan F, Lopez-Villafuerte L. The effect of topical virgin coconut oil on SCORAD index, transepidermal water loss, and skin capacitance in mild to moderate pediatric atopic dermatitis: a randomized, double-blind, clinical trial. Int J Dermatol 2014;53:100–8. https://doi.org/10.1111/ijd.12339.

[86]   Pazyar N, Yaghoobi R, Ghassemi MR, Kazerouni A, Rafeie E, Jamshydian N. Jojoba in dermatology: a succinct review. G Ital Dermatol Venereol 2013;148:687–91.

[87]   Lin T-K, Zhong L, Santiago JL. Anti-Inflammatory and Skin Barrier Repair Effects of Topical Application of Some Plant Oils. Int J Mol Sci 2017;19:70. https://doi.org/10.3390/ijms19010070.

[88]   Villa C, Trucchi B, Gambaro R, Baldassari S. Green procedure for the preparation of scented alcohols from carbonyl compounds. Int J Cosmet Sci 2008;30:139–44. https://doi.org/10.1111/j.1468-2494.2008.00431.x.

[89]   Jose A, Mahey R, Sharma JB, Bhatla N, Saxena R, Kalaivani M, et al. Comparison of ferric Carboxymaltose and iron sucrose complex for treatment of iron deficiency anemia in pregnancy-randomized controlled trial. BMC Pregnancy Childbirth 2019;19:54. https://doi.org/10.1186/s12884-019-2200-3.

[90]   Thring TS, Hili P, Naughton DP. Antioxidant and potential anti-inflammatory activity of extracts and formulations of white tea, rose, and witch hazel on primary human dermal fibroblast cells. J Inflamm (Lond) 2011;8:27. https://doi.org/10.1186/1476-9255-8-27.

[91]   Tang S-C, Yang J-H. Dual Effects of Alpha-Hydroxy Acids on the Skin. Molecules 2018;23:863. https://doi.org/10.3390/molecules23040863.

[92] Telang PS. Vitamin C in dermatology. Indian Dermatol Online J 2013;4:143–6. https://doi.org/10.4103/2229-5178.110593.

[93] Gold MH. Use of hyaluronic acid fillers for the treatment of the aging face. Clin Interv Aging 2007;2:369–76.

[94] Mukherjee S, Date A, Patravale V, Korting HC, Roeder A, Weindl G. Retinoids in the treatment of skin aging: an overview of clinical efficacy and safety. Clin Interv Aging 2006;1:327–48.

[95] Arif T. Salicylic acid as a peeling agent: a comprehensive review. Clin Cosmet Investig Dermatol 2015;8:455–61. https://doi.org/10.2147/CCID.S84765.

[96] Pazyar N, Yaghoobi R, Bagherani N, Kazerouni A. A review of applications of tea tree oil in dermatology. Int J Dermatol 2013;52:784–90. https://doi.org/10.1111/j.1365-4632.2012.05654.x.

[97] Lin P-H, Sermersheim M, Li H, Lee PHU, Steinberg SM, Ma J. Zinc in Wound Healing Modulation. Nutrients 2017;10:16. https://doi.org/10.3390/nu10010016.

[98] Ahsan A, tian wenxia, Farooq M, Khan D. An overview of hydrogels and their role in transdermal drug delivery. International Journal of Polymeric Materials 2020;70. https://doi.org/10.1080/00914037.2020.1740989.

[99] Defraeye T, Bahrami F, Rossi RM. Inverse Mechanistic Modeling of Transdermal Drug Delivery for Fast Identification of Optimal Model Parameters. Front Pharmacol 2021;12:641111. https://doi.org/10.3389/fphar.2021.641111.

[100] Kováčik A, Kopečná M, Vávrová K. Permeation enhancers in transdermal drug delivery: benefits and limitations. Expert Opin Drug Deliv 2020;17:145–55. https://doi.org/10.1080/17425247.2020.1713087.

[101] Mishra A, Pathak A. Plasticizers: A Vital Excipient in Novel Pharmaceutical Formulations. Current Research in Pharmaceutical Sciences 2017;7:1–10. https://doi.org/10.24092/CRPS.2017.070101.

[102] Otterbach A, Lamprecht A. Enhanced Skin Permeation of Estradiol by Dimethyl Sulfoxide Containing Transdermal Patches. Pharmaceutics 2021;13:320. https://doi.org/10.3390/pharmaceutics13030320.

[103] Alkilani AZ, Nasereddin J, Hamed R, Nimrawi S, Hussein G, Abo-Zour H, et al. Beneath the Skin: A Review of Current Trends and Future Prospects of Transdermal Drug Delivery Systems. Pharmaceutics 2022;14:1152. https://doi.org/10.3390/pharmaceutics14061152.

[104] Akrami-Hasan-Kohal M, Tayebi L, Ghorbani M. Curcumin-loaded naturally-based nanofibers as active wound dressing mats: morphology, drug release, cell proliferation, and cell adhesion studies. New J Chem 2020;44:10343–51. https://doi.org/10.1039/D0NJ01594F.

[105] Mishra S, Bishnoi R, Maurya R, Jain D. BOSWELLIA SERRATA ROXB. -A BIOACTIVE HERB WITH VARIOUS PHARMACOLOGICAL ACTIVITIES. Asian Journal of Pharmaceutical and Clinical Research 2020;13:33. https://doi.org/10.22159/ajpcr.2020.v13i11.39354.

[106]   Chinnasamy G, Chandrasekharan S, Koh TW, Bhatnagar S. Synthesis, Characterization, Antibacterial and Wound Healing Efficacy of Silver Nanoparticles From Azadirachta indica. Front Microbiol 2021;12:611560. https://doi.org/10.3389/fmicb.2021.611560.

[107]   Sengsuk T, Songtipya P, Kalkornsurapranee E, Johns J, Songtipya L. Active Bio-Based Pressure-Sensitive Adhesive Based Natural Rubber for Food Antimicrobial Applications: Effect of Processing Parameters on Its Adhesion Properties. Polymers 2021;13:199. https://doi.org/10.3390/polym13020199.

[108]   Bauer AW, Kirby WM, Sherris JC, Turck M. Antibiotic susceptibility testing by a standardized single disk method. Am J Clin Pathol 1966;45:493–6.

[109]   Nematpour N, Farhadian N, Ebrahimi KS, Arkan E, Seyedi F, Khaledian S, et al. Sustained release nanofibrous composite patch for transdermal antibiotic delivery. Colloids and Surfaces A: Physicochemical and Engineering Aspects 2020;586:124267. https://doi.org/10.1016/j.colsurfa.2019.124267.

[110]   Al-Hazeem NZA, Al-Hazeem NZA. Nanofibers and Electrospinning Method. IntechOpen; 2018. https://doi.org/10.5772/intechopen.72060.

[111]   Chinnappan BA, Krishnaswamy M, Xu H, Hoque ME. Electrospinning of Biomedical Nanofibers/Nanomembranes: Effects of Process Parameters. Polymers (Basel) 2022;14:3719. https://doi.org/10.3390/polym14183719.

[112]   Barhoum A, Bechelany M, Hamdy Makhlouf AS. Handbook of Nanofibers. 2019. https://doi.org/10.1007/978-3-319-53655-2.

[113]   Yarin A, Koombhongse S, Reneker D. Taylor Cone and Jetting from Liquid Droplets in Electrospinning of Nanofibers. Journal of Applied Physics 2001;90:4836–46. https://doi.org/10.1063/1.1408260.

[114]   Barhoum A, Pal K, Rahier H, Uludag H, Kim IS, Bechelany M. Nanofibers as new-generation materials: From spinning and nano-spinning fabrication techniques to emerging applications. Applied Materials Today 2019;17:1–35. https://doi.org/10.1016/j.apmt.2019.06.015.

[115]   Nayl AA, Abd-Elhamid AI, Awwad NS, Abdelgawad MA, Wu J, Mo X, et al. Review of the Recent Advances in Electrospun Nanofibers Applications in Water Purification. Polymers (Basel) 2022;14:1594. https://doi.org/10.3390/polym14081594.

[116]   Dokuchaeva AA, Timchenko TP, Karpova EV, Vladimirov SV, Soynov IA, Zhuravleva IY. Effects of Electrospinning Parameter Adjustment on the Mechanical Behavior of Poly-ε-caprolactone Vascular Scaffolds. Polymers (Basel) 2022;14:349. https://doi.org/10.3390/polym14020349.

[117]   Li H, Chen X, Lu W, Wang J, Xu Y, Guo Y. Application of Electrospinning in Antibacterial Field. Nanomaterials (Basel) 2021;11:1822. https://doi.org/10.3390/nano11071822.

[118]   Luraghi A, Peri F, Moroni L. Electrospinning for drug delivery applications: A review. J Control Release 2021;334:463–84. https://doi.org/10.1016/j.jconrel.2021.03.033.

[119]   Xue J, Wu T, Dai Y, Xia Y. Electrospinning and Electrospun Nanofibers: Methods, Materials, and Applications. Chem Rev 2019;119:5298–415. https://doi.org/10.1021/acs.chemrev.8b00593.

[120] Sun G, Sun L, Xie H, Liu J. Electrospinning of Nanofibers for Energy Applications. Nanomaterials (Basel) 2016;6:129. https://doi.org/10.3390/nano6070129.

[121] Zhang C, Feng F, Zhang H. Emulsion electrospinning: Fundamentals, food applications and prospects. Trends in Food Science & Technology 2018;80:175–86. https://doi.org/10.1016/j.tifs.2018.08.005.

[122] Tian Y, Zhou J, He C, He L, Li X, Sui H. The Formation, Stabilization and Separation of Oil–Water Emulsions: A Review. Processes 2022;10:738. https://doi.org/10.3390/pr10040738.

[123] Wu Y-K, Wang L, Fan J, Shou W, Zhou B-M, Liu Y. Multijet Electrospinning with Auxiliary Electrode: The Influence of Solution Properties. Polymers (Basel) 2018;10:572. https://doi.org/10.3390/polym10060572.

[124] Varesano A, Carletto RA, Mazzuchetti G. Experimental investigations on the multijet electrospinning process. Journal of Materials Processing Technology 2009;209:5178–85. https://doi.org/10.1016/j.jmatprotec.2009.03.003.

[125] Mohammadalizadeh Z, Bahremandi-Toloue E, Karbasi S. Recent advances in modification strategies of pre- and post-electrospinning of nanofiber scaffolds in tissue engineering. Reactive and Functional Polymers 2022;172:105202. https://doi.org/10.1016/j.reactfunctpolym.2022.105202.

[126] Ding B, Kimura E, Sato T, Fujita S, Shiratori S. Fabrication of blend biodegradable nanofibrous nonwoven mats via multijet electrospinning. Polymer 2004;45:1895–902. https://doi.org/10.1016/j.polymer.2004.01.026.

[127] Xue J, Xie J, Liu W, Xia Y. Electrospun Nanofibers: New Concepts, Materials, and Applications. Acc Chem Res 2017;50:1976–87. https://doi.org/10.1021/acs.accounts.7b00218.

[128] Li D, Yue G, Li S, Liu J, Li H, Gao Y, et al. Fabrication and Applications of Multi-Fluidic Electrospinning Multi-Structure Hollow and Core–Shell Nanofibers. Engineering 2022;13:116–27. https://doi.org/10.1016/j.eng.2021.02.025.

[129] Yu D-G, Li J-J, Zhang M, Williams GR. High-quality Janus nanofibers prepared using three-fluid electrospinning. Chem Commun (Camb) 2017;53:4542–5. https://doi.org/10.1039/c7cc01661a.

[130] Yu D-G, Yang C, Jin M, Williams GR, Zou H, Wang X, et al. Medicated Janus fibers fabricated using a Teflon-coated side-by-side spinneret. Colloids Surf B Biointerfaces 2016;138:110–6. https://doi.org/10.1016/j.colsurfb.2015.11.055.

[131] Zheng X, Kang S, Wang K, Yang Y, Yu D-G, Wan F, et al. Combination of structure-performance and shape-performance relationships for better biphasic release in electrospun Janus fibers. International Journal of Pharmaceutics 2021;596:120203. https://doi.org/10.1016/j.ijpharm.2021.120203.

[132] Lu Y, Huang J, Yu G, Cardenas R, Wei S, Wujcik EK, et al. Coaxial electrospun fibers: applications in drug delivery and tissue engineering. WIREs Nanomed Nanobiotechnol 2016;8:654–77. https://doi.org/10.1002/wnan.1391.

[133] Pant B, Park M, Park S-J. Drug Delivery Applications of Core-Sheath Nanofibers Prepared by Coaxial Electrospinning: A Review. Pharmaceutics 2019;11:305. https://doi.org/10.3390/pharmaceutics11070305.

101

[134] Rathore P, Schiffman JD. Beyond the Single-Nozzle: Coaxial Electrospinning Enables Innovative Nanofiber Chemistries, Geometries, and Applications. ACS Appl Mater Interfaces 2021;13:48–66. https://doi.org/10.1021/acsami.0c17706.

[135] Liu Y, Chen X, Liu Y, Gao Y, Liu P. Electrospun Coaxial Fibers to Optimize the Release of Poorly Water-Soluble Drug. Polymers 2022;14:469. https://doi.org/10.3390/polym14030469.

[136] Baykara T, Taylan G. Coaxial electrospinning of PVA/Nigella seed oil nanofibers: Processing and morphological characterization. Materials Science and Engineering: B 2021;265:115012. https://doi.org/10.1016/j.mseb.2020.115012.

[137] Liu W, Ni C, Chase D, Rabolt J. Preparation of Multilayer Biodegradable Nanofibers by Triaxial Electrospinning. ACS Macro Letters 2013;2:466–8. https://doi.org/10.1021/mz4000688.

[138] Liu X, Yang Y, Yu D-G, Zhu M-J, Zhao M, Williams GR. Tunable zero-order drug delivery systems created by modified triaxial electrospinning. Chemical Engineering Journal 2019;356:886–94. https://doi.org/10.1016/j.cej.2018.09.096.

[139] Yu D, Wang M, Xiaoyan L, Liu X, Zhu L-M, Bligh S. Multifluid electrospinning for the generation of complex nanostructures. Wiley Interdisciplinary Reviews: Nanomedicine and Nanobiotechnology 2019;12:e1601. https://doi.org/10.1002/wnan.1601.

[140] Zulkifli MZA, Nordin D, Shaari N, Kamarudin SK. Overview of Electrospinning for Tissue Engineering Applications. Polymers 2023;15:2418. https://doi.org/10.3390/polym15112418.

[141] Zhang X, Chi C, Chen J, Zhang X, Gong M, Wang X, et al. Electrospun quad-axial nanofibers for controlled and sustained drug delivery. Materials & Design 2021;206:109732. https://doi.org/10.1016/j.matdes.2021.109732.

[142] Gonçalves S. Use of enzymes in cosmetics: proposed enzymatic peel procedure 2021;1:29–35.

[143] Bié J, Sepodes B, Fernandes PCB, Ribeiro MHL. Enzyme Immobilization and Co-Immobilization: Main Framework, Advances and Some Applications. Processes 2022;10:494. https://doi.org/10.3390/pr10030494.

[144] Basso A, Serban S. Overview of Immobilized Enzymes' Applications in Pharmaceutical, Chemical, and Food Industry. Methods Mol Biol 2020;2100:27–63. https://doi.org/10.1007/978-1-0716-0215-7_2.

[145] White-Chu EF, Reddy M. Dry skin in the elderly: complexities of a common problem. Clin Dermatol 2011;29:37–42. https://doi.org/10.1016/j.clindermatol.2010.07.005.

[146] Clark EW. A brief history of lanolin. Pharm Hist (Lond) 1980;10:5–6.

[147] Ertas IF, Uzun M, Altan E, Kabir MH, Gurboga M, Ozakpinar OB, et al. Investigation of silk fibroin-lanolin blended nanofibrous structures. Materials Letters 2023;330:133263. https://doi.org/10.1016/j.matlet.2022.133263.

[148] Thau P. Glycerin (glycerol): Current insights into the functional properties of a classic cosmetic raw material. J Cosmet Sci 2002;53:229–36.

[149]   Fluhr JW, Gloor M, Lehmann L, Lazzerini S, Distante F, Berardesca E. Glycerol accelerates recovery of barrier function in vivo. Acta Derm Venereol 1999;79:418–21. https://doi.org/10.1080/000155599750009825.

[150]   Gonçalves MM, Lobsinger KL, Carneiro J, Picheth GF, Pires C, Saul CK, et al. Morphological study of electrospun chitosan/poly(vinyl alcohol)/glycerol nanofibres for skin care applications. International Journal of Biological Macromolecules 2022;194:172–8. https://doi.org/10.1016/j.ijbiomac.2021.11.195.

[151]   Movahedi M, Asefnejad A, Rafienia M, Khorasani MT. Potential of novel electrospun core-shell structured polyurethane/starch (hyaluronic acid) nanofibers for skin tissue engineering: In vitro and in vivo evaluation. International Journal of Biological Macromolecules 2020;146:627–37. https://doi.org/10.1016/j.ijbiomac.2019.11.233.

[152]   Fan L, Cai Z, Zhang K, Han F, Li J, He C, et al. Green electrospun pantothenic acid/silk fibroin composite nanofibers: fabrication, characterization and biological activity. Colloids Surf B Biointerfaces 2014;117:14–20. https://doi.org/10.1016/j.colsurfb.2013.12.030.

[153]   Gehring W, Gloor M. Effect of topically applied dexpanthenol on epidermal barrier function and stratum corneum hydration. Results of a human in vivo study. Arzneimittelforschung 2000;50:659–63. https://doi.org/10.1055/s-0031-1300268.

[154]   Biro K, Thaçi D, Ochsendorf FR, Kaufmann R, Boehncke W-H. Efficacy of dexpanthenol in skin protection against irritation: a double-blind, placebo-controlled study. Contact Dermatitis 2003;49:80–4. https://doi.org/10.1111/j.0105-1873.2003.00184.x.

[155]   Kazsoki A, Palcsó B, Alpár A, Snoeck R, Andrei G, Zelkó R. Formulation of acyclovir (core)-dexpanthenol (sheath) nanofibrous patches for the treatment of herpes labialis. Int J Pharm 2022;611:121354. https://doi.org/10.1016/j.ijpharm.2021.121354.

[156]   Jin YH, Lee SJ, Chung MH, Park JH, Park YI, Cho TH, et al. Aloesin and arbutin inhibit tyrosinase activity in a synergistic manner via a different action mechanism. Arch Pharm Res 1999;22:232–6. https://doi.org/10.1007/BF02976355.

[157]   Wahedi HM, Jeong M, Chae JK, Do SG, Yoon H, Kim SY. Aloesin from Aloe vera accelerates skin wound healing by modulating MAPK/Rho and Smad signaling pathways in vitro and in vivo. Phytomedicine 2017;28:19–26. https://doi.org/10.1016/j.phymed.2017.02.005.

[158]   Zhu W, Gao J. The use of botanical extracts as topical skin-lightening agents for the improvement of skin pigmentation disorders. J Investig Dermatol Symp Proc 2008;13:20–4. https://doi.org/10.1038/jidsymp.2008.8.

[159]   Gupta S, Dutta P, Acharya V, Prasad P, Roy A, Bit A. Accelerating skin barrier repair using novel bioactive magnesium-doped nanofibers of non-mulberry silk fibroin during wound healing. Journal of Bioactive and Compatible Polymers 2022;37:38–52. https://doi.org/10.1177/08839115211061737.

[160]   Liu Y, Qin Y, Bai R, Zhang X, Yuan L, Liu J. Preparation of pH-sensitive and antioxidant packaging films based on κ-carrageenan and mulberry polyphenolic extract. International Journal of Biological Macromolecules 2019;134:993–1001. https://doi.org/10.1016/j.ijbiomac.2019.05.175.

OPEN JOURNAL OF
NANO

[161]   Hakozaki T, Minwalla L, Zhuang J, Chhoa M, Matsubara A, Miyamoto K, et al. The effect of niacinamide on reducing cutaneous pigmentation and suppression of melanosome transfer. Br J Dermatol 2002;147:20–31. https://doi.org/10.1046/j.1365-2133.2002.04834.x.

[162]   Nada A, Hassabo A, Mohamed A, Zaghloul S. Encapsulation of Nicotinamide into Cellulose Based Electrospun Fibers. Journal of Applied Pharmaceutical Science 2016;6:013–21. https://doi.org/10.7324/JAPS.2016.60803.

[163]   Katiyar SK, Ahmad N, Mukhtar H. Green tea and skin. Arch Dermatol 2000;136:989–94. https://doi.org/10.1001/archderm.136.8.989.

[164]   Sadri .Minoo, Arab-Sorkhi S, Vatani H, Bagheri Pebdeni A. New wound dressing polymeric nanofiber containing green tea extract prepared by electrospinning method. Fibers and Polymers 2015;16:1742–50. https://doi.org/10.1007/s12221-015-5297-7.

[165]   De Spirt S, Stahl W, Tronnier H, Sies H, Bejot M, Maurette J-M, et al. Intervention with flaxseed and borage oil supplements modulates skin condition in women. Br J Nutr 2009;101:440–5. https://doi.org/10.1017/S0007114508020321.

[166]   Hadad S, Goli S. Improving Oxidative Stability of Flaxseed Oil by Encapsulation in Electrospun Flaxseed Mucilage Nanofiber. Food and Bioprocess Technology 2019;12. https://doi.org/10.1007/s11947-019-02259-1.

[167]   Hadad S, Goli S. Fabrication and characterization of electrospun nanofibers using flaxseed (Linum usitatissimum) mucilage. International Journal of Biological Macromolecules 2018;114. https://doi.org/10.1016/j.ijbiomac.2018.03.154.

[168]   Staniforth V, Chiu L-T, Yang N-S. Caffeic acid suppresses UVB radiation-induced expression of interleukin-10 and activation of mitogen-activated protein kinases in mouse. Carcinogenesis 2006;27:1803–11. https://doi.org/10.1093/carcin/bgl006.

[169]   Saija A, Tomaino A, Trombetta D, De Pasquale A, Uccella N, Barbuzzi T, et al. In vitro and in vivo evaluation of caffeic and ferulic acids as topical photoprotective agents. Int J Pharm 2000;199:39–47. https://doi.org/10.1016/s0378-5173(00)00358-6.

[170]   Vilchez A, Acevedo F, Cea M, Seeger M, Navia R. Applications of Electrospun Nanofibers with Antioxidant Properties: A Review. Nanomaterials 2020;10:175. https://doi.org/10.3390/nano10010175.

[171]   Kaya S, Yilmaz DE, Akmayan I, Egri O, Arasoglu T, Derman S. Caffeic Acid Phenethyl Ester Loaded Electrospun Nanofibers for Wound Dressing Application. J Pharm Sci 2022;111:734–42. https://doi.org/10.1016/j.xphs.2021.09.041.

[172]   Wang Q-J, Gao X, Gong H, Lin X-R, Saint-Leger D, Senee J. Chemical stability and degradation mechanisms of ferulic acid (FA) within various cosmetic formulations. J Cosmet Sci 2011;62:483–503.

[173]   Vashisth P, Kumar N, Sharma M, Pruthi V. Biomedical applications of ferulic acid encapsulated electrospun nanofibers. Biotechnol Rep (Amst) 2015;8:36–44. https://doi.org/10.1016/j.btre.2015.08.008.

[174]   Charurin P, Ames JM, del Castillo MD. Antioxidant activity of coffee model systems. J Agric Food Chem 2002;50:3751–6. https://doi.org/10.1021/jf011703i.

104

[175]   Sheng X, Fan L, He C, Zhang K, Mo X, Wang H. Vitamin E-loaded silk fibroin nanofibrous mats fabricated by green process for skin care application. Int J Biol Macromol 2013;56:49–56. https://doi.org/10.1016/j.ijbiomac.2013.01.029.

[176]   Taepaiboon P, Rungsardthong U, Supaphol P. Vitamin-loaded electrospun cellulose acetate nanofiber mats as transdermal and dermal therapeutic agents of vitamin A acid and vitamin E. Eur J Pharm Biopharm 2007;67:387–97. https://doi.org/10.1016/j.ejpb.2007.03.018.

[177] Israili ZH. Antimicrobial properties of honey. Am J Ther 2014;21:304–23. https://doi.org/10.1097/MJT.0b013e318293b09b.

[178]   Ediriweera ERHSS, Premarathna NYS. Medicinal and cosmetic uses of Bee's Honey - A review. Ayu 2012;33:178–82. https://doi.org/10.4103/0974-8520.105233.

[179]   Pakolpakçıl A, Draczynski Z. Green Approach to Develop Bee Pollen-Loaded Alginate Based Nanofibrous Mat. Materials 2021;14:2775. https://doi.org/10.3390/ma14112775.

[180]   Ionescu OM, Mignon A, Iacob AT, Simionescu N, Confederat LG, Tuchilus C, et al. New Hyaluronic Acid/Polyethylene Oxide-Based Electrospun Nanofibers: Design, Characterization and In Vitro Biological Evaluation. Polymers (Basel) 2021;13:1291. https://doi.org/10.3390/polym13081291.

[181]   Pugazhenthi K, Kapoor M, Clarkson AN, Hall I, Appleton I. Melatonin accelerates the process of wound repair in full-thickness incisional wounds. J Pineal Res 2008;44:387–96. https://doi.org/10.1111/j.1600-079X.2007.00541.x.

[182] Morganti P. Melatonin and immunostimulating substance-based compositions. EP1991222B1, 2016.

[183]   Mirmajidi T, Chogan F, Rezayan AH, Sharifi AM. In vitro and in vivo evaluation of a nanofiber wound dressing loaded with melatonin. Int J Pharm 2021;596:120213. https://doi.org/10.1016/j.ijpharm.2021.120213.

[184]   Rahman S, Carter P, Bhattarai N. Aloe Vera for Tissue Engineering Applications. JFB 2017;8:6. https://doi.org/10.3390/jfb8010006.

[185]   Barbosa R, Villarreal A, Rodriguez C, De Leon H, Gilkerson R, Lozano K. Aloe Vera extract-based composite nanofibers for wound dressing applications. Mater Sci Eng C Mater Biol Appl 2021;124:112061. https://doi.org/10.1016/j.msec.2021.112061.

Determination of Swelling Kinetics and Diffusion Mechanisms of Chemically Crosslinked Porous Chitosan Hydrogels

[1] Hanife Songül Kaçoğlu (iD), [2] Özgür Ceylan (iD), [*3] Mithat Çelebi (iD)

[1] Yalova University, Polymer Materials Engineering, Institute of Graduate Studies, Yalova, Turkey,
[2] Yalova University, Central Research Laboratory Research and Application Centre, Yalova, Turkey
[3] Yalova University, Polymer Materials Engineering Dept., Faculty of Engineering, Yalova, Turkey
 * Corresponding author, e-mail: mithat.celebi@yalova.edu.tr, https://orcid.org/0000-0002-2013-5354

Abstract - Chitosan hydrogels have gained popularity in a variety of industrial applications due to their biocompatibility, biodegradability, and various physicochemical features. Understanding these hydrogels' swelling dynamics and diffusion processes is crucial to improve their efficiency in drug delivery, tissue engineering, and wound healing applications. This work aims to examine the chemically crosslinked porous chitosan hydrogels in swelling and diffusion processes. The swelling kinetics of the hydrogels were investigated using Fick's diffusion mathematical model to determine the effects of different molecular weights on its swelling behavior at pH: 2.0, 5.6 and 7.4. It was observed that the swelling percentages of hydrogels prepared with low molecular weight chitosan and 1% glutaraldehyde were higher. Chitosan hydrogels cross-linked with glutaraldeyhde exhibited Super Case II Diffusion according to Fick's laws of diffusion. In addition, optical microscopy was used to analyze pictures of porous chitosan hydrogels that were generated using two different molecular weight chitosan.

Keywords: hydrogel, freeze-drying, Fick's law, swelling kinetic, diffusion coefficient

Kimyasal Olarak Çapraz Bağlı Gözenekli Kitosan Hidrojellerin Şişme Kinetiği ve Difüzyon Mekanizmalarının Belirlenmesi

Öz - Kitosan hidrojelleri biyouyumlulukları, biyobozunurlukları ve çeşitli fizikokimyasal özelliklerinden dolayı çeşitli endüstriyel uygulamalarda popülerlik kazanmıştır. Bu hidrojellerin şişme dinamiklerini ve difüzyon süreçlerini anlamak, ilaç salınımı, doku mühendisliği ve yara iyileştirme uygulamalarındaki etkinliklerinin arttırılması açısından çok önemlidir. Bu çalışma kimyasal olarak çapraz bağlı gözenekli kitosan hidrojellerde şişme ve difüzyon süreçlerini incelemeyi amaçlamaktadır. Hidrojellerin şişme kinetiği, pH: 2.0, 5.6 ve 7.4' te kitosanın farklı moleküler ağırlıklarının şişme davranışı üzerindeki etkilerini belirlemek için Fick Kanunu difüzyon matematiksel modeli kullanılarak araştırıldı. Düşük molekül ağırlığında kitosan ve %1 lik glutaraldehit ile hazırlanan hidrojellerin şişme yüzdeleri daha yüksek olduğu görüldü. Glutaraldehit ile çapraz bağlanan kitosan hidrojelleri, Fick'in difüzyon yasalarına göre Süper Durum II Difüzyonu gösterdi. Ayrıca iki farklı molekül ağırlıklı kitosan ile hazırlanan porous kitosan hidrojellerin optik mikroskop ile görüntüleri incelendi.

Anahtar kelimeler: hidrojel, dondurarak kurutma, Fick Yasası, şişme kinetiği, difüzyon katsayısı

1. Introduction

Hydrogels are polymeric materials with a hydrophilic structure that allows them to absorb large amounts of water into their three-dimensional networks. Natural polymers including proteins (collagen and gelatin) and polysaccharides (chitosan, starch, alginate, and agarose) can form hydrogels. Hydrogel-based products are widely used in various industrial, and environmental applications [1]. Hydrogels are often produced by cross-linking biodegradable polysaccharides including starch and chitosan. These natural polymers possess distinctive characteristics such as biocompatibility, biodegradability, low prices, and rapid gelation, owing to their hydrophilic nature[2]. The swelling characteristics of hydrogels are determined by the polymer's solvent compatibility, cross-linking degree, and its nature. [3]. The deacetylation degree (DD) is critical for changing the swelling characteristics of chitosan for a variety of applications. The deacetylation

106

degree indicates the percentage of free amino groups in the chitosan molecule. The degree of deacetylation is a crucial factor that influences the behavior of chitosan in terms of its physicochemical characteristics, including reactivity, crystallinity, and swelling degree[4], [5].

Chitosan is a copolymer composed of glucosamine and N-acetylglucosamine repeat units, with the repeat units defined by the degree of deacetylation of crustacean shell chitin [6]. Chitosan's deacetylation degree determines the ratio of D-glucosamine to N-acetyl-d-glucosamine units in polymer chains. Chitosan is defined as DD > 50%, while chitin is defined as DD < 50% [7], [8]. Chitosan is soluble in dilute acids at acidic pHs. However, it is not soluble at pH 7.4, non-protonated chitosan may absorb huge volumes of water. The swelling characteristic of chitosan, even in the absence of chemical cross-linking, may be explained by the swelling theory of polymer networks, which includes crystalline structures and physical entanglements[4], [5]. According to Zhou et al., the molecular weight and the degree of chitosan deacetylation have strong influence on the pH value, turbidity, viscosity, and thermosensitive properties of chitosan-based hydrogels crosslinked with glycerophosphate [9]. Although, chitosan has been used for many years in a variety of fields, including agriculture, health, sensors, wastewater treatment, metal removal, and cosmetics. It has specific limitations when used as a scaffold, especially in controlled fertilizer, or drug release applications. Here, chemical modification has been proven to overcome these constraints, cross-linked chitosan hydrogels have thus become increasingly important in relevant recent research on drug, fertilizer release, and tissue engineering. Modifying chitosan improves its intrinsic properties such as biocompatibility, chemical versatility, biodegradability, and low toxicity. These adjustments can be made to fit in a specific application. Chitosan's physical and chemical properties can be effectively and practically enhanced for its use in practical applications by crosslinking with crosslinking agents such as sodium tripolyphosphate or glutaraldehyde [10]. Physical hydrogels are hydrophilic structures formed by non-covalent cross-links from ionic, hydrogen, Van Der Waals, or hydrophobic interactions, whose formation depends on thermodynamic parameters like temperature, pH, and ionic strength. The primary drawbacks of physically cross-linked systems are potential mechanical instability and the possibility of system breakdown caused by extremely pH-sensitive swelling [11], [12]. Sodium tripolyphosphate (STPP) is used as a ionic physical crosslinker. STPP-based hydrogels are non-toxic and have low mechanical strength, while they have high swelling capacity [13]. However, chemical cross-linking's irreversible gelation creates stable, mechanically strong hydrogels with resistance to dissolution, making them ideal for chitosan applications due to their physicochemical stability and resistance to extreme pH conditions[14]. The main disadvantage of this system is that most of the cross-linkers used for the cross-linking process are relatively toxic and their effects on the living body are not fully known due to the lack of data on their biocompatibility. The most used chemical crosslinkers in studies on chitosan hydrogels are dialdehydes (such as glutaraldehyde or glyoxal) and genipin. Dialdehydes allow direct reaction in aqueous media, under mild conditions and without the addition of auxiliary molecules such as reducers, which is advantageous in terms of biocompatibility. However, the use of these cross-linkers that exhibit toxic properties requires an additional purification and verification step before application [15]. As mentioned above, chemically cross-linked hydrogels exhibit superior mechanical strength and reduced swelling degree compared to physically cross-linked hydrogels. Chitosan-based hydrogels exhibit different characteristics in swelling behavior at various pH conditions. Mathematical modeling of swelling is critical to understanding the behavior and application of hydrogels under various environmental circumstances[16].

Several mathematical models are used to describe the kinetics of a hydrogel's swelling, t among which, the dominant model is Fickian diffusion, that describes the dispersion of a liquid into the gel matrix as the hydrogel swells or collapses. This model demonstrates a linear increase in the swelling fraction with the square root of time until it reaches 0.4 for diffusion exponential. Additionally, the swelling curve never exhibits a sigmoidal shape. The second model, also known as collective diffusion, establishes a connection between the stress gradient and swelling of the gel

107

as well as the network. None of these two models can adequately explains the significant sigmoidal swelling curves that occur due to large volume changes and are often used to describe non-Fickian diffusion. The Fickian diffusion is characterized by the occurrence of sigmoidal swelling when the movement of the gel surface is precise [16]. The swelling dynamics of hydrogels can be categorized as either diffusion-controlled (Fickian) or relaxation-controlled (non-Fickian) [3]. In this study, glutaraldehyde was preferred as a very reactive chemical crosslinker. Glutaraldehyde is easier to obtain and less costly. The formation of hydrogel using glutaraldehyde occurs more rapidly. However, the crosslinker of glutaraldehyde has toxic properties. Therefore, this disadvantage of glutaraldehyde eliminated by washing the unbound glutaraldehyde from the hydrogel environment after the cross-linking process. Different molecular weight chitosan was used to prepare hydrogels at varying glutaraldehyde concentrations. Hydrogels' swelling properties were examined for their diffusion coefficient and percentages equilibrium swelling. The order of kinetics was further examined using the Fickian diffusion mathematical model. The purpose of this study was to produce porous gels using freeze treatment to examine how the microstructure of the gels affects their swelling process. The effect of the change in the molecular weight of chitosan on the swelling kinetics and optical properties of the hydrogels was investigated.

2. Materials and Methods

Low and medium molecular weight chitosan with a deacetylation degree of at least 75% was obtained from Sigma-Aldrich. Other chemicals including acetic acid (glacial) 100% anhydrous, hydrochloric acid (puris ≥37%), sodium hydroxide (puris 98-100%), glutaraldehyde (25% solution in water) for analysis along with other chemicals obtained from Sigma Aldrich chemicals, disodium hydrogen phosphate (sodium phosphate dibasic) (Na_2HPO_4) purity ≥99.0%, potassium phosphate monobasic (KH_2PO_4) purity ≥99.5%, and disodium citrate (purum p.a., ≥99.0%) were also provided.

The buffer solutions (pH: 2.0 and 7.4) were prepared based on the compositions provided in the Merck laboratory handbook [17]and their precision was verified using a pH meter. The composition and proportions of the buffer solutions are shown in Table 1. Only distilled water was used to prepare the pH:5.6 solution. When required, 0.1 M solution of NaOH and 0.1 M solution of HCl were used to adjust the pH of the solution to desired pH.

Table 1. Chemicals and their ratios used in preparing buffer solutions

pH	Chemicals used in solution preparation and their usage amounts
2.0	0.1 M Disodium citrate (C6H7O7Na2) – 0.1 M Hydrochloric acidt (HCl) 30.2 mL (C6H7O7Na2) + 69.8 mL HCl is completed to 1 L with distilled water.
7.4	0.067 M Potassium dihydrogen phosphate – 0.067 M Disodium hydrogen phosphate Prepare a solution by combining 19.7 mL of KH2PO4 and 80.3 mL of Na2HPO4 with distilled water to a total volume of 1 L.

2.1. Hydrogel Preparation

Figure 1 illustrates the procedural stages for manufacturing chitosan hydrogels cross-linked with glutaraldehyde through a chemical approach. 2 grams of chitosan (2% w/v) were prepared in 100 mL acetic acid (2% w/v) solution. After chitosan was dissolved in acetic acid, the air bubbles were eliminated by using an ultrasonic bath. Then, 1% glutaraldehyde solution was prepared from 25% glutaraldehyde solutionHydrogels were synthesized by adding glutaraldehyde solution at various concentrations ranging from 1% to 10% into solution, depending on the quantity of chitosan [8]. After the hydrogels were frozen in the freezer at -18°C, they were dried with a lyophilizerto form a porous structure. Freeze-drying process was performed with using Labconco FreeZone Freeze-Dry System (cold trap temperature: -40 °C, vacuum degree: ≤30 Pa).
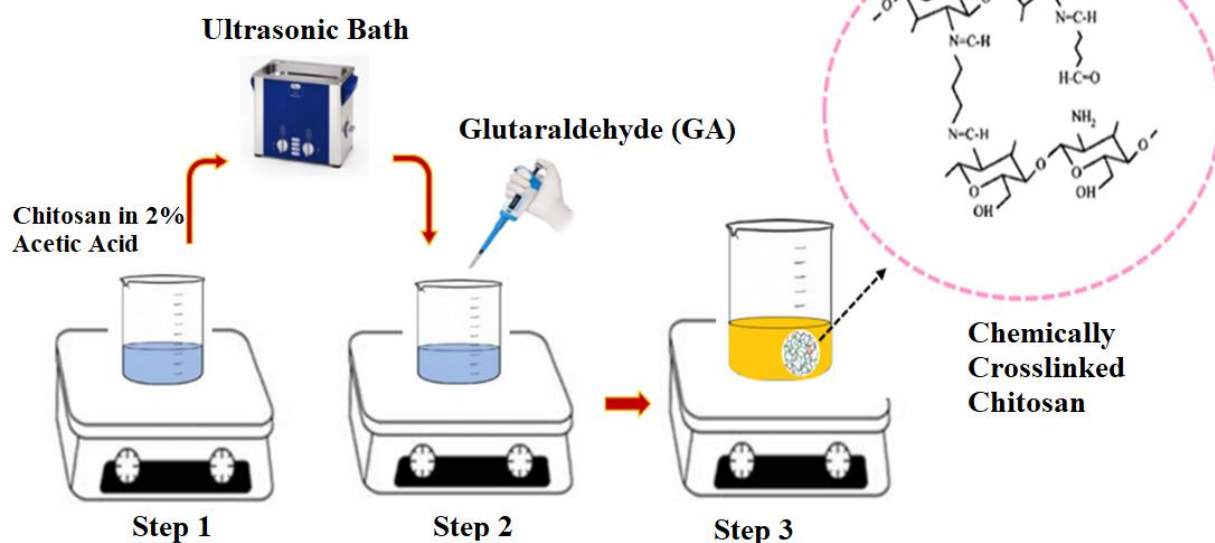
OPEN JOURNAL OF
NANO

Figure 1. Preparation procedure of chitosan hydrogels

2.2. Swelling Ratio

The swelling ratios of the hydrogels were determined according to Jin et. al.[18]. The gravimetric method was employed to evaluate the gels' swelling under various circumstances at room temperature. Initially, the gel's mass was measured, and then, it was placed in the media solution. The hydrogels were kept 6 hours in the media solution. The media solution was pH:2.0, 5,6 and 7.4. Periodically, the hydrogel was removed from the media solution, and it was dried to eliminate any remaining water on its surface. Once the hydrogel's mass was measured, it was placed back into the solution [18]. As the water molecules penetrate the gel, they encounter the cross-linkers' resistance in the network structure after a certain point and this is known as the elastic resistance. The moment when this resistance, which affects the swelling in the opposite direction, and the osmotic pressure force acting in favor of the swelling are equalized, the swelling reaches its maximum [19]. Equation 1 is used to determine the hydrogels' water content when they reached their maximum swelling value at this equilibrium moment.

$$Eq_w = \frac{m_d - m_0}{m_0} * 100 \qquad (1)$$

Eq_w; maximum swelling percentage of the hydrogel at equilibrium.

m_d; hydrogel weight at equilibrium.

m_0; hydrogel dry weight.

2.3. Swelling kinetics and diffusion mechanism

The Fickian diffusion model, which is widely used in modeling the absorption behavior of hydrogels, is explained by the second-order kinetic equation given below [10], [16], [20].

$$\frac{dS}{dT} = k_s (S_{eq} - S)^2 \qquad (2)$$

109

$dS/_{dT}$: swelling rate; k_s: swelling rate constant; S_{eq}: the swelling value at the time of equilibrium; S: refers to the swelling value at time t.

The mechanism of swelling proceeds from the zero order and is expressed by the Fick's law equation given below.

$$F = k \cdot t \, \frac{M_t}{M_d} \tag{3}$$

F is the ratio of the solvent amount absorbed by the hydrogel at t moment to the amount of solvent absorbed at the equilibrium, M_t; the amount of solvent absorbed at t moment, M_d; the amount of solvent absorbed at the equilibrium, t; the diffusion time, n; the diffusion exponent and k is a characteristic constant that varies according to the polymer's structure. By applying the logarithm to this equation, the diffusion exponent, n, is calculated. The parameter "n" facilitates the identification of the diffusion type. This value will give an idea of the diffusion of the solvent into the gel or gel into the solvent [18]. To determine the nature of diffusion mechanism which the diffusion of water into the chitosan hydrogels follows according to Akakuru and Isiuku [10]

$$\log F = \log k + n \cdot \log t \tag{4}$$

The value of n is calculated by the log(t) graph's slope, drawn against the log(F) value at a time when 60% of the solvent is absorbed by the polymer network (F < 0.60), and thus, the diffusion mechanism is determined [10], [16].

2.4. Optical microscopy

Both the visible light images, and the chitosan hydrogels' morphologies prepared at different molecular weights and glutaraldehyde (GA) concentrations were examined by using SOIF MD50 model optical microscope.

3. Results and Discussion

Swelling ratios of the hydrogels were assessed via water absorption. Hydrogels with 1, 3, 5, 7, and 10 wt.% GA were immersed in water to determine their swelling ratios (Fig. 2 and Fig. 3). Such hydrogels, cross-linked with GA, reached maximum swelling at the end of 6 hours. Both L-Mw and M-Mw chitosan gels showed a decrease in %s of swelling values with increased GA concentrations at all different pH mediums. The hydrogel prepared with a lower concentration of cross-linker (1 wt.%) exhibited more swelling compared to the one with a higher percentage of cross-linker (10 wt.%), respectively.

Chitosan hydrogels cross-linked with GA showed higher swelling values compared to non-crosslinked chitosan gels. It can be said that this is because gels with low cross-linking density have a more permeable structure. Zielińska et al. reported a similar result [21]. Silva et al. reported that chitosan membranes with low cross-link ratio (1 wt. % of GA) achieved a higher degree of equilibrium swelling compared to non-crosslinked chitosan, arguing that low crystallinity increases the accessibility of water molecules. Silva et al. observed that the increase in the cross-linking amount (10 wt. % and 20 wt. % of GA) was effective in reducing the degree of equilibrium swelling [22]. Similarly, Wegrzynowska et al. found that neat chitosan films left into the solvent medium exhibited a swelling degree that is twice as low as the cross-linked ones [23].

In cationic gels, less protonation of free amino groups at high pH values (pH>6) increases the hydrophobicity along the chitosan chain. The decrease in the ionization and electrostatic repulsion effect at the basic environment causes shrinkage, and decrease in swelling equilibrium values by reducing the pore area through which the gel absorbs water [24]. Hamedi et al. reported that chitosan hydrogels have low swelling values because they do not cause protonation at neutral and
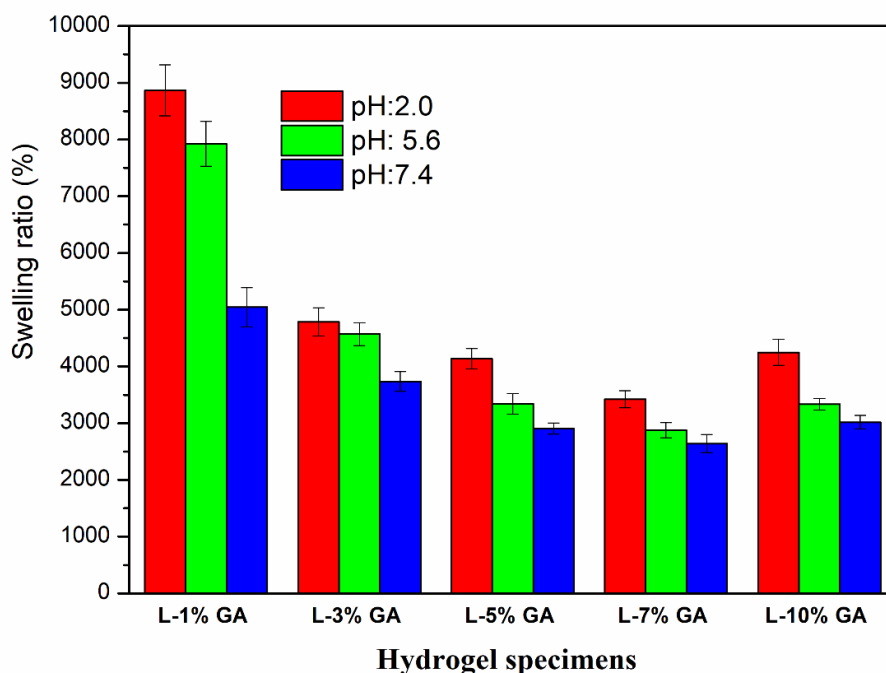
basic conditions [15].

Figure 2. Swelling percentages of low molecular weight chitosan (L-) hydrogels crosslinked with different amounts of glutaraldehyde (GA)
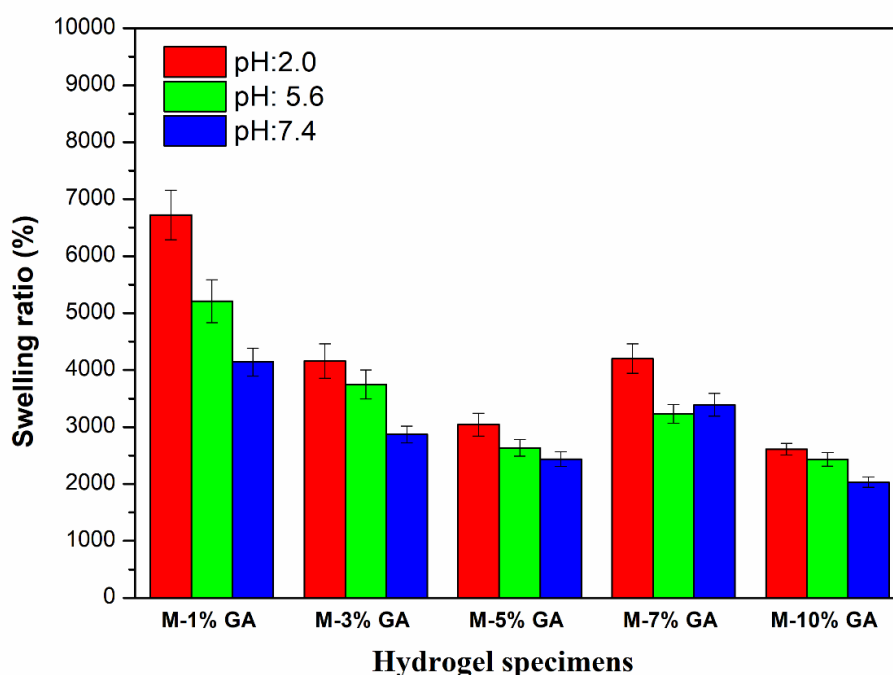
Figure 3. Swelling percentages of medium molecular weight chitosan (M-) hydrogels crosslinked with the different amounts of glutaraldehyde (GA).

On the other hand, it was observed that the swelling values decreased noticeably with the increasing molecular weight. Gupta et al. prepared microspheres with chitosan in three different molecular weights: low, medium and high, and examined their swelling properties. Chitosan chains with a greater molecular weight are longer and more entangled, which reduces swelling ability by increasing resistance to chain mobility and hydration when dispersed in water. They concluded that

111

the increase in molecular weight showed a lower swelling degree because it caused strong intermolecular interactions. The study reveals that higher molecular weight chitosan has reduced swelling due to increased interchain interactions and reduced chain mobility [6].

Table 2 demonstrates the highest water absorption capacity per gram of hydrogel at various concentrations of GA. At pH 2, one gram of hydrogel containing 1 wt.% of GA absorbs ~90 times of its weight in water, while one gram of hydrogel containing 10 wt.% of GA by weight exhibited a maximum water absorption corresponding to ~44 times of its weight.

Table 2. The maximum swelling ratio (g/g) of the hydrogels.

GA (%)	Absorbed water (g)/ g of hydrogel for low molecular weight chitosan.			Absorbed water (g)/ g of hydrogel for medium molecular weight chitosan.		
	pH:2.0	pH: 5.6	pH: 7.4	pH:2.0	pH: 5.6	pH: 7.4
1	89.7	80.3	59.3	68.2	53.1	41.4
3	48.9	46.7	37.0	42.6	38.5	29.1
5	42.3	34.4	29.5	31.4	27.3	24.9
7	35.2	29.8	26.1	43.0	33.3	33.8
10	43.5	34.3	29.6	27.1	25.3	19.8

Once cross-linked structures are immersed in an appropriate solvent, they expand as the solvent permeates their network. This scenario continues until the rate at which the solvent enters the network structure is the same as the pace at which it is released. The moment at which inflation reaches its highest value is known as the equilibrium point. Generating swelling curves of cross-linked polymers that demonstrate swelling behavior is highly significant for elucidating the kinetics of swelling and the diffusion mechanism of [11].

Swelling kinetics were investigated to better understand the swelling characteristics and diffusion mechanisms of hydrogels that reached the equilibrium at swelling point. The swelling curves of cross-linked polymers exhibiting swelling behavior is extremely important in explaining the swelling kinetics and the diffusion mechanism. The relationship between the diffusion exponent (n) and the diffusion mechanisms were shown in Table 3 [10].

Table 3. The relationship between diffusion exponent (n) and the diffusion mechanism.

Diffusion Exponential (n)	Diffusion Mechanism
$n \leq 0.5$	Fick Type Diffusion
$0.5 < n < 1$	Non-Fick Type Diffusion
$n \geq 1$	Super case II Diffusion

Graphs of the swelling behavior of L-Mw and M-Mw chitosan hydrogels containing different concentrations of GA in distilled water, pH 2.0 and 7.4 environments are presented in Figure 4.
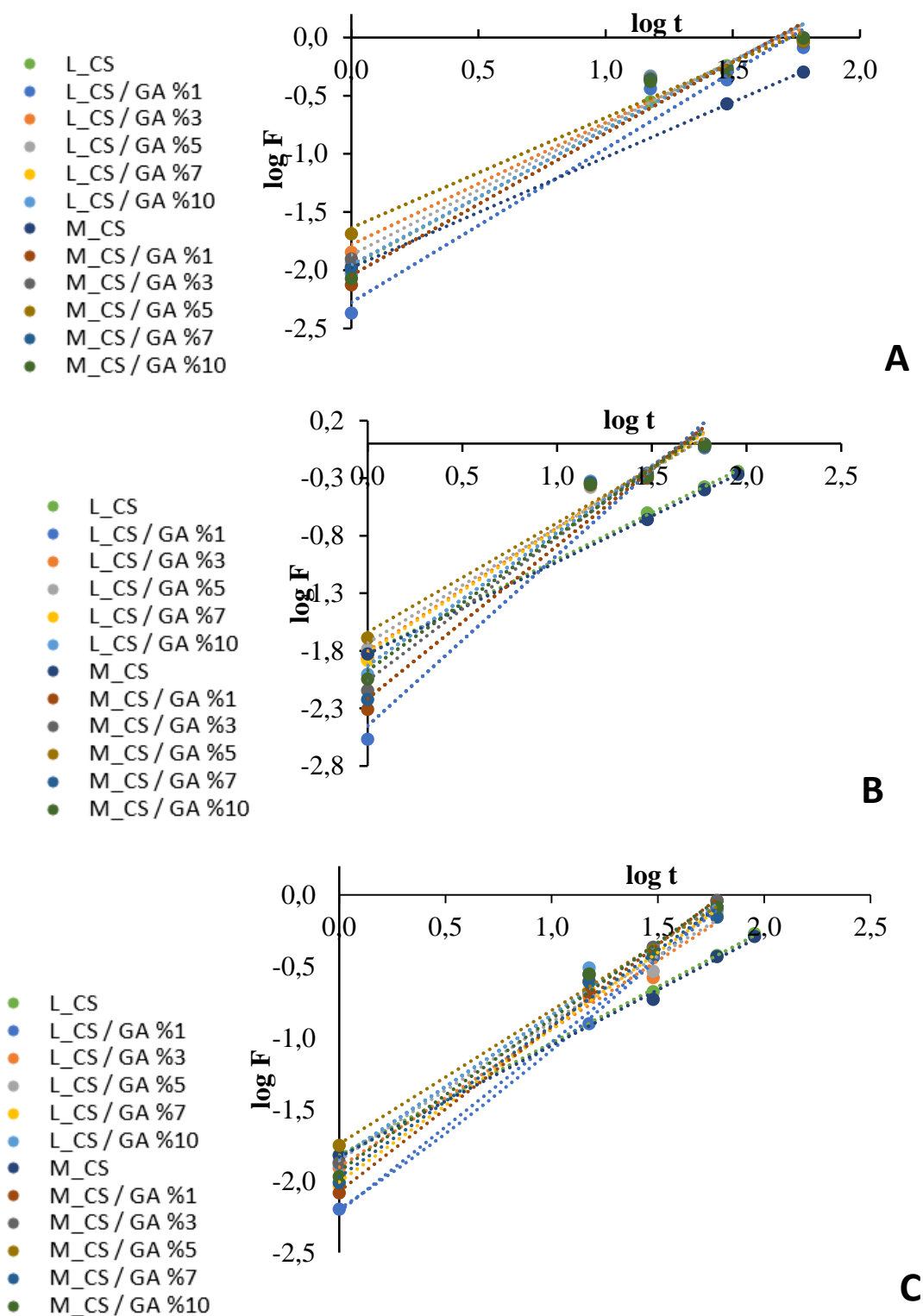
Figure 4. Swelling behavior of chitosan hydrogels cross-linked with GA in (A) Distilled water (B) pH 2.0 and (C) pH 7.4 according to Fick's Law

Because of the thermodynamic compatibility of the polymer chains and water, when a polymer network meets an aqueous medium, it begins to swell. The cross-linked webs' retraction force balances the swelling force, and when these two forces are equal, the swelling reaches the equilibrium. Since the polymer networks' thermodynamic behavior cannot be certainly predicted,

113

no theory can predict the diffusion mechanism, as well. Fickian diffusion analysis, on the other hand, allows making realistic evaluations [25]. Both the diffusion exponent (n) of chitosan hydrogels was determined at pH: 2.0, 5.6 and 7.4, respectively, and their diffusion mechanisms were examined. The 'n' values of pure chitosan hydrogels without GA were in the range of $0.5<n<1$ based on the data presented in Table 4 [18].

Table 4. Diffusion parameters of chitosan hydrogels (pH 2.0, pH: 5.6/distilled water and pH 7.4) cross-linked by GA

Specimens	n			k			R^2		
	pH: 2.0	pH: 5.6	pH: 7.4	pH 2.0	pH: 5.6	pH 7.4	pH 2.0	pH: 5.6	pH 7.4
L-CS	0.813	0.968	0.786	1.820	1.972	1.819	0.9997	0.9993	0.9997
L-CS/1% GA	1.481	1.321	1.186	2.450	2.277	2.214	0.9538	0.9652	0.9965
L-CS/3% GA	1.068	1.049	0.962	1.801	1.780	1.902	0.9705	0.9700	0.9915
L-CS/5% GA	1.001	1.116	0.949	1.731	1.869	1.852	0.9775	0.9694	0.9930
L-CS/7% GA	1.072	1.164	1.071	1.816	1.955	2.006	0.9697	0.9702	0.9956
L-CS/10% GA	1.155	1.164	1.001	1.928	1.953	1.842	0.9669	0.9657	0.9825
M-CS	0.799	0.949	0.779	1.829	1.978	1.831	0.9999	0.9999	0.9978
M-CS/1% GA	1.329	1.222	1.150	2.217	2.045	2.071	0.9631	0.9676	0.9993
M-CS/3% GA	1.240	1.071	1.032	2.059	1.837	1.852	0.9658	0.9698	0.9954
M-CS/5% GA	0.949	0.946	0.933	1.639	1.636	1.740	0.9773	0.9758	0.9985
M-CS/7% GA	1.276	1.149	1.057	2,130	1.928	1.971	0.9614	0.9734	0.9899
M-CS/10% GA	1.171	1.189	1.067	1.972	2.001	1.931	0.9687	0.9732	0.9900

This means that their swelling behavior is non-Fickian, in which the diffusion rate of the solvent into the gel is greater and faster than the polymer chains' relaxation rate. The swelling rate of gels of this type is determined by the rate of relaxation of polymer chains. Chitosan hydrogels cross-linked with GA appear to have $n \geq 1$ value in all three media with different pHs. This situation, called as superposition diffusion, means that both the diffusion, and the relaxation rate have the same effect on the swelling rate.

The high number of ionic groups at pH 2 has led to a higher diffusion rate compared to other different media. Among the cross-linked samples, M-CS/GA 5% exhibited non-Fickian type diffusion behavior, unlike its other counterparts. This condition is thought to be related to the sol content. Since NH_2 groups that participate in the cross-linking reaction have less interest in water than the other groups that do not participate in the reaction, as they affect the swelling in a decreasing direction.

An optical microscope was used to analyze both the images using 40× magnification lenses and morphologies of chitosan hydrogels that were produced at various molecular weights and GA concentrations under visible light.
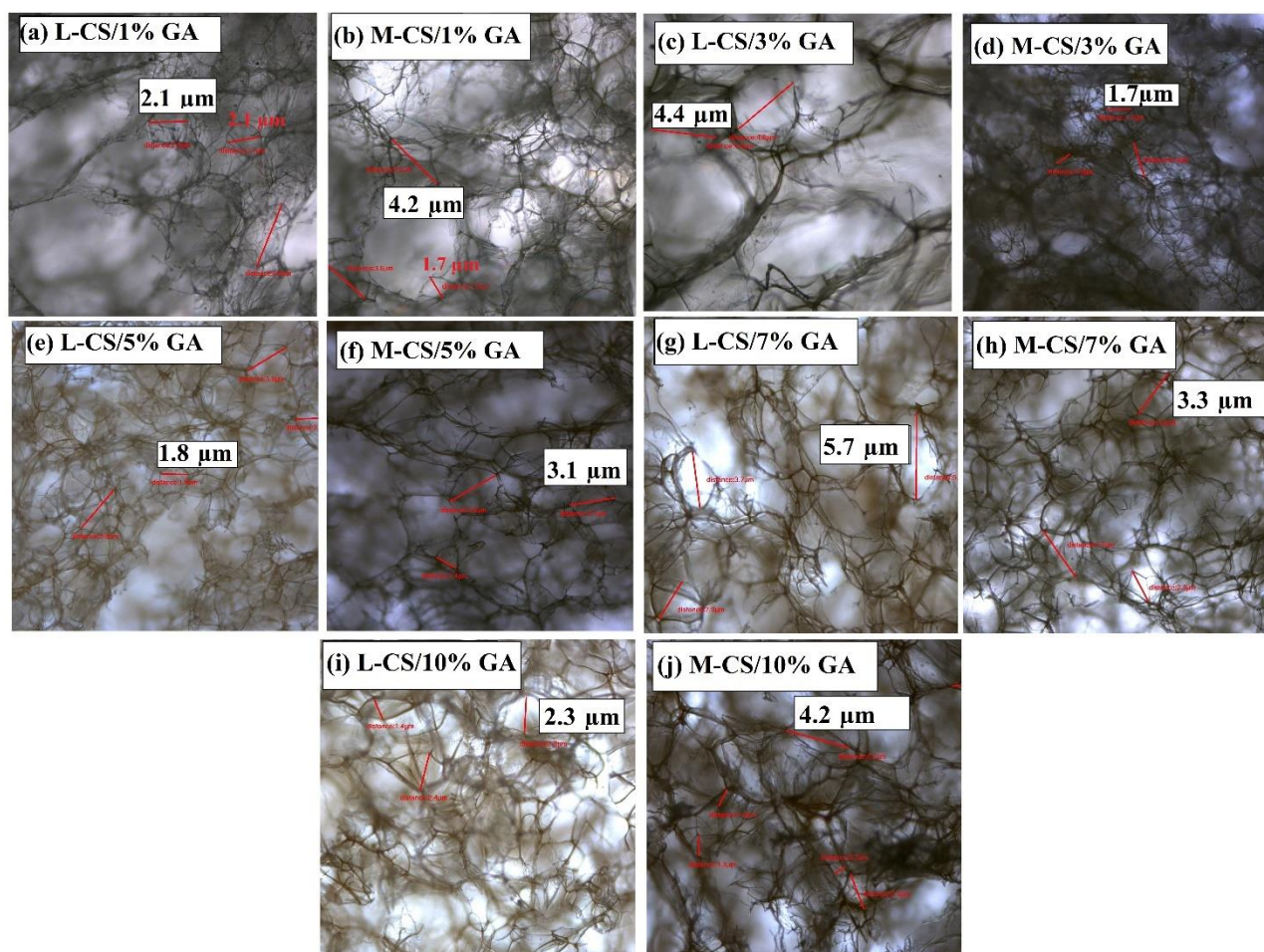
Figure 5. Optical microscope images of cross-linked chitosan hydrogels with GA at different ratios

Optical microscope images of the dry chitosan hydrogels cross-linked with 1-3-5-7-10% GA by weight is shown in Figure 5. It can be observed that hydrogels' pore sizes decrease as the cross-linking ratio in the hydrogel matrix increases. This situation directly affects such gels' swelling behavior. Mirzaei et al. analyzed the relationship between the pore sizes and swelling values by cross-linking chitosan hydrogels that were used as drug delivery systems with GA at different ratios. The experimental results revealed that pore diameters were decreased from 500 μm down to 100 μm upon increasing the GA ratio from 0.068% to 0.30%, and thus the equilibrium swelling values were observed to decrease from 1200% down to 600% [26] [26]. M-CS-3% and L-CS-7% hydrogel specimens seem to have larger pore sizes than expected, which is associated with the fact that the sol content of these gels is higher than the other ones. As a matter of fact, during the swelling trials, it was reported that the groups with high sol content exhibited high swelling values due to absorbing more water. Additionally, hydrogels prepared with medium molecular weight chitosan appear to be opaquer. It is thought that the increase in molecular weight causes the increase in entanglements, resulting in a decrease in light transmittance.

4. Conclusions

The swelling values exhibited significant decrease along with increasing in molecular weight. The hydrogel formulated with lower concentration of cross-linker demonstrated a greater extent of swelling in comparison to the hydrogel containing a higher proportion of cross-linker for both different molecular weight chitosans. The findings indicate that the level of cross-linking had a significant impact on the degree of swelling. 1% GA cross-linked chitosan-based hydrogels showed the highest swelling percentage. The swelling ratio (g/g) of low molecular weight chitosan hydrogels

115

crosslinked with 1% GA was measured as 89.7, 80.3 and 59.3 for pH: 2.0, 5.6 and 7.4, respectively. However, the lowest swelling percentages were observed in hydrogels prepared with 10% GA and medium molecular weight chitosan. Maximum swelling ratio (g/g) of medium molecular weight chitosan hydrogels crosslinked with 10% GA was determined as 27.1, 25.3 and 19.8 for pH: 2.0, 5.6 and 7.4, respectively.

As the molecular weight of chitosan increase from low to medium molecular weight, there is often a corresponding alteration in the size and chain structure of the molecule. The alterations have the potential to impact the physical characteristics of chitosan, thereby influencing its diffusion coefficient. As the molecular weight increased, the diffusion coefficient (k) of chitosan generally decreased. Because diffusion of larger molecules may be more difficult. The absorption and release of solvent by a gel is commonly explained by a straightforward process that is regulated by diffusion, which is known as Fick's law of diffusion. The diffusion coefficient generally showed an inverse relationship with molecular weight. The diffusion mechanism of porous low and medium molecular weight chitosans, which were synthesized without the addition of crosslinks, was identified as non-Fick Type. The diffusion mechanism of all hydrogels produced with GA, except for the M-CS/5% GA hydrogel, was determined as Super CASE II.

Based on the optical microscope images, this shows that the increased GA amount reduces the pore size in the gel structure and leads to reduced water-holding capacity. Generally, low molecular weight chitosan formed a more homogeneous structure, while medium molecular weight chitosan tended to form larger pores.

References

[1] E. M. Ahmed, "Hydrogel: Preparation, characterization, and applications: A review," *Journal of Advanced Research*, vol. 6, no. 2. 2015. doi: 10.1016/j.jare.2013.07.006.

[2] N. Sarhan, E. G. Arafa, N. Elgedawy, K. N. M. Elsayed, and F. Mohamed, "Urea intercalated encapsulated microalgae composite hydrogels for slow-release fertilizers," *Sci Rep*, vol. 14, no. 1, Dec. 2024, doi: 10.1038/s41598-024-58875-1.

[3] A. Martínez-Ruvalcaba, J. C. Sánchez-Díaz, F. Becerra, L. E. Cruz-Barba, and A. González-Álvarez, "Swelling characterization and drug delivery kinetics of polyacrylamide-co-itaconic acid/chitosan hydrogels," *Express Polym Lett*, vol. 3, no. 1, 2009, doi: 10.3144/expresspolymlett.2009.5.

[4] M. A. Gámiz-González *et al.*, "Determining the influence of N-acetylation on water sorption in chitosan films," *Carbohydr Polym*, vol. 133, 2015, doi: 10.1016/j.carbpol.2015.07.020.

116

[5]   A. Dilmi, T. Bartil, N. Yahia, and Z. Benneghmouche, "Hydrogels based on 2-hydroxyethylmethacrylate and chitosan: Preparation, swelling behavior, and drug delivery," *International Journal of Polymeric Materials and Polymeric Biomaterials*, vol. 63, no. 10, 2014, doi: 10.1080/00914037.2013.854221.

[6]   K. C. Gupta and F. H. Jabrail, "Glutaraldehyde cross-linked chitosan microspheres for controlled release of centchroman," *Carbohydr Res*, vol. 342, no. 15, 2007, doi: 10.1016/j.carres.2007.06.009.

[7]   M. A. Gámiz-González, D. M. Correia, S. Lanceros-Mendez, V. Sencadas, J. L. Gómez Ribelles, and A. Vidaurre, "Kinetic study of thermal degradation of chitosan as a function of deacetylation degree," *Carbohydr Polym*, vol. 167, pp. 52–58, 2017, doi: 10.1016/j.carbpol.2017.03.020.

[8]   H. S. Kaçoğlu, Ö. Ceylan, and M. Çelebi, "Comparative study of the effect of cross-linking degree on chitosan hydrogels synthesized with low and medium molecular weight chitosan," *Polym Eng Sci*, Mar. 2024, doi: 10.1002/pen.26619.

[9]   H. Y. Zhou, X. G. Chen, M. Kong, C. S. Liu, D. S. Cha, and J. F. Kennedy, "Effect of molecular weight and degree of chitosan deacetylation on the preparation and characteristics of chitosan thermosensitive hydrogel as a delivery system," *Carbohydr Polym*, vol. 73, no. 2, pp. 265–273, 2008, doi: 10.1016/j.carbpol.2007.11.026.

[10]   O. Akakuru and B. O. Isiuku, "Chitosan Hydrogels and their Glutaraldehyde-Crosslinked Counterparts as Potential Drug Release and Tissue Engineering Systems - Synthesis, Characterization, Swelling Kinetics and Mechanism," *J Phys Chem Biophys*, vol. 07, no. 03, 2017, doi: 10.4172/2161-0398.1000256.

[11]   J. Berger, M. Reist, J. M. Mayer, O. Felt, N. A. Peppas, and R. Gurny, "Structure and interactions in covalently and ionically crosslinked chitosan hydrogels for biomedical applications," *European Journal of Pharmaceutics and Biopharmaceutics*, vol. 57, no. 1, pp. 19–34, 2004, doi: 10.1016/S0939-6411(03)00161-9.

[12]   F. Croisier and C. Jérôme, "Chitosan-based biomaterials for tissue engineering," *European Polymer Journal*, vol. 49, no. 4. 2013. doi: 10.1016/j.eurpolymj.2012.12.009.

[13]   H. C. Yang and M. H. Hon, "The effect of the degree of deacetylation of chitosan nanoparticles and its characterization and encapsulation efficiency on drug delivery," *Polymer - Plastics Technology and Engineering*, vol. 49, no. 12, 2010, doi: 10.1080/03602559.2010.482076.

[14]   J. Fu, F. Yang, and Z. Guo, "The chitosan hydrogels: from structure to function," *New Journal of Chemistry*, vol. 42, no. 21, pp. 17162–17180, 2018, doi: 10.1039/C8NJ03482F.

[15]   H. Hamedi, S. Moradi, S. M. Hudson, and A. E. Tonelli, "Chitosan based hydrogels and their applications for drug delivery in wound dressings: A review," *Carbohydr Polym*, vol. 199, no. June, pp. 445–460, 2018, doi: 10.1016/j.carbpol.2018.06.114.

[16]   S. Nangia, D. N. Katyal, and S. G. Warkar, "Kinetics , absorption and diffusion mechanism of crosslinked Chitosan Kinetics , absorption and diffusion mechanism of crosslinked Chitosan Hydrogels," *Indian Journal of Engineering and Materials Sciences*, vol. 28, no. October, pp. 374–384, 2021.

[17]   "Merck Laboratuvar El Kitabı," 2007.

[18]   S. Jin, F. Bian, M. Liu, S. Chen, and H. Liu, "Swelling mechanism of porous P(VP-co-MAA)/PNIPAM semi-IPN hydrogels with various pote sizes prepared by a freeze treatment," *Polym Int*, vol. 58, no. 2, pp. 142–148, 2009, doi: 10.1002/pi.2504.

[19]   Y. Zhou *et al.*, "Photopolymerized water-soluble maleilated chitosan/methacrylated poly (vinyl alcohol) hydrogels as potential tissue engineering scaffolds," *Int J Biol Macromol*, vol. 106, pp. 227–233, 2018, doi: 10.1016/j.ijbiomac.2017.08.002.

[20] A. Jastram, T. Lindner, C. Luebbert, G. Sadowski, and U. Kragl, "Swelling and diffusion in polymerized ionic liquids-based hydrogels," *Polymers (Basel)*, vol. 13, no. 11, p. 1834, 2021, doi: 10.3390/polym13111834.

[21] K. Zielińska, W. Kujawski, and A. G. Chostenko, "Chitosan hydrogel membranes for pervaporative dehydration of alcohols," *Sep Purif Technol*, vol. 83, no. 1, pp. 114–120, 2011, doi: 10.1016/j.seppur.2011.09.023.

[22] R. Silva, G. Silva, O. Coutinho, J. Mano, and R. L. Reis, "Preparation and characterisation in simulated body conditions of glutaraldehyde crosslinked chitosan membranes," *J Mater Sci Mater Med*, vol. 15, no. 10, pp. 1105–1112, 2004, doi: 10.1023/B:JMSM.0000046392.44911.46.

[23] K. Wegrzynowska-Drzymalska *et al.*, "Crosslinking of chitosan with dialdehyde chitosan as a new approach for biomedical applications," *Materials*, vol. 13, no. 15, pp. 1–27, 2020, doi: 10.3390/ma13153413.

[24] S. J. Kim, S. U. Ryon Shin, N. G. Kim, and S. I. Kim, "Swelling behavior of semi-interpenetrating polymer network hydrogels based on chitosan and poly(acryl amide)," *Journal of Macromolecular Science - Pure and Applied Chemistry*, vol. 42 A, no. 8, pp. 1073–1083, 2005, doi: 10.1081/MA-200065934.

[25] T. Erşen Dudu and D. Alpaslan, "Eco-friendly and biodegradable dimethylacrylamide/starch hydrogels for controlled release of urea and its water retention," *MANAS Journal of Engineering*, vol. 10, no. 2, pp. 116–128, 2022, doi: 10.51354/mjen.1194756.

[26] E. Mirzaei B., A. Ramazani, M. Shafiee, and M. Danaei, "Studies on glutaraldehyde crosslinked chitosan hydrogel properties for drug delivery systems," *International Journal of Polymeric Materials and Polymeric Biomaterials*, vol. 62, no. 11, pp. 605–611, 2013, doi: 10.1080/00914037.2013.769165.

Extraction and Purification of Eriocitrin from *Mentha piperita*

[1]Duygu Mısırlı ⓘD, [2]Merve Soy ⓘD, *[1]**Zafer Ömer Özdemir** ⓘD, [1]Mahfuz Elmastaş ⓘD

[1] Health Sciences University, Hamidiye Faculty of Pharmacy, Hamidiye Pharmacy Program, Istanbul, Turkey.
[2] University of Health Sciences, Hamidiye Institute of Health Sciences, Pharmacognosy (PhD), Istanbul, Turkey.
* Corresponding author, e-mail: ozdemirz@gmail.com

Abstract - Currently, the practice of using plants for treatment is a multidisciplinary field referred to as "phytotherapy." The presence of secondary metabolites in plants is one of the main reasons for their utilization in the pharmaceutical sector. Research assessing the scientific use of plants utilized in Traditional and Complementary Medicine (GETAT) inside modern medicine would enhance the healthcare system by delivering highly efficient pharmacological molecules with minimal adverse effects, potentially stimulating the country's economy. In this article, the levels of 16 specific phenolic compounds in *Mentha piperita*, *Mentha dumoretum*, *Mentha spicata* and *Mentha villosa nervata* were investigated and the purification of eriocitrin from *Mentha piperita* was attempted. Eriocitrin is a secondary metabolite that has been shown to have various benefits for human health. The process of purifying bioflavonoid combinations containing eriocitrin from local natural sources is becoming increasingly important. The HPLC analysis revealed that the butanol extract of *Mentha piperita* contained the highest concentrations of eriocitrin. Therefore, the purification process was carried out utilizing these extracts obtained from *Mentha piperita*. This research has yielded eriocitrin with a purity of 92%.

Keywords: Extraction, Mentha species, Chromatography, Eriocitrin

Mentha piperita'dan Eriositrin'in Ekstraksiyonu ve Saflaştırılması

Öz - Günümüzde, bitkileri tedavi amaçlı kullanma uygulaması "fitoterapi" olarak adlandırılan çok disiplinli bir alandır. Bitkilerdeki sekonder metabolitlerin varlığı, bunların ilaç sektöründe kullanılmasının başlıca nedenlerinden biridir. Geleneksel ve Tamamlayıcı Tıpta (GETAT) kullanılan bitkilerin modern tıpta bilimsel kullanımını değerlendiren araştırmalar, en az yan etkiye sahip yüksek verimli farmakolojik moleküller sunarak sağlık sistemini geliştirecek ve potansiyel olarak ülke ekonomisini canlandıracaktır. Bu makalede *Mentha piperita*, *Mentha dumoretum*, *Mentha spicata* ve *Mentha villosa nervata*'daki 16 spesifik fenolik bileşiğin düzeyleri araştırılmıştır ve *Mentha piperita*'dan eriositrin saflaştırılmasına çalışılmıştır. Eriositrin insan sağlığı için çeşitli faydaları bulunduğu gösterilmiş bir sekonder metabolittir. Yerel doğal kaynaklardan eriositrin içeren biyoflavonoid kombinasyonlarının saflaştırılması süreci giderek daha önemli hale gelmektedir. HPLC analizi, *Mentha piperita*'nın butanol özütünün en yüksek eriositrin konsantrasyonlarını içerdiğini ortaya koymuştur. Bu nedenle, saflaştırma işlemi *Mentha piperita*'dan elde edilen bu özütler kullanılarak gerçekleştirilmiştir. Bu araştırma sonucunda %92 saflıkta eriositrin elde edilmiştir.

Anahtar kelimeler: Ekstraksiyon, Mentha türleri, Kromatografi, Eriositrin

1. Introduction

Nowadays, treatment with plants is an interdisciplinary science known as "phytotherapy". The Green Wave or Green Medicine, known as the movement of returning to nature in treatment, has become a growing interest worldwide (Yadav et al., 2024). One of the primary factors for the use of plants in the pharmaceutical industry is the secondary metabolites they contain. These metabolites are used not only as raw materials for the pharmaceutical industry but also in cosmetics, food additives, agricultural pesticides, and many other chemical sectors. The use of herbal additives in various industrial fields is quite common in Europe. To enhance the efficacy of organic compounds

---

[1] Corresponding author: ozdemirz@gmail.com

derived from natural sources and to develop modified new drugs, the isolation and characterization of secondary metabolites have gained importance, leading to significant research in this area in recent years. Although Türkiye has rich flora, it cannot utilize this wealth adequately due to the lack of scientific and technological applications. Consequently, Türkiye has not achieved its deserved place in the global market regarding herbal products. Studies evaluating the scientific usage of plants used in the field of Traditional and Complementary Medicine (GETAT) in modern medicine will contribute to the health system by introducing low-side-effect effective drug molecules and potentially boost the country's economy (Talhaoğlu, 2021; Uçar et al., 2020). It is known that flavonoid-structured secondary metabolites, which are widespread in plants, have been a particularly noteworthy group in recent years (Demirtas et al., 2013; Erenler et al., 2024).

There are 15 species of mint, including 6 hybrids, in the flora of Türkiye. Among these, the spearmint group (*M. spicata* and *M. villosa nervata*), rich in carvone, is used in spices, food, and cosmetics, while the peppermint group (*M. piperita*) is primarily used for pharmaceutical and essential oil production. The commercial value of naturally distributed Mentha species is limited. Among these species, the hybrid *M. dumetorum* is an interspecific hybrid of *M. aquatica* and *M. longifolia*. This species has been identified in the flora of Türkiye in recent years. Due to its limited distribution and less preferred aroma, studies on it are quite limited. Although it was not recorded in the flora of Türkiye researched by Davis, recent studies have identified it in the Black Sea region (Yesilada, 2005). In addition to its natural distribution in Türkiye, it has been noted that it is cultivated as an ornamental plant in Anatolia due to its more attractive appearance than other mint species. Cultural genotypes collected from various regions have been examined for yield and essential oil characteristics (Saka et al., 2024).
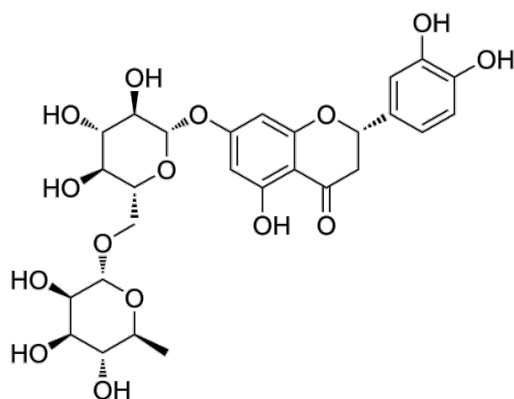

Figure 1. Structure of eriocitrin.

Studies on the phenolic compound content in mint species have identified numerous compounds. Rosmarinic acid, as with all species belonging to the Labiatae family, is an important phenolic acid in mint species. Additionally, eriocitrin is a highly valuable compound isolated in mint species (Akşit et al., 2014). Mint species have various uses beyond essential oils, including spices (*M. spicata*, *M. villoso nervata*) and herbal tea (*M. piperita*). Due to their antioxidant activities, plants have become important in functional food mixtures in preventive medicine in recent years. Among the phenolic acids in mint species, rosmarinic acid, caffeic acid, flavonoids such as eriocitrin, and luteolin are important antioxidants (Fatih et al., 2017; Teğin et al., 2022).

In the literature, articles related to citrus species are encountered in the purification of the eriocitrin compound. Citrus species are important due to the bioflavonoids they contain, which are used in the treatment of cancer, liver disorders, and many inflammation-related conditions. Scientific studies have shown that many plants with records of use in cardiovascular diseases, varicose veins, and hemorrhoid treatments contain flavonoid compounds. Numerous scientific studies have been conducted on the biological activities of flavonoids (Ángeles Ávila-Gálvez et al., 2021; Liu et al.,

2019). The health effects of these compounds vary depending on the amount consumed and their bioavailability (Ferreira et al., 2020).

Unlike citrus species, recent studies on the eriocitrin compound found in mint species report that it has no side effects but possesses anticancer, cholesterol-lowering, and antioxidant activities. Furthermore, it has been documented to counteract diet-induced hepatic steatosis, exhibit efficacy in the management of cardiovascular disorders, and be employed in the prevention of neurodegenerative conditions such as Alzheimer's and Parkinson's owing to its cholinesterase inhibitory properties (Ferreira et al., 2021; Guo et al., 2019; Kwon & Choi, 2020). Considering these studies, it is predicted that the eriocitrin compound will become a prospective raw material for the health, food, cosmetic, and pharmaceutical industries. Therefore, the production or purification of this compound will become an important issue in the future. Currently, it is observed that the research use of this compound is sold at high prices. The price of 1 mg of 98% pure eriocitrin for analytical purposes is €264 in chemical catalogs (Sigma Aldrich). Dietary supplements containing small amounts of eriocitrin, such as lemon bioflavonoid mixture capsules (containing 60 capsules), are sold online for prices ranging from €7-12. Hence, the purification of bioflavonoid mixtures containing eriocitrin from local natural sources is gaining importance.

The objective of this study is to extract compounds from four species of Mentha plants - *Mentha spicata*, *Mentha piperita*, *Mentha dumetorum*, and *Mentha villosa nervata* - using different solvents. The goal is to identify the species with the highest concentration of eriocitrin and subsequently purify the eriocitrin compound.

2. Experimental

The mint samples were acquired from Prof. İsa TELCİ, who is affiliated with the Faculty of Agriculture at Isparta University of Applied Sciences.

The procedures were carried out separately for each plant. 20 g of *M. dumetorum*, *M. villosa nervata*, *M. spicata*, and *M. piperita* plants were weighed. 600 mL of pure water was added to each, and after boiling for 30 minutes, the mixture was filtered. Another 600 mL of water was added to the remaining plants, and the process was repeated twice. Liquid-liquid extraction was initiated with each of the obtained water extracts. Additionally, the previously applied process was repeated, and this time the water extracts were subjected to lyophilization. HPLC analyses were performed after lyophilization.

The initial water extracts were subjected to liquid-liquid extraction first with ethyl acetate and then with butanol. The liquid-liquid extractions were performed in two repetitions. The first ethyl acetate liquid-liquid extraction was carried out at a ratio of 1:5 (water:ethyl acetate), and the second at a ratio of 1:2 (water:ethyl acetate). The solvents of the ethyl acetate extracts were removed using a Rotary Evaporator under low pressure. The last part, obtained after extracting with these two solvents, is referred to as the "Remaining Water Extract" and generally has a lower concentration of chemicals.

For quantitative analysis, a Shimadzu Nexera-i LC-2040C 3D Plus HPLC device was used. A DAD detector (scanned at 254 nm) was used for detection, and separation was performed using a Phenylhexyl 4.6 x 150 mm, 3 μm (UP) (GL Sciences Inter Sustain Made in Japan) C6 reverse phase column. The mobile phases were 0.1% formic acid/deionized water (Solvent A) and acetonitrile (Solvent B) (Merck, HPLC grade), following the pump program in Table 1. The flow rate of the mobile phase was set to 1 mL/min throughout the analysis. Samples and standards were injected into the device at 10 μL. The column temperature was set to 30 °C.

OPEN JOURNAL OF
NANO

Table 1. HPLC pump program.

Steps	Flow rate (mL/min)	Time (min.)	% Solvent B (acetonitrile)	% Solvent A (% 0,1 formic acid/deionize water)
Step 1	1.00	0,01	5	95
Step 2	1.00	7	9,5	90,5
Step 3	1.00	20	17	83
Step 4	1.00	35	40	60
Step 5	1.00	40	0	100
Step 6	1.00	40,01	Stop	

Using the method described in Table 1, 16 phenolic compounds were analyzed. The wavelength at which each phenolic compound exhibited maximum absorbance was determined, and all were scanned at their respective maximum wavelengths.

Since there was no detection of Vanilic acid and Salicylic acid in the mint species examined, these acids are not given in the Table 2.

3. Results and Discussions

Following the extraction procedure outlined in the experimental section. The results of the analysis of 16 phenolic compounds are presented in Table 2.

Table 2. HPLC Analysis Results of Lyophilized Water Extracts, Ethyl Acetate Extracts, Butanol Extracts, and Remaining Water Extracts (Values are given as means ± standard deviation)

			Mentha dumetorum mg/g	*Mentha villosa nervata* mg/g	*Mentha spicata* mg/g	*Mentha piperita* mg/g
1	**Gallic Acid**	Lyophilized water extract	1.79±0.417	0.677±0.027	0.82±0.036	0.43±0.018
		Ethyl acetate	0.581±0.011	0.177±0.006	0.152±0.007	0.202±0.001
		Butanol	1.187±0.005	0.622±0.022	0.507±0.020	0.226±0.005
		Remaining Water Extract	1.43±0.217	0.569±0.021	0.675±0.037	0.472±0.012
2	**4-Hydroxyibenzoic Acid**	Lyophilized water extract	0.025±0.000	0	0	0
		Ethyl acetate	0	0	0.097±0.001	0
		Butanol	0	0	0	0
		Remaining Water Extract	0	0	0.135±0.018	0
3	**Chlorogenic Acid**	Lyophilized water extract	1.545±0.411	2.039±0.813	2.307±0.915	1.774±0.107
		Ethyl acetate	12.335±1.717	24.037±1.717	22.898±1.917	17.317±1.007
		Butanol	0	1.789±0.403	1.504±0.210	0.425±0.033
		Remaining Water Extract	0	0	0,163	0
4	**Caffeic Acid**	Lyophilized water extract	0.032±0.000	0.167±0.003	0.419±0.045	0.031±0.000
		Ethyl acetate	0	0	0	0
		Butanol	0	0.717±0.025	0.509±0.097	0.209±0.012

122

		Remaining Water Extract	0	0	0	0
4	Epicatechin	Lyophilized water extract	0	0.548±0.032	0	0
		Ethyl acetate	0	0.539±0.065	0.379±0.067	0.919±0.081
		Butanol	0	0	0	0
		Remaining Water Extract	0	0	0	0
6	p-Coumaric Acid	Lyophilized water extract	0	0.244±0.013	0.033±0.000	0.041±0.000
		Ethyl acetate	0.028±0.000	0	0	0
		Butanol	0	0.258±0.005	0	0
		Remaining Water Extract	0	0	0	0
7	Ferulic Acid	Lyophilized water extract	0	0.061±0.000	0.178±0.010	0
		Ethyl acetate	0	0	0	0
		Butanol	0	0.226±0.023	0.072±0.000	0.018±0.000
		Remaining Water Extract	0	0	0	0
8	Eriocitrin	Lyophilized water extract	**132.599**±13.497	0.239	4.323±0.437	**198.936**±11.616
		Ethyl acetate	**285.342**±15.623	0	9.769±0.967	**336.036**±16.417
		Butanol	**369.717**±17.417	0	7.587±0.987	**389.486**±19.417
		Remaining Water Extract	0	0	0	**6.204**±0.697
9	Rutin	Lyophilized water extract	12.519±1.417	3.949±0.918	3.219±0.618	8.526±0.717
		Ethyl acetate	34.417±6.915	1.838±0.317	3.96±0.417	14.779±3.567
		Butanol	51.857±7.419	3.319±0.818	14.021±5.234	27.632±8.498
		Remaining Water Extract	0	0	0.317±0.007	3.791±0.187
10	Rosmarinic Acid	Lyophilized water extract	43.078±0.417	93.892±8.643	112.465±9.413	41.45±0.989
		Ethyl acetate	406.523±20.619	907.247±43.717	713.634±37.417	346.336±19.369
		Butanol	36.302±7.455	179.327±8.634	200.115±9.917	31.002±3.428
		Remaining Water Extract	0.6±0.007	3.804±0.098	6.448±0.537	1.413±0.088
11	Apigenin-7-glucoside	Lyophilized water extract	0.953±0.063	1.562±0.319	1.096±0.413	0.462±0.068
		Ethyl acetate	3.053±0.735	1.141±0.228	1.878±0.419	0.506±0.098
		Butanol	3.567±0.652	2.054±0.605	1.776±0.619	0.646±0.058

123

		Remaining Water Extract	0	0.718±0.081	0.543±0.023	0.194±0.022
12	**Cinnamic Acid**	Lyophilized water extract	0.06±0.000	0	0	0
		Ethyl acetate	0	0	13.967	0
		Butanol	0	0.369±0.074	0.029±0.000	0
		Remaining Water Extract	0	0.029±0.002	0.071±0.001	0.121±0.010
13	**Quercetin**	Lyophilized water extract	0.179±0.029	0.164±0.005	0.669±0.079	0.47±0.028
		Ethyl acetate	3.476±0.088	2.091±0.098	3.968±0.187	3.731±0.117
		Butanol	0	0.428±0.087	0.359±0.058	0.183±0.056
		Remaining Water Extract	0.153±0.013	0.192±0.023	0.757±0.037	0.588±0.026
14	**Naringenin**	Lyophilized water extract	0.398±0.035	0.176±0.018	1.785±0.185	0.067±0.003
		Ethyl acetate	5.327±0.095	0.388±0.078	8.811±0.789	2.368±0.058
		Butanol	0	0.016±0.001	0.791±0.019	0
		Remaining Water Extract	0	0.118±0.091	1.566±0.213	0

The table shows that in lyophilized water extracts, the highest concentration of phenolic compounds was found in *Mentha piperita* (198.936±11.616 mg/g extract) and *Mentha dumetorum* (132.599±13.497 mg/g extract) with eriocitrin. Additionally, rosmarinic acid levels were also high compared to other phenolic compounds and among the other species, with the highest concentrations found in *Mentha villosa nervata* (93.892±0.417 mg/g extract) and *Mentha spicata* (112.465±9.413 mg/g extract).

The table also indicates that in ethyl acetate extracts, the highest concentration of phenolic compounds was rosmarinic acid in *M. villosa nervata* (907.247±43.717 mg/g extract) and *M. spicata* (713.634±37.417 mg/g extract). High levels of rosmarinic acid were also observed in other species (*M. dumetorum*: (406.523±20.619 mg/g extract), *M. piperita*: (346.336±19.369 mg/g extract). In *M. villosa nervata* and *M. spicata*, aside from rosmarinic acid, the highest phenolic compound was chlorogenic acid (24.037±1.717 mg/g extract) and (22.898±1.917 mg/g extract, respectively). Following rosmarinic acid, eriocitrin was found to be the highest phenolic compound in *M. dumetorum* (285.342±15.623 mg/g extract) and *M. piperita* (336.036±16.417 mg/g extract). In these two plant species, rutin was also found to be high (*M. dumetorum*: (34.417±6.915 mg/g extract), *M. piperita*: (14.779±3.567 mg/g extract).

In butanol extracts, the highest concentration of phenolic compounds was also eriocitrin, found in *M. dumetorum* (369.717±17.417 mg/g extract) and *M. piperita* (389.486±19.417 mg/g extract). Additionally, besides eriocitrin, rutin was also found to be high in these two species *M. dumetorum*: (51.857±7.419 mg/g extract), *M. piperita*: (27.632±8.498 mg/g extract). Rosmarinic acid levels were higher in *M. villosa nervata* (179.327±8.634 mg/g extract) and *M. spicata* (200.115±9.917 mg/g extract).

The findings reported here are in agreement with the results that were acquired from the previous research.

In their study, Kapp et al. examined the qualitative and quantitative polyphenolic contents in the infusions of 27 commercial peppermint (*M. piperita* L.) tea samples sourced from 10 different countries using HPLC–UV-MS/MS analysis (Kapp et al., 2013).

124

In another study conducted by Athanasiadis et al., deep eutectic solvents (DES) composed of glycerol-choline chloride (GL-ChCl), 60% aqueous ethanol (AqEt), and water were used as extraction solvents. Peppermint (*M. piperita* L.) samples, dried and packaged in plastic, air-tight containers, were obtained from local stores in Greece and analyzed using HPLC. The analytical polyphenolic composition of the extracts produced with GL-ChCl, AqEt, and water revealed that eriocitrin was the predominant compound in all extracts. The yields of eriocitrin were 36.60 ± 1.99 mg g^{-1} dm, 35.42 ± 2.22 mg g^{-1} dm, and 23.65 ± 1.88 mg g^{-1} dm, respectively (Athanasiadis et al., 2023).

It was observed that, consistent with findings from previous studies, eriocitrin emerged as the predominant polyphenolic compound (Areias et al., 2001; Athanasiadis et al., 2023; Atoui et al., 2005; Dorman et al., 2003; Duband et al., 1992; Fecka & Turek, 2007; Guédon & Pasquier, 1994; Kapp et al., 2013; Sroka et al., 2005).

Consequently, this investigation found that the greatest concentration of the phenolic component in the remaining water extracts was eriocitrin in *Mentha piperita* (6.204 mg/g extract), consistent with the findings in the literature. Rosmarinic acid concentrations were determined to be elevated in *Mentha spicata* (6.448 mg/g extract).

The butanol extract of *Mentha piperita* was found to have the highest concentrations of eriocitrin, as shown by the results of the HPLC analysis. Following this, the process of purification was carried out with the use of these extracts that were generated from *Mentha piperita*.

3.1. Purification Process

The butanol extract was first processed in a rotary and then in a lyophilized (HyperCOOL, Korea) to become powder.

The powdered extract of *M. piperita* was dissolved in water at a concentration of 1 mg/mL in a volume of 9 mL and loaded onto a 40 cm long chromatographic column with a 2 cm internal diameter, packed with Sephadex LH-20 (General Electric (GE) Healthcare (Cytiva)). The purification process was conducted at a flow rate of 0.1 mL/min. The eluent was collected in 20 mL fractions in test tubes at the column exit, and the water from these tubes was subsequently removed by lyophilization. Analytical HPLC was performed on a C6 reverse-phase column, resulting in the isolation of eriocitrin in pure form in fractions 36 and 37. The HPLC chromatogram indicated that the eriocitrin achieved 92% purity.

A sample solution of 1000 ppm concentration was prepared from the powdered extract and analyzed by HPLC (Shimadzu Nexera-i LC-2040C 3D Plus) on a C6 reverse-phase column Phenylhexyl 3 μm, 4.6 mm x 150 mm (GL Sciences InterSustain, Japan). The analysis was performed with a DAD detector, scanning at 280 nm.
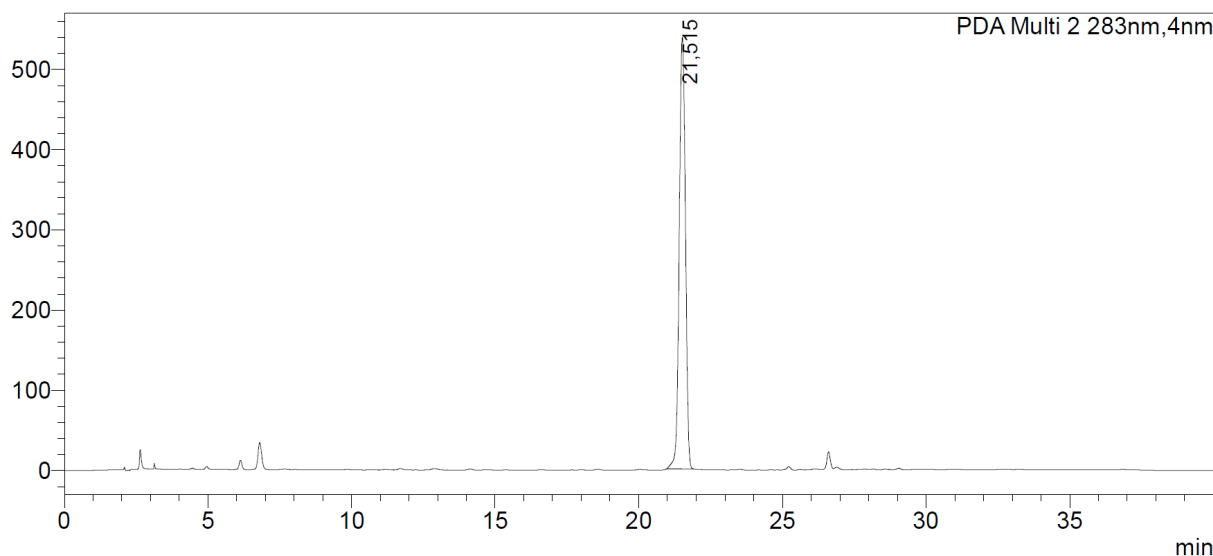

Figure 2. The HPLC chromatogram of eriocitrin obtained from tube 36.

4. Conclusions

In this study, industrial scale grinding tests were carried out for the fabrication of nano calcite. The normal capacity of the mill used in the tests is 20 tph. However, it was not possible to produce nano-sized calcite with this capacity. Therefore, the capacity of the mill has been reduced. In other words, the amount of calcite feed is reduced. This increases the contact time between the calcite and the balls. When the residence time of Calcite in the mill was increased by 4 times, the fineness (d_{90}) of the products obtained fell below 4 microns. When the mill capacity was 20, 10 and 5 tph, respectively, the fineness of the products was 60, 20, and 3.8 microns, respectively. These results were obtained in case of grinding with conventional balls. In case of using Cylpebs instead of conventional balls, the product fineness was 30, 10 and 1.3 microns, respectively. According to these results; the fineness of the products is inversely proportional to the mill capacity. As the mill capacity is reduced, finer products are obtained. This is due to increased grinding time and material-to-ball contact.

As a result, mill capacity is an important operating parameter in the fabrication of nano-sized calcite. It is not possible to fabricate nano-sized material with a conventional ball mill operated with normal capacity (20 tph). If the capacity is reduced by 75%, it is possible to produce nano-sized material. Furthermore, cylpebs should be used instead of conventional balls in this grinding process. Cylpebs gives finer products than conventional spherical balls.

References

Akşit, H., Çelik, S. M., Şen, Ö., Erenler, R., Demirtaş, I., Telci, I., & Elmastaş, M. (2014). Complete isolation and characterization of polar portion of Mentha dumetorum water extract. *Records of Natural Products*, *8*(3).

Ángeles Ávila-Gálvez, M., Antonio Giménez-Bastida, J., González-Sarrías, A., & Espín, J. C. (2021). New Insights into the Metabolism of the Flavanones Eriocitrin and Hesperidin: A Comparative Human Pharmacokinetic Study. *Antioxidants*, *10*(3).

Areias, F. M., Valentão, P., Andrade, P. B., Ferreres, F., & Seabra, R. M. (2001). Phenolic fingerprint of peppermint leaves. *Food Chemistry*, *73*(3). https://doi.org/10.1016/S0308-8146(00)00302-2

Athanasiadis, V., Palaiogiannis, D., Grigorakis, S., Bozinou, E., Lalas, S. I., & Makris, D. P. (2023). Food-grade deep eutectic solvent extraction of antioxidant polyphenols from peppermint (Mentha × piperita L.): Screening, optimization and metabolite profile. *Journal of Applied Research on Medicinal and Aromatic Plants*, *33*. https://doi.org/10.1016/j.jarmap.2022.100456

Atoui, A. K., Mansouri, A., Boskou, G., & Kefalas, P. (2005). Tea and herbal infusions: Their antioxidant activity and phenolic profile. *Food Chemistry*, *89*(1). https://doi.org/10.1016/j.foodchem.2004.01.075

Demirtas, I., Erenler, R., Elmastas, M., & Goktasoglu, A. (2013). Studies on the antioxidant potential of flavones of Allium vineale isolated from its water-soluble fraction. *Food Chemistry*, *136*(1), 34–40. https://doi.org/10.1016/j.foodchem.2012.07.086

Dorman, H. J. D., Koşar, M., Kahlos, K., Holm, Y., & Hiltunen, R. (2003). Antioxidant properties and composition of aqueous extracts from Mentha species, hybrids, varieties, and cultivars. *Journal of Agricultural and Food Chemistry*, *51*(16). https://doi.org/10.1021/jf034108k

Duband, F., Carnat, A. P., Carnat, A., Petitjean-Freytet, C., Clair, G., & Lamaison, J. L. (1992). COMPOSITION AROMATIQUE ET POLYPHENOLIQUE DE L'INFUSE DE MENTHE, MENTHA X PIPERITA L. *Annales Pharmaceutiques Francaises*, *50*(3).

Erenler, R., Yıldız, İ., Geçer, E. N., Yıldırım Kocaman, A., Alma, M. H., Demirtas, İ., Başar, Y., Hosaflıoğlu, İ., & Behçet, L. (2024). Phytochemical analyses of Ebenus haussknechtii flowers: Quantification of phenolics, antioxidants effect, and molecular docking studies. *Bütünleyici ve Anadolu Tıbbı Dergisi*, *5*(2), 1–9. https://doi.org/10.53445/batd.1479874

Fatih, B., Madani, K., Chibane, M., & Duez, P. (2017). Chemical Composition and Biological Activities of Mentha Species. In *Aromatic and Medicinal Plants - Back to Nature*. InTech. https://doi.org/10.5772/67291

Fecka, I., & Turek, S. (2007). Determination of water-soluble polyphenolic compounds in commercial herbal teas from Lamiaceae: Peppermint, melissa, and sage. *Journal of Agricultural and Food Chemistry*, *55*(26), 10908–10917. https://doi.org/10.1021/jf072284d

Ferreira, P. S., Manthey, J. A., Nery, M. S., & Cesar, T. B. (2021). Pharmacokinetics and Biodistribution of Eriocitrin in Rats. *Journal of Agricultural and Food Chemistry*, *69*(6).

Ferreira, P. S., Manthey, J. A., Nery, M. S., Spolidorio, L. C., & Cesar, T. B. (2020). Low doses of eriocitrin attenuate metabolic impairment of glucose and lipids in ongoing obesogenic diet in mice. *Journal of Nutritional Science*. https://doi.org/10.1017/jns.2020.52

Guédon, D. J., & Pasquier, B. P. (1994). Analysis and Distribution of Flavonoid Glycosides and Rosmarinic Acid in 40 Mentha X piperita Clones. *Journal of Agricultural and Food Chemistry*, *42*(3). https://doi.org/10.1021/jf00039a015

Guo, G., Shi, W., Shi, F., Gong, W., Li, F., Zhou, G., & She, J. (2019). Anti-inflammatory effects of eriocitrin against the dextran sulfate sodium–induced experimental colitis in murine model. *Journal of Biochemical and Molecular Toxicology*, *33*(11).

Kapp, K., Hakala, E., Orav, A., Pohjala, L., Vuorela, P., Püssa, T., Vuorela, H., & Raal, A. (2013). Commercial peppermint (Mentha×piperita L.) teas: Antichlamydial effect and polyphenolic composition. *Food Research International*, *53*(2), 758–766. https://doi.org/10.1016/j.foodres.2013.02.015

Kwon, E. Y., & Choi, M. S. (2020). Eriocitrin Improves Adiposity and Related Metabolic Disorders in High-Fat Diet-Induced Obese Mice. *Journal of Medicinal Food*, *23*(2).

Liu, J., Huang, H., Huang, Z., Ma, Y., Zhang, L., He, Y., Li, D., Liu, W., Goodin, S., Zhang, K., & Zheng, X. (2019). Eriocitrin in combination with resveratrol ameliorates LPS-induced inflammation in RAW264.7 cells and relieves TPA-induced mouse ear edema. *Journal of Functional Foods*, *56*, 321–332. https://doi.org/10.1016/j.jff.2019.03.008

Saka, A. K., Uğur, A., & Açıkgöz, M. A. (2024). Assessment of Agronomic Traits and Essential Oil Yield in Various Local Mint (Mentha piperita L.) Genotypes. *Akademik Ziraat Dergisi*, *13*(1), 1–12. https://doi.org/10.29278/azd.1465733

127

Sroka, Z., Fecka, I., & Cisowski, W. (2005). Antiradical and Anti-H2O2 Properties of Polyphenolic Compounds from an Aqueous Peppermint Extract. *Zeitschrift Fur Naturforschung - Section C Journal of Biosciences*, *60*(11–12). https://doi.org/10.1515/znc-2005-11-1203

Talhaoğlu, D. (2021). Geleneksel ve Tamamlayıcı Tedavi Uygulamaları. *Bütünleyici ve Anadolu Tıbbı Dergisi*, *3*(1), 16–29. https://doi.org/10.53445/batd.945893

Teğin, İ., Hallaç, B., Özden, H., & Fidan, M. (2022). Determination of Metal Content and Biological Activities of Radish Plant Consumed as Turnip by Public in Siirt Region. *Open Journal of Nano*, *7*(1), 26–30. https://doi.org/10.56171/ojn.1035703

Uçar, D., Tayfun, K., Müslümanoğlu, A. Y., & Kalaycı, M. Z. (2020). Koronavirüs ve Fitoterapi. *Bütünleyici Ve Anadolu Tıbbı Dergisi*, *1*(2), 49–57.

Yadav, S., Pandey, A., & Mali, S. N. (2024). From lab to nature: Recent advancements in the journey of gastroprotective agents from medicinal chemistry to phytotherapy. In *European Journal of Medicinal Chemistry* (Vol. 272). Elsevier Masson s.r.l. https://doi.org/10.1016/j.ejmech.2024.116436

Yesilada, E. (2005). Past and future contributions to traditional medicine in the health care system of the Middle-East. In *Journal of Ethnopharmacology* (Vol. 100, Issues 1–2, pp. 135–137). Elsevier Ireland Ltd. https://doi.org/10.1016/j.jep.2005.06.003

Investigation of the Effects of Electrospinning Parameters on the Diameter of PMMA Fibers

*[1] İbrahim GELEN (ID), [1] Harun GÜL (ID)

[1] Sakarya Uygulamalı Bilimler Üniversitesi, Metalurji ve Malzeme Mühendisliği Bölümü, Sakarya, Türkiye.
* Sorumlu yazar, e-mail: ibrahimgelenn@gmail.com

Abstract - In this study, fibers were produced by electrospinning method using Polymethyl Methacrylate (PMMA) polymer. In this research, the effects of different parameters on the thickness of the fibers were investigated and the morphology of the obtained fibers were examined. The effects of solution concentration, applied voltage, collector rotation speed and flow rate on the diameter and shape of nanofibers were investigated. As a result of the tests, it was seen that the fibers with the smallest diameter could be obtained as a result of the experiments performed using the parameters of flow rate 4 mL h^{-1}, applied voltage 14 kV, DMF (Dimetilformamid) ratio in the solution 15%, collector rotation speed 80 rpm. More homogeneous fibers were obtained with 15% solvent ratio. Fiber diameters ranging from 1,278 μm to 2,840 μm were obtained. While bead-like and filamentous structures were observed in nanofibers, the thinnest fiber diameter was measured as 1.278 μm.

Keywords: Nanofiber, Electrospinning, PMMA, DMF

Elektroeğirme Parametrelerinin PMMA Fiberlerinin Çapı Üzerine Etkilerinin Araştırılması

Öz - Bu çalışmada, Polimetil Metakrilat (PMMA) polimeri kullanılarak, elektroeğirme (Elektrospinning) yöntemiyle fiberler üretilmiştir. Farklı parametreler çalışılarak yapılan bu araştırmada fiberlerin kalınlıklarına bu parametrelerin etkileri araştırılmış ve elde edilen fiberlerin morfolojileri incelenmiştir. Çözelti konsantrasyonu, uygulanan voltajın, kolektör dönme hızı ve akış hızının nanofiberlerin çapı ve şekli üzerindeki etkileri araştırılmıştır. Yapılan testlerin sonucunda akış hızı 4 mL h^{-1}, uygulanan voltaj 14 kV, çözeltideki DMF (Dimetilformamid) oranı %15, kolektör dönüş hızı 80 rpm parametreleri kullanılarak yapılan deneyler sonucunda en küçük çapa sahip fiberlerin elde edilebildiği görülmüştür. % 15 çözücü oranı ile daha homojen fiberler elde edilmiştir. 1,278 μm - 2,840 μm arasında değişen fiber çapları söz konusu olmuştur. Nanofiberlerde boncuksu ve ipliksi yapılar görülürken en ince fiber çapı 1,278 μm olarak ölçülmüştür.

Anahtar kelimeler: Nanofiber, Elektroeğirme, PMMA, DMF

1. Giriş

Elektroeğirme, yüksek yüzey alanı-hacim oranı, ayarlanabilir gözeneklilik ve çeşitli malzemeleri birleştirme yeteneği gibi benzersiz özelliklere sahip nanofiberler üretmek için çok yönlü ve etkili bir teknik olarak ortaya çıkmıştır. Bu yöntem, bir polimer çözeltisine veya eriyiğine yüksek voltaj uygulanmasını ve topraklanmış bir alt tabaka üzerinde toplanan liflerin oluşturulmasını içerir. Basitliği ve uyarlanabilirliği nedeniyle elektroeğirme, filtrasyon, biyomedikal mühendisliği, enerji depolama ve sensör teknolojisi gibi çeşitli alanlarda uygulama alanı bulmuştur. Elektroeğirme kullanılan birçok polimer arasında polimetil metakrilat (PMMA) olağanüstü optik şeffaflığı, kimyasal direnci ve mekanik mukavemeti ile öne çıkmaktadır. Bu özellikler PMMA'yı optik cihazlar,

---

[1] Corresponding author: Tel: 0 505 254 40 89
E-mail: ibrahimgelenn@gmail.com

129

membranlar ve doku mühendisliği için iskelelerdeki uygulamalar için cazip bir malzeme haline getirmektedir [1, 2].

Elektroeğirme yoluyla üretilen PMMA lifleri, polimer konsantrasyonu, çözücü seçimi ve uygulanan voltaj gibi işleme parametrelerini ayarlayarak uyarlanabilen bir dizi morfoloji ve özellik sergiler. Özellikle çözücü seçimi, çözeltinin viskozitesini, iletkenliğini ve yüzey gerilimini etkilediği için lif kalitesinin belirlenmesinde kritik bir rol oynar. Ayrıca, elektroeğirme işlemi PMMA fiberlerine fonksiyonel katkı maddelerinin dahil edilmesine olanak tanıyarak gelişmiş işlevlere sahip kompozit malzemelerin geliştirilmesini sağlar [3,4].

PMMA fiberlerinin çok yönlülüğü, çeşitli yüksek performanslı uygulamalarda kullanılmalarına yol açmıştır. Biyomedikal alanda, elektrospun PMMA iskeleleri, biyouyumlulukları ve ayarlanabilir mekanik özellikleri nedeniyle hücre büyümesi ve doku rejenerasyonu için kullanılmaktadır. Çevresel uygulamalarda, PMMA nanofiberleri ince partikülleri ve kirleticileri hava ve sudan uzaklaştırabilen etkili filtrasyon membranları olarak hizmet vermektedir. Ayrıca, optik netlikleri ve termal kararlılıkları PMMA fiberlerini ışık kılavuzları ve ekranlar gibi fotonik ve optoelektronik cihazlarda kullanım için uygun hale getirir. Elektroeğirmenin uyarlanabilirliği, gelişmiş işlevlere sahip PMMA bazlı kompozit fiberlerin oluşturulmasını da kolaylaştırarak ileri teknolojilerdeki uygulama potansiyellerini daha da genişletmektedir [4,5].

Polimer nanofiberler, kalıp senteziyle, çekme, faz ayırma ve elektroeğirme gibi farklı yöntemlerle üretilebilmektedir. Elektroeğirme, elektrohidrodinamik temelli polimerik çözümlerden mikro ölçekten nano ölçeğe kadar malzemeler üretmek için kullanılır. Malzeme değişiklikleri, geleneksel ve yeni uygulamalar için laboratuvardan endüstriyel ölçeğe kadar çeşitli malzeme mimarileri üreten fiziksel ve kimyasal proseslerle elde edilir. Nanomalzemeleri ekonomik olarak daha az maliyette ve en basit şekilde üretmek için elektrospinning, avantajlarından dolayı daha çok tercih edilen bir yöntemdir. Bu işlemin temel prensibi; bir polimer çözeltisine veya eriyiğine yüksek voltajlı bir yük uygulayarak ve bu yükü kullanarak çözeltiyi bir iğne ucundan topraklanmış bir toplayıcıya çekerek süper ince nanofiberler üreten bir işlemdir. Bu işlem sistemi temel olarak polimer çözeltisini tutmak için bir şırıngadan, iki elektrottan ve polimerin yüzey gerilim kuvvetlerini aşmak için yeterli olan kV aralığında bir DC voltaj kaynağından oluşur. Yüklü polimerin serbest yüzeyi, topraklanmış toplayıcıya doğru çekilen çok ince sıvı jetleri üretir. Bu etki, topraklanmış toplayıcıya yaklaştıkça hızla katılaşan liflerin önemli ölçüde çekilmesine neden olur. Lif, topraklanmış toplayıcının yüzeyinde bir lif ağı olarak toplanır [6-8].

Polimerlerden PMMA'nın özellikle biyomedikal, sensör, optik, polimer, polimer elektrotlar, moleküler ayrılma, vizkozite uygulamaları dikkat çekmektedir. İnsan vücudu ile uyumlu olmasından dolayı biyomedikal alanında, kimyasal kararlılık ve yüksek yüzey alanı ve dolayısıyla gözenekli yapıya sahip olduğundan filtrasyon işlemlerinde ve su arıtımında, amorf yapısı ve termal kararlılık nitelikleriyle elektronik ve enerji uygulamalarında elektrolit membranların rijitliğini arttırmada ve yüksek moleküler ağırlığından dolayı vizkozite arttırmada kullanılır [9]. Ayrıca karbon nanotüp (CNT) işlevselli PMMA, biyosensörlerde kullanılmakta olup, tercih edilmesine; yüksek iletkenlik, daha büyük ve aktif yüzeyle beraber gelişmiş elektron transfer kinetiği etmen olmuştur [10]. Camara ve arkadaşları, fotokatalitik uygulamalar için onbir adet farklı polimeri inceleyerek araştırmalar yapmıştır. Bu araştırmada TiO$_2$ kaplamalı ve kaplamasız bir şekilde güneş radyasyonuna maruz bırakılmış olup, PMMA'nın optik ve mekanik özellikleri desteklediği ve hatta koruduğu, UV direncinden ötürü ve fotokatalitik destek malzemesi olarak uygunluğu ile ön plana çıkmıştır. Sararma yapmaması ve ışık geçirgenliğini koruması nedeniyle güneş panellerinin ömrünü uzatacağı ön görülmektedir [11]. Ayrıca, PMMA, akrilat ailesine ait amorf polimerlerden olup, 100 °C ila 130 °C camsı geçiş sıcaklığı aralığınadır. Bu polimer 130 °C'de erir, %0,3 su emiciliği, %0,3 ila %0,33 dengede nem emilimi vardır. Oda sıcaklığında 1,20 g cm^{-3} yoğunluğuna sahip berraktır ve renksiz bir polimerdir [12-14].

Bu çalışma, elektroeğirme yoluyla PMMA fiber üretiminin kapsamlı bir şekilde anlaşılmasını sağlamayı, kritik parametreleri vurgulamayı ve ileri malzeme bilimindeki potansiyel uygulamaları keşfetmeyi amaçlamaktadır. Ayrıca bu çalışma ile PMMA polimerinden fiber üretiminde elektroeğirme parametrelerinden üç farklı akış hızı, iki farklı kolektör hızı, üç farklı uygulanan voltaj ve iki farklı çözücü oranının (DMF) etkileri araştırılmış ve en küçük fiber çapının hangi etkiler sonucu elde edilebildiği ortaya konmuştur.

2. Materyal ve Yöntem

Çalışmada ilk aşamada PMMA ve DMF kullanılarak elektroeğirme de kullanılacak çözelti hazırlanmıştır. Bu çözeltilerin hazırlanmasında kullanılan bileşenler ve oranları tablo 1'de detaylı olarak verilmiştir. Söz konusu oranlar kullanılarak hazırlanan karışım manyetik karıştırıcıda 800 rpm karıştırma hızı ile 6 saat süre boyunca karıştırılarak homeojen bir çözelti elde edilmesi sağlanmıştır.

Tablo 1. PMMA için elektroeğirme parametreleri.

	Numune 1	Numune 2	Numune 3	Numune 4	Numune 5
Akış Hızı (mL h^{-1})	4	4	8	9	4
Uygulanan Voltaj (kV)	12	14	14	20	14
Kolektör hızı (Rpm)	100	80	80	100	80
Çözelti DMF oranı	%15	%15	%15	%12	%12

Ardından hazırlanan çözeltiler tablo 1'de verilen eğirme parametreleriyle elektroeğirme (elektrospinning) işlemine tabi tutulmuştur. Bu işlemden sonra ise 24 saat 60 °C sıcaklığında etüv fırınında kurutma işlemine tabi tutulmuştur. Nihai olarak elde edilen numuneler taramalı elektron mikroskobu ile (SEM, Scanning Electron Microscope) ile gözlemlenmiştir. Yapılan bu işlemler şematik olarak Şekil 1'de gösterilmiştir. Elektrospinning parametrelerinin fiber kalınlıları üzerine etkileri incelenmiş olup kıyaslamalar yapılmıştır.

Çözelti Hazırlama   Elektrospinning İşlemi   PMMA Fiberleri
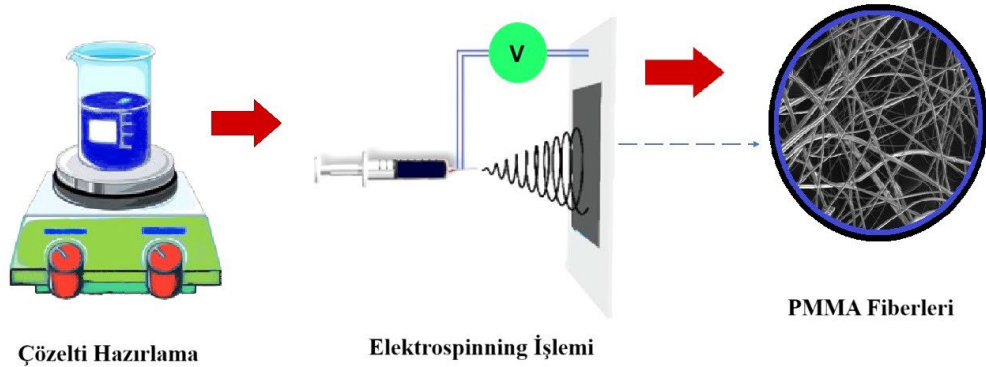
Şekil 1. PMMA fiberlerinin elektrospinning işlemi ile üretim sürecinin şematik gösterimi

3. Bulgular ve Tartışma

Tablo 1'de verilen parametreler ve çalışma koşulları ile üretilen PMMA fiberlere ait bilgiler tablo 2'de verilmiştir. Fiberlerin boyutları ve çap bilgileri incelendiğinde kolektör dönüş hızının fiber boyutları üzerinde etkili bir parametre olduğu görülmüştür. Ayrıca benzer şekilde çözücü oranı ve akış hızınında fiber çapları üzerinde değişimlere sebep olan parametreler oldukları anlaşılmıştır. Kullanım alanlarında ki farklılıklara bağlı olarak, çapın küçülmesiyle birlikte yüzey/hacim oranı arttığından biyomedikal alanında özellikle hücre yapışması ve ilaç salımı gibi proseslere avantaj sağlarken, ince lifler daha kırılgan olacağından mekanik dayanım düşmektedir. Ayrıca ince lifler ağın yapısındaki gözenekliliği de arttıracağından sıvı ve gaz difüzyonunu artırır. Kalın fiberler ise mekanik dayanımı arttırırken biyomedikal uygulamalarda hücre tutunmasını zorlaştırır. Bununla birlikte, termal iletkenliği veya elektriksel iletkenliği arttırarak avantajlı hale geldiği durumlarda olabilir [15]. Tüm bu koşullar kullanım alanına bağlı olarak avantaj ve dezavantaj olarak faklılık gösterebilir. Bazı

131

sektörlerde düşük çap avantaj sağlarken bazı sektörlerde yüksek çap kalınlıkları avantaj sağlayabilmektedir.

Tablo 2. Elektroeğirme sonucu elde edilen fiber boyutları ve parametre ilişkisi.

	Numune 1	Numune 2	Numune 3	Numune 4	Numune 5
Akış Hızı (mL h⁻¹)	4	4	8	9	4
Uygulanan Voltaj (kV)	12	14	14	20	14
Kolektör hızı (Rpm)	100	80	80	100	80
Çözelti DMF oranı	%15	%15	%15	%12	%12
Fiber Kalınlığı (µm)	1,278	1,673	2,840	2,190	2,645

Farklı kolektör hızlarında, farklı çözücü oranın kullanımı durumunda ve farklı uygulanan voltaj değerlerinde yapılan deneylerde elde edilen fiber kalınlıkları gösterilmiştir.

Yapılan çalışmada numune 1'de fiber çapı 1,278 µm numune 2'de 1,673 µm ve numune 3'te ise 2,840 µm olduğu gözlemlenmiştir. 2 ve 3 numaralı numuneler eldesinin sağlandığı parametreler aynı olmakla beraber sadece akış hızı farklı olduğundan akış hızının düşmesiyle fiber çapının da inceldiği/düştüğü gözlemlenmiştir. Bu veriler Numune 1'in parametreleri ile kıyaslandığında ise kolektör dönüş hızının 100 rpm iken numune 2 ve 3'de 80 rpm, uygulanan voltaj numune 1'de 12 kV iken numune 2 ve 3'de 14 kV'dır. Voltajın artması ve bununla beraber kolektör hızının düşmesi fiber çapını arttırmıştır.

Şekil 2'de Numune 3 ve Numune 5'te görülen boncuksu yapılar çözücünün hızlı buharlaşmasından kaynaklandığı düşünülmektedir. Ayrıca çözelti yoğunluğu arttığında polimer çözeltisinin vizkozitesi artmaktadır, böylelikle liflerin çekilmesi zorlaşır ve yavaş akışla jet kararlılığı düşer ve halkasal yapılar oluşabilir. Fazla halkasal yapının oluşması biyouyumluluğu arttırırken liflerin yapısal olarak dayanımını azaltabilir. Çözelti yoğunluğu halkasal yapıların üzerinde etkilidir. Bu nedenden ötürü elektrospinning parametrelerinin optimum seviyelerde ayarlanması gerekmektedir. Yoğunluğun optimum seviyelerde olmasıyla lifler homojen ve düzgün olurlarken, yoğunluğun düşük veya yüksek olmasıyla halkasal yapılar artabilir [15-18].
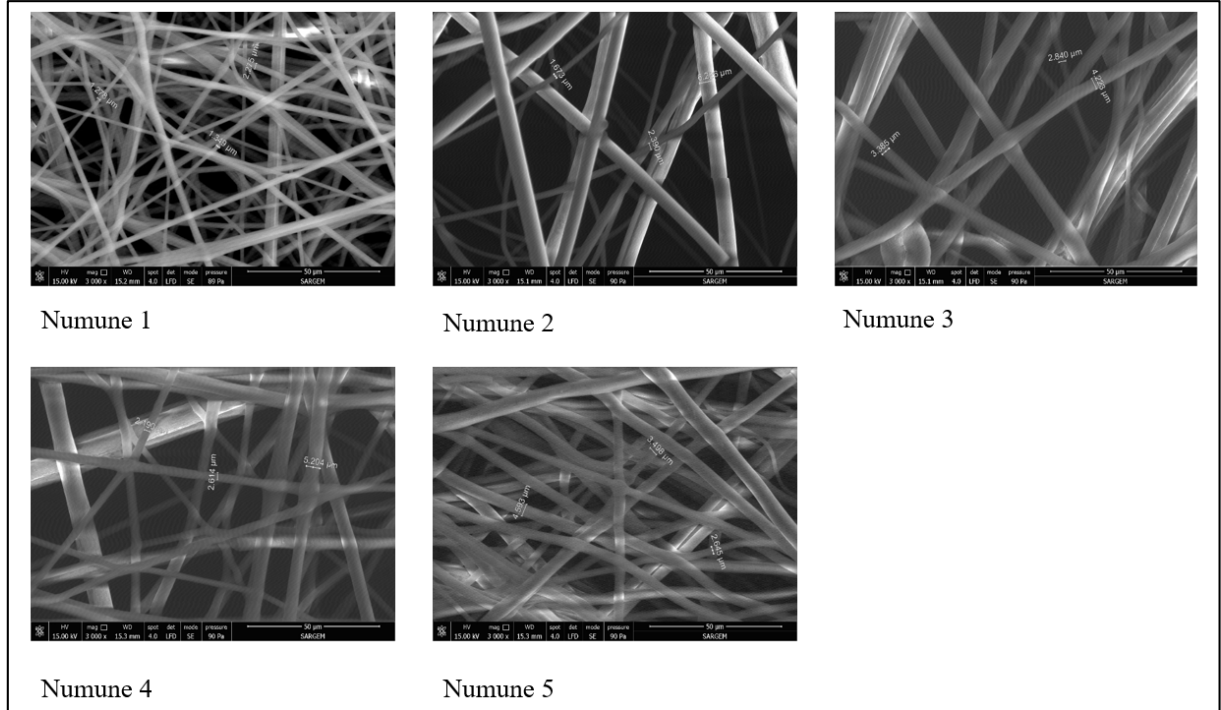
Şekil 2. PMMA numunelerine ait SEM görüntüsü.

4. Sonuçlar ve Öneriler

PMMA lifleri, ortam sıcaklığında DMF çözelti haline getirilerek elektroeğirme ile başarılı bir şekilde üretilmiştir. Elde edilen sonuçlar aşağıda maddeler halinde verilmiştir.

- Çözücü oranı, uygulanan voltaj, kolektör dönüş hızı, akış hızı parametrelerinin etkileri araştırılmış ve değerlendirilmiştir.
- %15 çözücü konsantrasyonuyla PMMA/DMF sisteminden düzgün lifler elde edilmiştir. Elde edilen yapılar SEM cihazı ile incelenmiş olup boncuksu ve ipliksi yapılar da saptanmıştır.
- Liflerin çaplarının farklı parametlerin etkisine bağlı olarak 1,278 µm - 2,840 µm arasında değişmekte olduğu görülmüştür.

Bu çalışmanın bir sonraki aşamasında PMMA'nın diğer parametrelerinin optimizasyonu sağlanabilir ve ayrıca üretilen fiberlerin biyomedikal, filtrasyon vb uygulamalarına uygunluğu test edilebilir.

Kaynakça

[1] Huang, Z.-M., Zhang, Y.-Z., Kotaki, M., & Ramakrishna, S. (2003). Elektrospinning ile polimer nanofiberler ve nanokompozitlerde uygulamaları üzerine bir inceleme. Composites Science and Technology, 63(15), 2223-2253.

[2] Rao, S. S., Srinivas, G., & Mahesh, K. (2012). PMMA ve karışımları: Bir inceleme. International Journal of Research in Chemistry and Environment, 2(1), 89-102.

[3] Reneker, D. H., & Chun, I. (1996). Elektrospinning ile üretilen nanometre çapında polimer lifler. Nanotechnology, 7(3), 216-223.

[4] Bhardwaj, N., & Kundu, S. C. (2010). Elektrospinning: Büyüleyici bir elyaf üretim tekniği. Biotechnology Advances, 28(3), 325-347.

[5] Agarwal, S., Greiner, A., & Wendorff, J. H. (2009). Polimerlerin elektrospinasyonu ile fonksiyonel malzemeler. Progress in Polymer Science, 34(8), 982-1025.

[6] Koysuren, O., & Koysuren, H. N. (2016). Characterization of poly(methyl methacrylate) nanofiber mats by electrospinning process. Journal of Macromolecular Science, Part A, 53(11), 691–698. https://doi.org/10.1080/10601325.2016.1224627

[7] Ji, D., Lin, Y., Guo, X. et al. Electrospinning of nanofibres. Nat Rev Methods Primers 4, 1 (2024).

[8] A. Gül, "Obtaining Activated Carbon Doped PA66 Nanofibers by Electrospinning Method and Fiber/Diameter Analysis," Journal of Green Technology and Environment , vol.2, no.2, pp.46-48, 2024

[9] Ali, U., Karim, K. J. B. A., & Buang, N. A. (2015). A Review of the Properties and Applications of Poly (Methyl Methacrylate) (PMMA). Polymer Reviews, 55(4), 678–705.

[10] Dai H, Xu G, Zhang S, Gong L, Li X, Yang C, et al. Carbon nanotubes functionalized electrospun nanofibers formed 3D electrode enables highly strong ECL of peroxydisulfate and its application in immunoassay. Biosens Bioelectron 2014;61:575–8.

[11] Camara, R.M.; Portela, R.; Gutierrez-Martin, F.; Sanchez B. "Evaluation of several

commercial polymers as support for TiO2 in photocatalytic applications", Global NEST Journal 2014, 6(3), 525–535.

[12] Charles, A.H.; Edward, M.P. Plastics Materials and Processes, in Concise Encyclopedia; Wiley: NJ, 2003, pp. 42–44.

[13] Van Krevelen, D.W.; Nijenhuis, K. T. Properties of Polymers; Elsevier: Amsterdam, 2000, pp. 106, 322.

[14] Charles, A.H. Handbook of Plastics Processes; Wiley: NJ, 2006, pp. 1–7.

[15] Zaszczyńska, A.; Kołbuk, D.; Gradys, A.; Sajkiewicz, P. Development of Poly(methyl methacrylate)/nano-hydroxyapatite (PMMA/nHA) Nanofibers for Tissue Engineering Regeneration Using an Electrospinning Technique. Polymers 2024, 16, 531.

[16] Aydogdu RB, Cetin MS, Karahan Toprakci HA, Toprakci O (2024) Investigation of electrospinning parameters and fiber collection methods on morphology of thermoplastic polyester elastomer fibers. Int J Nanomater Nanotechnol Nanomed 10(1): 035-044. DOI: 10.17352/2455-3492.000060

[17] Çetin, M. Ş., Demirel, A. S., Toprakcı, O., Toprakcı, H. A. K. (2022). The synergic effects of electrospinning solution properties on formation of polyvinyl chloride (pvc) fibers. Tekstil ve Mühendis , 29(126), 42 - 49. doi.org/10.7216/1300759920222912601

[18] İnan, A. T., & Şeker, M. M. (2021). Elektrospinning Yöntemiyle Üretilmiş Farklı Çaplardaki Yapay Damarların Mekanik Özelliklerinin İncelenmesi. International Journal of Advances in Engineering and Pure Sciences, 33(4), 687-693. https://doi.org/10.7240/jeps.993582

OPEN JOURNAL OF
NANO

Graphene, GO, and Borophene: Innovations in QCM-Based Humidity Sensors for Enhanced Sensitivity

[1] Zeynep Demirtaş (ID), [1] Mervenur Kirazoğlu (ID), [*1,2] **Birgül Benli** (ID)

[1] Istanbul Technical University, Nanoscience and Nanoengineering Program, Istanbul, Turkiye.
[2] Istanbul Technical University, Department of Mineral Processing Engineering, Istanbul, Turkiye.
* Corresponding author, e-mail: benli@itu.edu.tr

Abstract - Humidity measurements are crucial in daily life as they influence human comfort, health, safety, and product quality. Quartz Crystal Microbalance (QCM) sensors, known for their fast response times and high sensitivity, offer a significant advantage in humidity sensing due to their ability to provide highly linear and accurate measurements. These sensors are particularly valuable because they enable real-time, precise humidity detection with minimal calibration, making them ideal for various applications. This mini-review highlights the significance of QCM sensors, focusing on the sensing layers made from nanomaterial fillers integrated into composite matrices. Typical QCM sensor surfaces are could be coated with highly conductive materials such as graphene, graphene oxide (GO), and borophene, which offer excellent humidity-sensing capabilities due to their two-dimensional allotrope structure and unique properties of carbon and boron. This review begins with a brief overview of humidity measurement principles and QCM sensor characteristics. It then explores a variety of materials used for preparing QCM sensing layers, discussing their advantages and disadvantages for humidity sensor applications. Finally, the review presents future perspectives on the development of layer-by-layer self-assembled conductive polymeric films, novel GO-based composite QCM humidity sensors, and borophene-based humidity sensors, illustrating their potential for multifunctional composites.

Keywords: Quartz Crystal Microbalance (QCM), Quick-response, Highly sensitive, Graphene oxide (GO)-based humidity sensors, borophene-based humidity sensing platforms.

Grafen, GO ve Borofen: QCM Tabanlı Nem Sensörlerinde Artırılmış Hassasiyet için Yaklaşımlar

Öz - Ortam neminin belirlenmesi, insan konforu, sağlığı, güvenliği ve ürün kalitesini doğrudan etkilediği için günlük yaşamda büyük bir öneme sahiptir. Hızlı yanıt süreleri ve yüksek hassasiyetleri ile bilinen Quartz Kristal Mikroteraziler (QCM), nem algılama konusunda yüksek doğrulukla doğrusal ölçümler sağlayabilme yetenekleri sayesinde önemli bir avantaj sunar. Bu sensörler, gerçek zamanlı, hassas nem tespiti yapabilmeleri ve minimum kalibrasyon gerektirmeleri nedeniyle özellikle değerlidir, bu da onları çeşitli uygulamalar için ideal kılar. Bu mini derleme, QCM sensörlerinin önemini vurgulamakta olup, kompozit matrislere entegre edilmiş katkı malzemelerinden karbon ve bor bazlı nanomalzemelerden hazırlanan algılama katmanlarına odaklanmaktadır. Derlemede, grafen, grafen oksit (GO) ve borofen tabanlı malzemelere ağırlık verilecektir. Bu malzemeler, karbon ve borun benzersiz özellikleri ve iki boyutlu allotrop yapıları sayesinde mükemmel nem algılama yetenekleri sunar. Bu derleme, nem ölçüm ilkeleri ve QCM sensör özellikleri hakkında kısa bir genel bakışla başlamakta, ardından QCM algılama katmanlarını hazırlamak için kullanılan çeşitli malzemeleri incelemekte ve bu malzemelerin nem sensörü uygulamalarındaki avantajlarını ve dezavantajlarını tartışmaktadır. Son olarak, derleme, katmanlar arası kendiliğinden montaj edilen iletken polimerik filmler, yenilikçi GO tabanlı kompozit QCM nem sensörleri ve borofen tabanlı nem sensörlerinin geliştirilmesine yönelik gelecekteki perspektifleri sunarak, bunların çok fonksiyonlu kompozitler için potansiyelini ortaya koymaktadır.

Anahtar kelimeler: Quartz Kristal Mikrodengeleme (QCM), Hızlı Yanıtlı, Yüksek Hassasiyetli, Grafen Oksit (GO) Tabanlı Nem Sensörleri, Borofen Tabanlı Nem Algılama Platformları.

---

[1] Corresponding author: E-mail: benli@itu.edu.tr

135

GRAPHICAL ABSTRACT
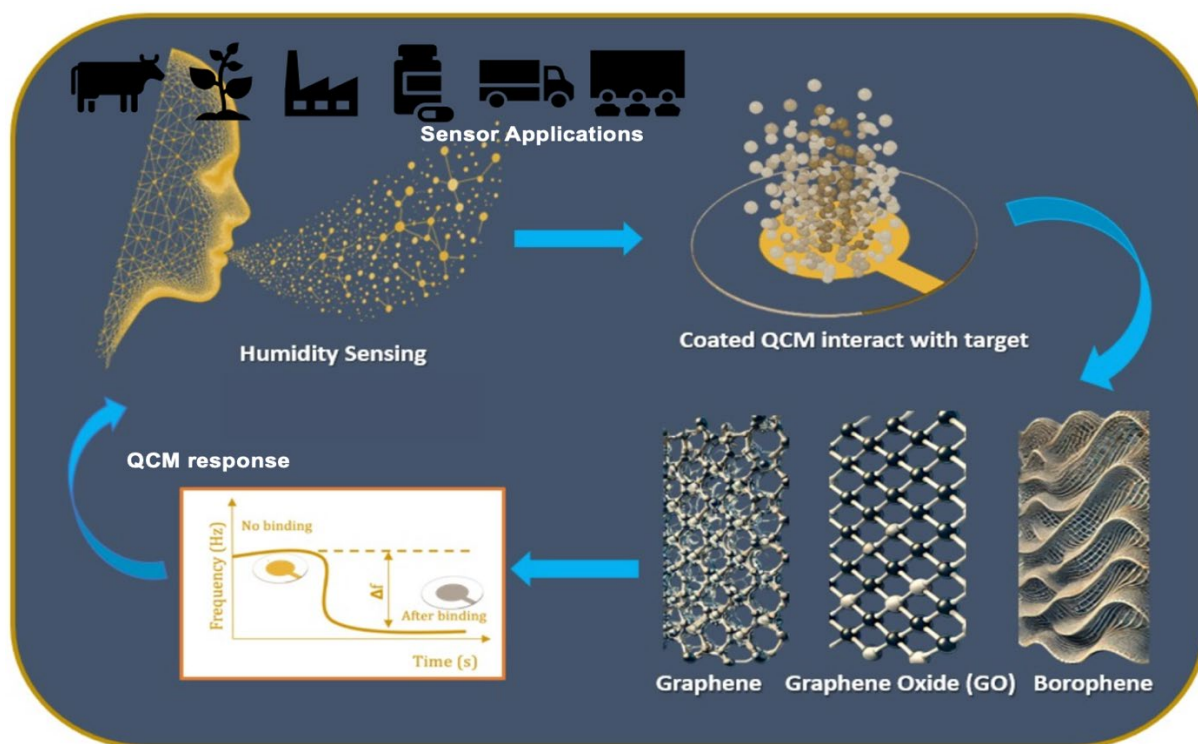
1. Introduction

Humidity and its control is crucial in many areas of our daily lives [1, 2], and therefore, humidity measurement has attracted significant attention since the 1900s [3]. Humidity measurement plays a vital role in various industries, such as weather forecasting [4], food safety [5,6], human comfort [7, 8], agricultural process control [9], and mining (for gas leakage monitoring) [10], among others. As a result, there has been an increasing demand for the development of rapid, cost-effective, and highly sensitive humidity sensors. Although a variety of methods have been developed, the quartz crystal microbalance (QCM) stands out as a leading candidate due to its outstanding advantages. QCM sensors offer excellent sensitivity to mass changes at the nanogram level, a wide measurement range, stability, and reliability under mild operational conditions. Additionally, they are compact and can be developed at a low cost [11]. These features make QCM sensors particularly attractive compared to other traditional methods, which may struggle with sensitivity or operational stability in certain conditions.

The schematic representation of QCM is shown in Figure 1. A quartz disk is positioned between two gold electrodes, and when a voltage is applied, oscillation at a specific frequency occurs. This oscillation results in a shift in the resonance frequency [12]. The mass change on the QCM surface is directly related to this shift in frequency, which can be accurately quantified using the Sauerbrey equation [13]. The resonance frequency shift (Δf) is typically measured over time, as the mass change on the quartz surface occurs due to the adsorption or desorption of materials.

$$\Delta f = -2.26x10^{-6}f_0^2 \frac{\Delta m}{A} \tag{1}$$

Here, the equation specifies that the mass change is represented by Δm (in grams), and the resonance frequency shift by Δf (in MHz). The original frequency of the quartz crystal is f_0 (in MHz), and A (in cm²) is the surface area of the quartz electrode. Importantly, the shift in frequency is not directly dependent on the applied voltage. However, the QCM's performance can be affected by voltage if it's part of a system designed for electromechanical resonance, but this is generally outside

136

the scope of the Sauerbrey equation. As shown in the Eq.1, there is a proportional relationship between Δm and Δf, indicating that as the mass on the quartz surface increases or decreases, the resonance frequency shifts accordingly. This relationship is fundamental for many piezoelectric sensing applications, as the frequency shift provides a sensitive and accurate method to quantify mass changes at the surface. For instance, Favrat et al. developed a QCM sensor for real-time measurement of fatty acid removal in a cleaning mechanism, which involved an aqueous solution containing anionic and non-ionic detergents [14]. The real-time measurement was performed by observing the frequency change in the quartz crystal during the cleaning process. In another study, Susilo et al. (2019) used spray coating to deposit reduced graphene oxide on the QCM surface to develop a piezoelectric biosensor [15]. Mass deposition on the QCM surface results in a decline in its resonant frequency. The crystal's thickness affects both the resonant frequency and the mass sensitivity, as a thinner crystal typically has a higher resonant frequency and greater sensitivity to mass changes.
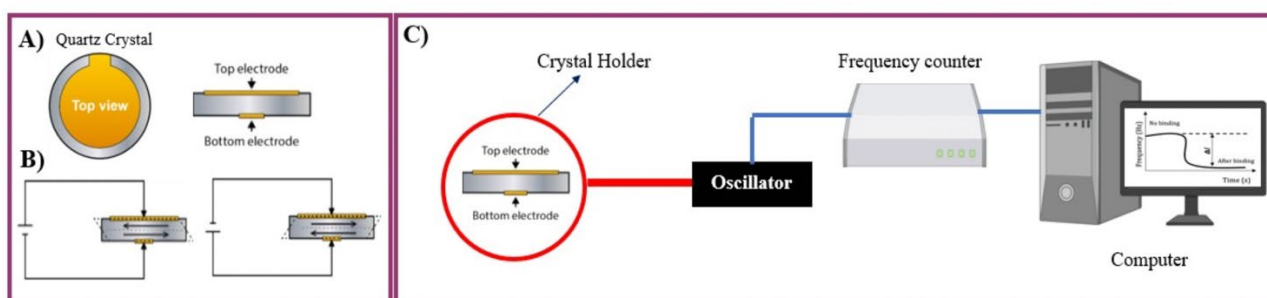

Figure 1. Schematic illustration of a QCM setup.

On the other hand, QCM is not functional by itself for humidity detection, and an additional sensing layer is necessary. Li et al. (2021) demonstrated that an uncoated QCM has a minimal response to humidity, whereas a coated QCM exhibited a high response to relative humidity [16]. Kosuru et al. (2016) investigated PVP and metal-organic framework coatings on the QCM surface for humidity sensing. They tested the sensitivity of uncoated QCM sensors alongside these coated sensors and found that uncoated QCM showed the lowest sensitivity [17].

The selection of materials and development methods for the sensing layer is of great importance [18], as the sensing layer also determines the characteristics of the QCM sensor. The sensing material is coated on the electrode of the QCM (as shown in Figure 1); note that the uncoated quartz is shown in Figure 1, as it represents the unmodified QCM setup. Therefore, in addition to the chemical structure and physical properties of the sensing layer, the mass and viscoelastic properties of the material used for the sensing layer also influence the QCM sensor response [19]. To ensure the humidity sensitivity of the QCM, the electrode surface is covered with various water-adsorbing materials, including polymers [20], ceramics [21], different chemical incorporations [11], nanostructures [22], and composites [23, 24]. For instance, molecularly imprinted polymers (MIPs) can offer good selectivity and sensitivity as a coating material on QCM sensors, but they are not suitable for relative humidity levels around 50%, and their structural and morphological instability is another issue that needs to be addressed [25]. On the other hand, ZnO, as an example of metal oxides, has the advantage of morphology-dependent sensing and has garnered significant attention for this reason [26]. Due to their high surface area for interactions, 1-dimensional ZnO nanomaterials are among the most promising candidates for applications [27]. Unfortunately, these materials lack hydrophilicity, which is an important parameter for humidity sensing [28, 29, 30].

For most humidity sensing applications, fast response/recovery times are essential to ensure real-time measurement. The key parameters affecting QCM (Quartz Crystal Microbalance) measurements include several factors related to both the crystal itself and the experimental conditions. The QCM crystal plays a fundamental role in the sensor's performance, as its properties directly influence the frequency response. The electrode surface also impacts the measurement by determining

the interaction between the crystal and the adsorbed material. The sensing material deposited on the electrode surface is another critical factor, as its physical and chemical properties influence the mass changes detected by the QCM. In addition, the thickness of the sensing material is important, as it determines the magnitude of the frequency shift for a given mass change. The electrode area also affects the sensitivity of the QCM, with larger areas generally providing higher sensitivity. Environmental factors, such as temperature and humidity, can further influence QCM measurements by affecting both the crystal's behavior and the properties of the sensing material. Together, these factors must be carefully controlled to ensure accurate and reliable QCM measurements. In such cases, surface properties play a crucial role [31]. For example, Qi et al. (2018) synthesized acidized multiwalled carbon nanotubes as a sensing layer on QCM surfaces and achieved relatively fast response and recovery times (49s / 6s) [32], while Gao et al. (2019) achieved even better results in terms of response and recovery times (10s / 3s) by fabricating colloidal tin oxide nanowires [33]. Furthermore, Horzum et al. (2011) demonstrated that the use of ZnO-based fibers can provide very fast response (0.5 s) and recovery (1.5 s) times when produced via electrospinning [34]. On the other hand, hydrophilic organic polymers are unable to meet these criteria, as recovery times after adsorption typically range from 25 to 75 s [35]. Dai et al. (2017) studied the humidity sensing properties of organic hybrid polymers and observed a 40 s recovery time [36]. These types of materials are not effective enough for enhanced humidity sensing in critical applications. Moreover, it has been shown that nanostructured materials offer better properties than their bulk counterparts for QCM sensors [37], as they have a larger surface area to volume ratio, higher mechanical modulus, and better chemical stability [38].

To achieve specific improvements, such as enhanced sensitivity for QCM humidity sensors, hybrid composite materials can be used, which combine two or more different materials. Essentially, two approaches can be applied: (1) using an additional nanostructured/porous material to enhance the specific surface area and increase interactions with water molecules and the surface, or (2) using another humidity-sensitive material to improve overall humidity sensitivity [11]. Composite materials for humidity sensors exhibit low hysteresis, excellent sensitivity, fast response/recovery times, enhanced selectivity, stability, and linearity [39]. Nanostructured innovative composites, also known as nanocomposites, with large surface areas and oxygen-rich functional groups, ensure excellent humidity sensing performance [40, 41].

Superior physicochemical features that make them commonly used materials in sensing, energy and biomedicine applications in addition to other utilizations. Carbon nanomaterials are taking attention because of their low weight, and high strength and conductivity [39]. The significant attention on carbon nanomaterials because of their chemical, mechanical, optical, electrical and thermal properties has provided enhancement in fundamental and applied science.

2. Graphene and Graphene Oxide (GO) nanomaterials

Graphene is one of the 2D structures of carbon that has various derivatives containing graphene oxide (GO) and reduced graphene oxide (rGO). Due to its superior properties such as mechanical strength, flexibility, high surface to volume ratio, good conductivity, different electrical and optical properties, simply modifiable, and thermal stability, graphene-based nanomaterials are the most popular nanomaterials for a while [42, 43, 44].

Graphene was discovered in 2004, but its history is not that new, as it represents a two-dimensional structure derived from the three-dimensional material graphite [45]. The most outstanding feature of graphene is that it is the thinnest and strongest material which is composed of 2D sheets less than 10 nm in thickness [45]. Even though graphene and its derivatives have basically the same 2D structure, there are slight differences which give various physicochemical properties to every one of them.

Graphene Oxide (GO), one of the main derivatives of graphene, can be obtained as result of chemical exfoliation and oxidizing of graphite powder and has hydrophilic functional groups on its carbon plane surface [46]. As it can be seen in Figure 2, GO is the oxidized state of graphene.
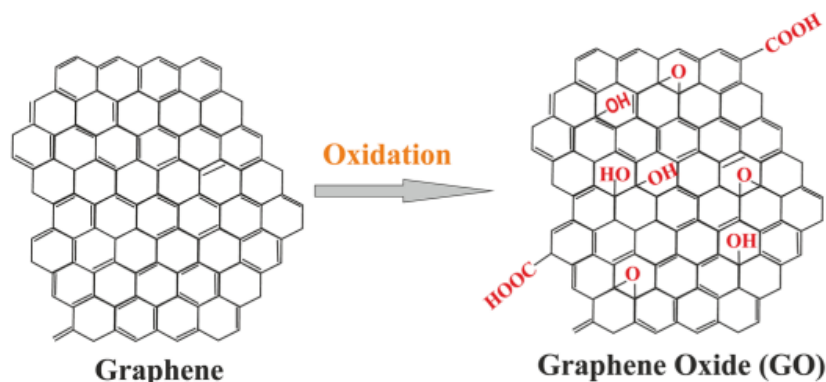

Figure 2. Conversion of graphene into GO [33].

GO has a cost effective and large-scale production, also the processing of GO is easier compared to graphene. Both graphene and GO demonstrate good mechanical, thermal and electrical properties thanks to their morphology. On the other hand, the most important difference between graphene and GO is their structure. While graphene is in a crystalline form, GO has both crystalline and amorphous regions. GO has oxygen-containing groups such as epoxy, hydroxyl, carboxylic and carbonyl which make GO hydrophilic and give an opportunity to use it in many fields from drug delivery to healthcare, solar cells to energy storage, etc [47]. In addition to mechanical, electrical and optical properties that GO has thanks to its oxygen-containing functional groups on the surface, it also gives the opportunity to be used in biotechnology by providing a large surface area and biocompatibility [48]. Therefore, GO is one of the most interesting carbon-based materials for biotechnological and nanotechnological applications.

3. Borophene Structures

Borophene is a newly developed material, designed as an alternative to graphene, which is one of the most extensively studied carbon-based 2D materials in recent years [49]. Borophene emerged initially through theoretical calculations and simulations, making it the first material to be conceptually predicted and later successfully synthesized. The first experimental synthesis of borophene was achieved in 2019, marking a significant breakthrough in materials science [50]. Since its synthesis, borophene has attracted widespread attention due to its exceptional chemical, electronic, mechanical, and thermal properties, which surpass those of graphene in several aspects. These remarkable properties suggest a vast potential for borophene in various advanced applications such as supercapacitors, batteries, hydrogen storage, and biomedical technologies [51].

Figure 3a shows the borophene structure which is obtained by extracting a slice from the bulk boron crystal. This slice forms a single-layer, two-dimensional sheet of boron, with different configurations that can be tailored depending on the specific synthesis conditions. Historically, the development of borophene has followed a theoretical path, starting with early predictions about its possible structures and properties. The theoretical models and their evolution are illustrated in Figure 3b, showing how the material was initially proposed and later refined through various simulations and experimental advancements [52].
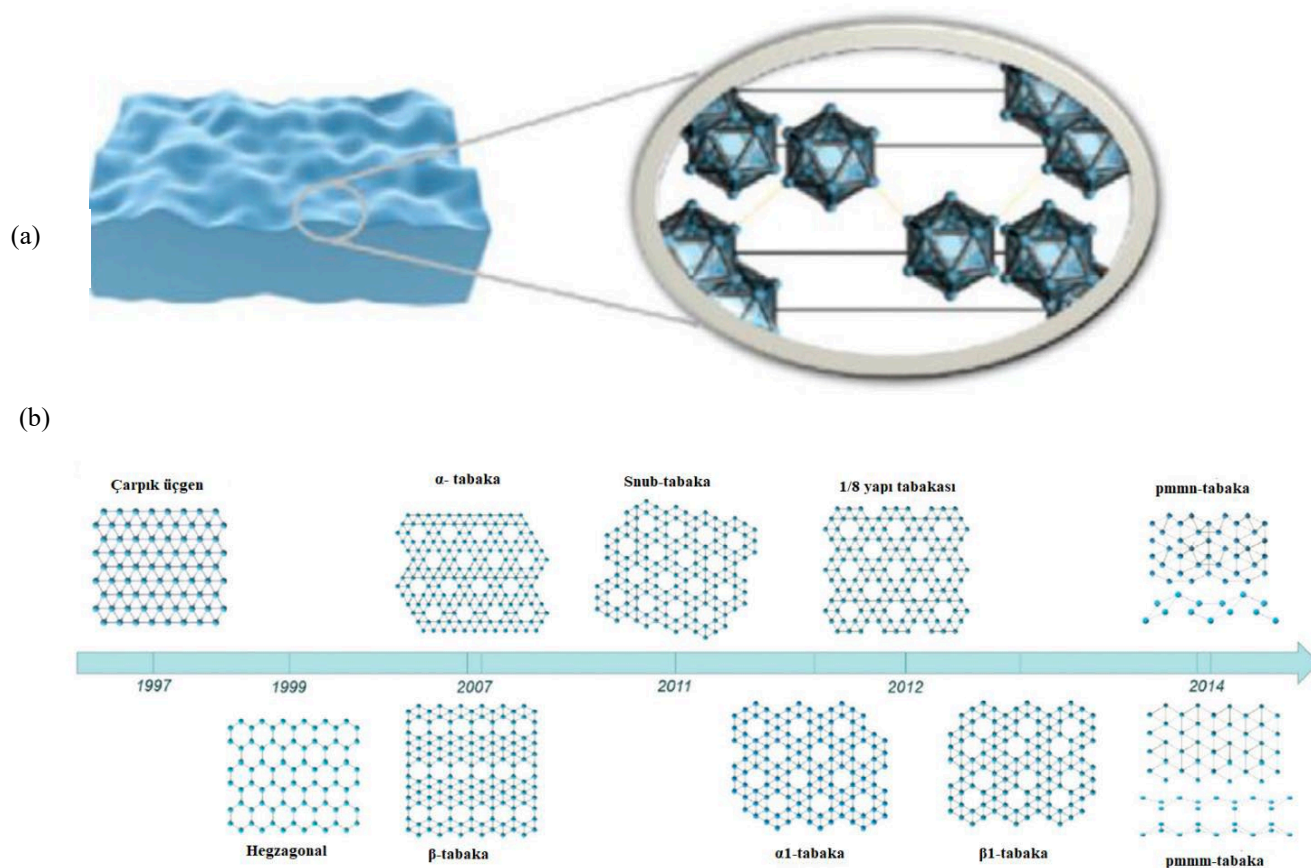
Open Journal of Nano
ISSN: 2147-0081
(2024) 9–2
Review Article

OPEN JOURNAL OF
NANO

Figure 3. Boron structure (a) and Developments of Borophene in history (b).

4. QCM humidity sensing applications

Three key factors that significantly influence the sensitivity and stability of QCM humidity sensors have been identified: flexibility, surface-to-volume ratio, and hydrophilicity [38]. To enhance these properties, researchers have been focusing on the development of novel materials and the combination of existing materials to create composites with improved performance characteristics [53]. Composites, which are materials made by combining two or more substances to achieve enhanced properties, have become a popular approach in the field.

For instance, Chen et al. (2020) introduced a composite-based QCM humidity sensor incorporating MOF-SnO$_2$/Chitosan, which demonstrated significant improvements in sensitivity, selectivity, response/recovery times, and stability [54]. Metal-organic frameworks (MOFs) are a class of novel functional materials with a porous structure and a high specific surface area, making them ideal for creating templates that facilitate the preparation of metal oxides like SnO$_2$. Chitosan, a biopolymer, also plays a crucial role in improving the sensor's performance due to its film-forming ability and hydrophilic nature, which are attributed to the presence of NH$_3^+$ and OH$^-$ groups in its structure.

SnO$_2$ is recognized for its excellent humidity sensing capabilities, its high stability, and its ease of fabrication, making it a favorable choice for the core component of the humidity sensor. When SnO$_2$ is combined with chitosan, the composite benefits from enhanced hydrophilicity, which aids in the adsorption of water molecules, ultimately improving humidity sensitivity. As a result, the QCM sensor coated with the MOF-SnO$_2$/Chitosan composite exhibits superior humidity sensing performance when compared to sensors based on MOF-SnO$_2$ or chitosan alone, as confirmed by various characterization methods [54].

140

Materials and surface coatings used to enhance the performance of sensors play a critical role. In recent years, two-dimensional materials such as graphene oxide (GO) and borophene have been increasingly favored for improving the humidity sensing capabilities of QCM sensors. In the following sections, we will explore the potential applications of these materials in QCM-based humidity sensing and discuss the advantages they offer in detail.

4.1. Graphene and Graphene Oxide in QCM humidity sensing applications

Similar to the examples mentioned above, various composite materials are being developed to functionalize the QCM by coating them on its electrode surface. Among these, graphene and its derivatives stand out due to their exceptional properties. Graphene is an extremely thin (about 34 nm) two-dimensional material that exhibits excellent physical properties such as high flexibility, intrinsic mobility, thermal and electrical conductivity, and high transmittance. In addition, graphene derivatives also possess unique mechanical, chemical, and electrical properties, making them highly attractive for use in composites for sensing applications. For example, graphene oxide (GO), a major derivative of graphene, is an excellent candidate for humidity sensing applications. On the other hand, reduced graphene oxide (rGO), a derivative and oxidized form of graphene, exhibits numerous chemical defects and good conductivity, but lacks significant water adsorption activity [55]. Humidity sensors developed using GO have enhanced sensitivity, short response/recovery times, and are suitable for flexible electronics, as GO possesses hydrophilic functional groups such as carboxyl, hydroxyl, epoxy, etc., on its surface [56, 57]. Table 1 shows the typical GO-based composite materials used in QCM sensing layer preparation method, and sensing properties with response time and humidity range. On the other hand, a typical humidity sensing application involves detecting the humidity in breath. The schematic illustration (Figure 4) for an ultrafast QCM humidity sensor demonstrates the goal of sensing humidity from exhaled breath [58].
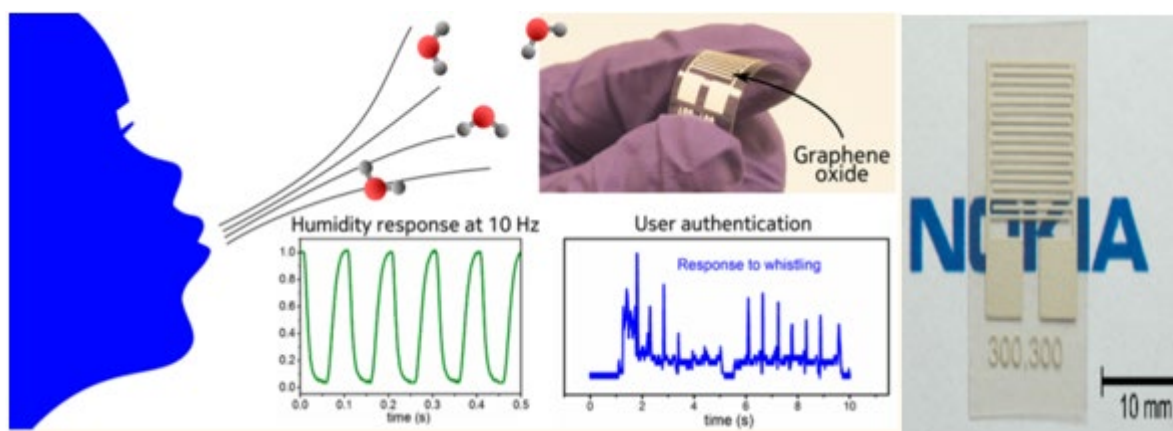

Figure 4. Schematic illustration for ultrafast QCM humidity sensor goal of sensing the humidity by breath, GO flexibility and graphical abstract of response time (left) and a photograph of GO sensing element (right) [58].

Table 1. GO-based composite materials for QCM humidity sensing applications.

Sensing layer	Method	Response Recovery time (s)	Humidity Range (%)	References
GO/ZnO composite thin film	Spray coating	9 s / 5 s	11.3%-97.3%	[59]
PANI/GO	Layer by layer self-assembly	8 s / 5 s	11%-97%	[57]
GO/SnO$_2$/PANI film	In-situ oxidative polymerization	7s / 2 s	0%-97%	[57]
GO/Cu(OH)$_2$ nanowires film	Drop-casting	1.9 s / 7.6 s	0%-80%	[60]
MoS$_2$/Graphene Oxide/C$_{60}$-OH	Drop-coating	1.3 s / 1.2 s	2%-97%	[61]

141

Open Journal of Nano
ISSN: 2147-0081
(2024) 9–2
Review Article

OPEN JOURNAL OF
NANO

GO/PEI	Spray coating	53 s / 18 s	11.3%-97.3%	[62]
GO/Nafion nanocomposite film	Spin coating	23 s / 5 s	11.3%-84.3%	[63]
C_{60}/GO	Drop-casting	4 s / 5 s	11%-97%	[64]

The figure includes a graphical abstract showing the sensor's response time on the left, highlighting its quick detection capabilities, and a photograph of the GO (Graphene Oxide) sensing element on the right, which is used to measure humidity levels. The GO material's flexibility contributes to the sensor's sensitivity and performance in detecting variations in humidity [58]. Borini et al. (2013) utilized the super-permeability property of GO to develop a fast humidity sensor [58]. They experimented with different thicknesses and preparation methods for the GO coating to achieve faster response/recovery times. Although they were able to obtain an ultrafast response/recovery time, a hysteresis effect occurred, and sensitivity was affected under certain conditions [58]. In another study, Yao et al. (2014) attempted to leverage the mechanical properties of GO, such as its high flexibility, to enhance the QCM sensor's performance at high relative humidity values [65]. They compared a GO-coated QCM humidity sensor with a PEG-coated one and demonstrated that the GO-based QCM humidity sensor outperformed the PEG-based one. However, they also found that the GO-based sensor exhibited poor selectivity at lower relative humidity values due to cross-sensitivity with the presence of certain gases. The humidity-sensing property of GO may decrease as a result of physical interactions between GO carboxyl groups and water molecules [65]. These drawbacks can be addressed by incorporating other materials, turning the GO coating into a GO-based composite for QCM humidity sensing applications.

As mentioned earlier, graphene oxide is a two-dimensional material with a large surface area and hydrophilicity due to its structural defects. This strong adsorption capacity of GO can lead to cross-sensitivity, but the incorporation of different polymers, such as polyaniline (PANI), can address this issue by improving the sensitivity of the QCM humidity sensor. Zhang et al. (2018) investigated a GO/SnO_2/PANI nanocomposite for coating the QCM surface to enhance humidity sensing. In their study, SnO_2 was in nanoparticle form, while PANI was in nanofiber form. PANI surrounded both GO and SnO_2, bringing them all into contact to form a nanocomposite film [57]. The materials in the nanocomposite provided different properties to the structure. For example, PANI ensured stability and ease of fabrication for repeatability, while SnO_2 contributed hydrophilicity for sensitive and rapid response/recovery times, and GO provided functional groups that enhance water adsorption onto the surface [66, 67].

In another study, Fang et al. (2020) used $Cu(OH)_2$ nanowires in combination with GO to create a composite film for real-time respiration monitoring by sensing humidity. The study showed fast response/recovery times, high sensitivity, and high linearity, with potential applications being investigated by measuring various breathing patterns such as normal breathing, speaking, etc. $Cu(OH)_2$ nanowires, with their large surface area-to-volume ratio and hydrogen groups, enhanced interactions between water molecules and the coating material. The addition of $Cu(OH)_2$ nanowires to the GO composite also helped overcome the limitations of GO, such as agglomeration and swelling. This is significant, as homogenization of composites remains an unresolved issue and is a major challenge in nanofiller-added hybrid composite structures. Fang et al. (2020) studied the change in sensing performance for GO-coated, $Cu(OH)_2$-coated, and $Cu(OH)_2$/GO composite-coated QCM layers, with the best results coming from the $Cu(OH)_2$/GO composite-coated QCM [60]. The findings from this study are promising for future medical monitoring applications of QCM humidity sensors.

Carboxyl graphene (G-COOH) specifically chosen for its high surface area and porosity added polystrene electrospun nanofibers directly deposited onto the QCM [68, 69]. In recent years, Hydroxylated graphene quantum dots (OH-GQDs), a novel class of nanomaterials, have emerged as an effective solution for increasing the number of active sites on the GO surface. This approach offers

a promising way to further enhance sensor sensitivity. Ding et al. (2024) was introducing OH-GQDs could provide additional active sites, potentially offering a more significant improvement in sensor performance [70]. Clay/GO/chitosan multilayer nanocoatings at high humidity suggested as high gas barrier to enhance the barrier properties of bio-based polymers for food packaging applications [71]. Two types of anionic nanoplatelets, graphene oxide (GO) and montmorillonite (MMT), with large aspect ratios (300–1000 and 200–1000, respectively), were compared for bilayered systems. The 23 nm thick CH/MMT/CH/GO hybrid coating also demonstrates good nanoplatelet exfoliation. While different mechanical properties were observed, the stiffer MMT exhibited distinct characteristics, whereas GO, due to its flexibility, resulted in the formation of wrinkles. The higher content of highly oriented and tightly packed nanoplatelets in the multilayer assembly contributed to this effect, as well as to enhanced transparency, low oxygen permeability, and minimal variation in oxygen permeability with increasing humidity [72].

4.2. Borophene in QCM humidity sensing applications

Borophene is another two-dimensional material consisting of a single layer of boron atoms. Similar to graphene, borophene possesses unique chemical and physical properties [73]. Although its features make borophene a remarkable candidate for sensor applications, the instability arising from its reactivity results in several drawbacks in real-world applications [74]. Therefore, borophene has been investigated in various heterostructure forms in the literature. However, as a new two-dimensional material, borophene cannot be easily fabricated into heterostructures using simple methods.

In recent years, researchers have achieved remarkable results in terms of response/recovery time, sensitivity, detection range, and limit of detection for gas sensing applications using borophene-based sensors [75, 76]. Typically, different hybrid composite materials like SnO_2 have been used to obtain stable heterostructures. Shen et al. (2020) indicated that borophene's sensitivity to CO_2 is weak when compared with other gases, such as NO, NH_3, or CO [75]. This is of great importance for carbon monoxide detection and CO detectors.

Hou et al. (2021) produced a borophene-graphene heterostructure in a hydrogen-rich environment for sensitive and fast humidity sensing by growing borophene on graphene surfaces [76]. They emphasized that the sensitivity of the sensor, which is 4,200%, is the highest among 2D material-based chemiresistive sensors, with a relatively short response (10.5 s) / recovery time (8.3 s). To prevent instability, the sensor was fabricated using the drop-coating method, and it remained stable over a wide RH range, from 0% to 85%. In another study, Hou et al. (2021) fabricated a special innovative borophene heterostructure that contains both borophene and MoS_2 [77]. This sensor showed even more enhanced sensitivity, reaching 15,500% at 97% RH. This study once again highlights that borophene-based sensors are promising candidates for future human health care and wearable electronic sensing devices.

5. Conclusion and Future Perspectives

Quartz Crystal Microbalance (QCM) sensors have emerged as a powerful tool for humidity sensing, offering high sensitivity, fast response times, and real-time monitoring capabilities. The integration of nanomaterials such as graphene, graphene oxide (GO), and borophene has significantly enhanced the performance of QCM humidity sensors. Graphene's exceptional surface area, flexibility, and electrical conductivity make it an ideal candidate for improving sensor sensitivity, while GO's tunable surface chemistry offers additional advantages in terms of functionality. However, challenges such as GO agglomeration and cross-sensitivity still need to be addressed, and these can be mitigated by incorporating complementary materials that provide greater mechanical stability and hydrophilicity.

Borophene, with its promising electrical and mechanical properties, represents an exciting frontier for humidity sensing. Nevertheless, its instability and limited application in real-world conditions present significant challenges. Exploring borophene-based composites, particularly with stabilizing agents like MoS_2 or other nanomaterials, could lead to breakthroughs in overcoming these limitations and creating highly efficient humidity sensors.

Despite the advances made in QCM-based humidity sensors, several critical areas require further research and development. One of the main challenges remains improving the long-term stability and resistance to environmental factors such as temperature variations, pH changes, and exposure to chemicals. Additionally, understanding the exact sensing mechanisms at the molecular level will be crucial for optimizing the materials used in QCM sensors, thereby enhancing their performance and accuracy.

Several promising directions for future research can be identified. First, further optimization of the nanocomposites used in QCM sensors is necessary, particularly by combining GO with other materials that enhance its mechanical stiffness and hydrophilicity. The design of hybrid nanomaterials could address current issues like swelling, agglomeration, and cross-sensitivity, resulting in more stable and reliable sensors. Additionally, stabilizing borophene through composite materials is an exciting avenue, with potential applications in humidity sensors that require higher performance and durability.

Another promising approach is the development of layer-by-layer self-assembled conductive polymeric films, which could offer enhanced tunability, flexibility, and sensor functionality. These films would allow for precise control over the properties of QCM sensors, potentially enabling multifunctional devices capable of detecting a range of environmental factors beyond humidity. Furthermore, the integration of QCM humidity sensors into wearable and portable electronics offers significant potential for real-time monitoring in fields such as healthcare, industrial safety, and environmental monitoring.

To fully realize the potential of QCM-based humidity sensors, it is also essential to address challenges related to large-scale fabrication and cost-effective production. Refining manufacturing techniques such as electrospinning and wet-spinning will be crucial to ensuring the consistent, high-quality production of QCM sensors. Additionally, sustainability efforts in material production, particularly for graphene and other nanomaterials, will play a key role in making these sensors more environmentally friendly and cost-efficient.

In conclusion, the development of advanced QCM humidity sensors is at the forefront of sensing technology, with promising advances in nanocomposites and sensor design. However, overcoming challenges such as material stability, scalability, and long-term reliability will require continued research and innovation. As the demand for real-time, highly sensitive, and durable humidity sensors grows across various industries, the collaboration between materials science, sensor engineering, and manufacturing techniques will be essential to drive the next generation of QCM-based humidity sensing technologies.

References

[1] Yao, Y., Huang, X., Chen, Q., Zhang, Z., & Ling, W. (2020). High sensitivity and high stability QCM humidity sensors based on polydopamine coated cellulose nanocrystals/graphene oxide nanocomposite. Nanomaterials, 10(11), 2210.

[2] Chen, W., Chen, B., Lv, R., Wu, M., Zhou, J., Lu, B., ... & Tang, L. (2021). Fabrication of quartz crystal microbalance humidity sensors based on super-hydrophilic cellulose nanocrystals. Cellulose, 28(6), 3409-3421.

[3] Buxton, P. A., & Mellanby, K. (1934). The measurement and control of humidity. Bulletin of Entomological Research, 25(2), 171-175.

[4] Singh, N., Chaturvedi, S., & Akhter, S. (2019, March). Weather forecasting using machine learning algorithm. In 2019 International Conference on Signal Processing and Communication (ICSC) (pp. 171-174). IEEE.

[5] Yousefi, H., Su, H. M., Imani, S. M., Alkhaldi, K., M. Filipe, C. D., & Didar, T. F. (2019). Intelligent food packaging: A review of smart sensing technologies for monitoring food quality. ACS sensors, 4(4), 808-821.

[6] Ayala-Zavala, J. F., Del-Toro-Sánchez, L., Alvarez-Parrilla, E., & González-Aguilar, G. A. (2008). High relative humidity in-package of fresh-cut fruits and vegetables: advantage or disadvantage considering microbiological problems and antimicrobial delivering systems?. Journal of Food Science, 73(4), R41-R47.

[7] Wang, X., Xu, W., Tavakkoli, H., & Lee, Y. K. (2020, September). Low-Cost parylene based micro humidity sensor for integrated human thermal comfort sensing. In 2020 IEEE 15th International Conference on Nano/Micro Engineered and Molecular System (NEMS) (pp. 134-138). IEEE.

[8] Duan, Z., Jiang, Y., & Tai, H. (2021). Recent advances in humidity sensor for human body related humidity detections. Journal of Materials Chemistry C.

[9] Lakhiar, I. A., Jianmin, G., Syed, T. N., Chandio, F. A., Buttar, N. A., & Qureshi, W. A. (2018). Monitoring and control systems in agriculture using intelligent sensor techniques: A review of the aeroponic system. Journal of Sensors, 2018.

[10] Zrelli, A., & Ezzedine, T. (2018). Design of optical and wireless sensors for underground mining monitoring system. optik, 170, 376-383. Chappanda et al., 2018

[11] Chappanda, K. N., Shekhah, O., Yassine, O., Patole, S. P., Eddaoudi, M., & Salama, K. N. (2018). The quest for highly sensitive QCM humidity sensors: The coating of CNT/MOF composite sensing films as case study. Sensors and Actuators B: Chemical, 257, 609-619.

[12] Torad, N. L., Zhang, S., Amer, W. A., Ayad, M. M., Kim, M., Kim, J., ... & Yamauchi, Y. (2019). Advanced nanoporous material–based QCM devices: A new horizon of interfacial mass sensing technology. Advanced Materials Interfaces, 6(20), 1900849.

[13] Sauerbrey, G. J. Z. P. (1959). The use of quartz oscillators for weighing thin layers and for microweighing. Z. Phys., 155, 206-222.

[14] Favrat, O., Gavoille, J., Aleya, L., & Monteil, G. (2013). Real time study of detergent concentration influence on solid fatty acid film removal processes. Journal of Surfactants and Detergents, 16(2), 213-219.

[15] Susilo, D., & Mujiono, T. (2019, August). QCM Coating With rGO Material as a Platform Developing Piezoelectric Biosensor. In 2019 International Seminar on Intelligent Technology and Its Applications (ISITIA) (pp. 52-55). IEEE.

[16] Li, R., Fan, Y., Ma, Z., Zhang, D., Liu, Y., & Xu, J. (2021). Controllable preparation of ultrathin MXene nanosheets and their excellent QCM humidity sensing properties enhanced by fluoride doping. Microchimica Acta, 188(3), 1-11.

[17] Kosuru, L., Bouchaala, A., Jaber, N., & Younis, M. I. (2016). Humidity detection using metal organic framework coated on QCM. Journal of Sensors, 2016.

[18] Wang, L., Gao, J., & Xu, J. (2019). QCM formaldehyde sensing materials: Design and sensing

145

mechanism. Sensors and Actuators B: Chemical, 293, 71-82.

[19] Fauzi, F., Rianjanu, A., Santoso, I., & Triyana, K. (2021). Gas and humidity sensing with quartz crystal microbalance (QCM) coated with graphene-based materials–A mini review. Sensors and Actuators A: Physical, 112837.

[20] Jaruwongrungsee, K., Tuantranont, A., Wanna, Y., Wisitsoraat, A., & Lomas, T. (2007, August). Quartz crystal microbalance humidity sensor using electrospun PANI micro/nano dots. In 2007 7th IEEE Conference on Nanotechnology (IEEE NANO) (pp. 316-319). IEEE.

[21] Yakuphanoglu, F. (2012). Semiconducting and quartz microbalance (QCM) humidity sensor properties of TiO2 by sol gel calcination method. Solid state sciences, 14(6), 673-676.

[22] Zhang, D., Song, X., Wang, Z., & Chen, H. (2021). Ultra-highly sensitive humidity sensing by polydopamine/graphene oxide nanostructure on quartz crystal microbalance. Applied Surface Science, 538, 147816.

[23] Tai, H., Zhen, Y., Liu, C., Ye, Z., Xie, G., Du, X., & Jiang, Y. (2016). Facile development of high performance QCM humidity sensor based on protonated polyethylenimine-graphene oxide nanocomposite thin film. Sensors and Actuators B: Chemical, 230, 501-509.

[24] Qi, P., Zhang, T., Shao, J., Yang, B., Fei, T., & Wang, R. (2019). A QCM humidity sensor constructed by graphene quantum dots and chitosan composites. Sensors and Actuators A: Physical, 287, 93-101.

[25] Hussain, M., Kotova, K., & Lieberzeit, P. A. (2016). Molecularly imprinted polymer nanoparticles for formaldehyde sensing with QCM. Sensors, 16(7), 1011.

[26] Shukla, S. K., Kushwaha, C. S., Shukla, A., & Dubey, G. C. (2018). Integrated approach for efficient humidity sensing over zinc oxide and polypyrole composite. Materials Science and Engineering: C, 90, 325-332.

[27] Wang, X., Xie, S., Liu, J., Kucheyev, S. O., & Wang, Y. M. (2013). Focused-ion-beam assisted growth, patterning, and narrowing the size distributions of ZnO nanowires for variable optical properties and enhanced nonmechanical energy conversion. Chemistry of Materials, 25(14), 2819-2827.

[28] Cha, X., Yu, F., Fan, Y., Chen, J., Wang, L., Xiang, Q., ... & Xu, J. (2018). Superhydrophilic ZnO nanoneedle array: Controllable in situ growth on QCM transducer and enhanced humidity sensing properties and mechanism. Sensors and Actuators B: Chemical, 263, 436-444.

[29] Ren, X., Zhang, D., Wang, D., Li, Z., & Liu, S. (2018). Quartz crystal microbalance sensor for humidity sensing based on layer-by-layer self-assembled PDDAC/graphene oxide film. IEEE Sensors Journal, 18(23), 9471-9476.

[30] Zhao, Q., Yuan, Z., Duan, Z., Jiang, Y., Li, X., Li, Z., & Tai, H. (2019). An ingenious strategy for improving humidity sensing properties of multi-walled carbon nanotubes via poly-L-lysine modification. Sensors and Actuators B: Chemical, 289, 182-185.

[31] Yao, Y., Zhang, H., Sun, J., Ma, W., Li, L., Li, W., & Du, J. (2017). Novel QCM humidity sensors using stacked black phosphorus nanosheets as sensing film. Sensors and Actuators B: Chemical, 244, 259-264.

[32] Qi, P., Zhao, C., Wang, R., Fei, T., & Zhang, T. (2018). High-performance QCM humidity sensors using acidized-multiwalled carbon nanotubes as sensing film. IEEE Sensors Journal, 18(13), 5278-5283.

[33] Gao, N., Li, H. Y., Zhang, W., Zhang, Y., Zeng, Y., Zhixiang, H., ... & Liu, H. (2019). QCM-based humidity sensor and sensing properties employing colloidal SnO2 nanowires. Sensors and Actuators B: Chemical, 293, 129-135.

[34] Horzum, N., Taşçıoglu, D., Okur, S., & Demir, M. M. (2011). Humidity sensing properties of ZnO-based fibers by electrospinning. Talanta, 85(2), 1105-1111.

[35] Dai, J., Zhao, H., Lin, X., Liu, S., Fei, T., & Zhang, T. (2020). Design strategy for ultrafast-response humidity sensors based on gel polymer electrolytes and application for detecting respiration. Sensors and Actuators B: Chemical, 304, 127270.

Open Journal of Nano
ISSN: 2147-0081
(2024) 9–2
Review Article

OPEN JOURNAL OF
NANO

[36] Dai, J., Zhang, T., Zhao, H., & Fei, T. (2017). Preparation of organic-inorganic hybrid polymers and their humidity sensing properties. Sensors and Actuators B: Chemical, 242, 1108-1114.

[37] Yao, Y., & Xue, Y. (2015). Impedance analysis of quartz crystal microbalance humidity sensors based on nanodiamond/graphene oxide nanocomposite film. Sensors and Actuators B: Chemical, 211, 52-58.

[38] Yao, Y., Huang, X. H., Zhang, B. Y., Zhang, Z., Hou, D., & Zhou, Z. K. (2020). Facile fabrication of high sensitivity cellulose nanocrystals based QCM humidity sensors with asymmetric electrode structure. Sensors and Actuators B: Chemical, 302, 127192.

[39] Velumani, M., Meher, S. R., & Alex, Z. C. (2019). Composite metal oxide thin film based impedometric humidity sensors. Sensors and actuators B: Chemical, 301, 127084.

[40] Na Songkhla, S., & Nakamoto, T. (2021). Overview of quartz crystal microbalance behavior analysis and measurement. Chemosensors, 9(12), 350.

[41] Qian, J., Tan, R., Feng, M., Shen, W., Lv, D., & Song, W. (2024). Humidity Sensing Using Polymers: A Critical Review of Current Technologies and Emerging Trends. Chemosensors, 12(11), 230.

[42] Han, W., Wu, Z., Li, Y., & Wang, Y. (2019). Graphene family nanomaterials (GFNs)—promising materials for antimicrobial coating and film: A review. Chemical Engineering Journal, 358, 1022-1037.

[43] Seifi, T., & Kamali, A. R. (2021). Anti-pathogenic activity of graphene nanomaterials: A review. Colloids and Surfaces B: Biointerfaces, 199, 111509.

[44] Mehmood, A., Mubarak, N. M., Khalid, M., Walvekar, R., Abdullah, E. C., Siddiqui, M. T. H., ... & Mazari, S. (2020). Graphene based nanomaterials for strain sensor application—a review. Journal of Environmental Chemical Engineering, 8(3), 103743.

[45] Tahriri, M., Del Monico, M., Moghanian, A., Yaraki, M. T., Torres, R., Yadegari, A., & Tayebi, L. (2019). Graphene and its derivatives: Opportunities and challenges in dentistry. Materials Science and Engineering: C, 102, 171-185.

[46] Dideikin, A. T., & Vul', A. Y. (2019). Graphene oxide and derivatives: the place in graphene family. Frontiers in Physics, 6, 149.

[47] Yu, W., Sisi, L., Haiyan, Y., & Jie, L. (2020). Progress in the functional modification of graphene/graphene oxide: A review. RSC Advances, 10(26), 15328-15345.

[48] Singh, D. P., Herrera, C. E., Singh, B., Singh, S., Singh, R. K., & Kumar, R. (2018). Graphene oxide: An efficient material and recent approach for biotechnological and biomedical applications. Materials Science and Engineering: C, 86, 173-197.

[49] Kumar, P., Singh, G., Bahadur, R., Li, Z., Zhang, X., Sathish, C. I., ... & Vinu, A. (2024). The rise of borophene. Progress in Materials Science, 101331.

[50] Mao, T., Wang, S., Yong, Z., Wang, X., Wang, X., Chen, H., ... & Wang, Z. (2021). High-stable, outstanding heat resistance ionogel electrolyte and the poly (3, 4-ethylenedioxythiophene) electrodes with excellent long-term stability for all-solid-state supercapacitor. Chemical Engineering Journal, 417, 129269.

[51] Chaudhary, V., Sonu, S., Taha, B. A., Raizada, P., Rustagi, S., Chahal, S., ... & Nguyen, V. H. (2024). Borophene-based nanomaterials: Promising candidates for next-generation gas/vapor chemiresistors. Journal of Materials Science & Technology.

[52] Ou, M., Wang, X., Yu, L., Liu, C., Tao, W., Ji, X., & Mei, L. (2021). The emergence and evolution of borophene. Advanced Science, 8(12), 2001801.

[53] Gutiérrez, J., Robein, Y. N., Juan, J., Di Nezio, M. S., Pistonesi, C., González, E. A., ... & Pistonesi, M. F. (2024). A combined experimental and DFT study on the zero valent iron/reduced graphene oxide doped QCM sensor for determination of trace concentrations of As using a Flow-batch system. Sensors and Actuators B: Chemical, 404, 135233.

[54] Chen, H., Zhang, D., Pan, Q., & Song, X. (2020). Highly sensitive QCM humidity sensor

147

based on MOFs-derived SnO2/chitosan hybrid film. IEEE Sensors Journal, 21(4), 4385-4390.

[55]   Wang, S., Xie, G., Su, Y., Su, L., Zhang, Q., Du, H., ... & Jiang, Y. (2018). Reduced graphene oxide-polyethylene oxide composite films for humidity sensing via quartz crystal microbalance. Sensors and Actuators B: Chemical, 255, 2203-2210.

[56]   Lee, S. W., Choi, B. I., Kim, J. C., Woo, S. B., Kim, Y. G., Yoo, J., & Seo, Y. S. (2019). Reduction and compensation of humidity measurement errors at cold temperatures using dual QCM humidity sensors based on graphene oxides. Sensors and Actuators B: Chemical, 284, 386-394.

[57]   Zhang, D., Wang, D., Li, P., Zhou, X., Zong, X., & Dong, G. (2018). Facile fabrication of high-performance QCM humidity sensor based on layer-by-layer self-assembled polyaniline/graphene oxide nanocomposite film. Sensors and Actuators B: Chemical, 255, 1869-1877.

[58]   Borini, S., White, R., Wei, D., Astley, M., Haque, S., Spigone, E., ... & Ryhanen, T. (2013). Ultrafast graphene oxide humidity sensors. ACS nano, 7(12), 11166-11173.

[59]   Yuan, Z., Tai, H., Bao, X., Liu, C., Ye, Z., & Jiang, Y. (2016a). Enhanced humidity-sensing properties of novel graphene oxide/zinc oxide nanoparticles layered thin film QCM sensor. Materials Letters, 174, 28-31.

[60]   Fang, H., Lin, J., Hu, Z., Liu, H., Tang, Z., Shi, T., & Liao, G. (2020). Cu(OH)2 nanowires/graphene oxide composites based QCM humidity sensor with fast-response for real-time respiration monitoring. Sensors and Actuators B: Chemical, 304, 127313.

[61]   Tang, K., Chen, X., Ding, X., Yu, X., & Yu, X. (2021). MoS2/Graphene Oxide/C60-OH Nanostructures Deposited on a Quartz Crystal Microbalance Transducer for Humidity Sensing. ACS Applied Nano Materials, 4(10), 10810-10818.

[62]   Yuan, Z., Tai, H., Ye, Z., Liu, C., Xie, G., Du, X., & Jiang, Y. (2016). Novel highly sensitive QCM humidity sensor with low hysteresis based on graphene oxide (GO)/poly (ethyleneimine) layered film. Sensors and Actuators B: Chemical, 234, 145-154.

[63]   Chen, X., Chen, X., Li, N., Ding, X., & Zhao, X. (2016). A QCM humidity sensors based on GO/Nafion composite films with enhanced sensitivity. IEEE Sensors Journal, 16(24), 8874-8883.

[64]   Ding, X., Chen, X., Chen, X., Zhao, X., & Li, N. (2018). A QCM humidity sensor based on fullerene/graphene oxide nanocomposites with high quality factor. Sensors and Actuators B: Chemical, 266, 534-542.

[65]   Yao, Y., Chen, X., Li, X., Chen, X., & Li, N. (2014). Investigation of the stability of QCM humidity sensor using graphene oxide as sensing films. Sensors and Actuators B: Chemical, 191, 779-783.

[66]   Zhu, Y., Chen, J., Li, H., Zhu, Y., & Xu, J. (2014). Synthesis of mesoporous SnO2–SiO2 composites and their application as quartz crystal microbalance humidity sensor. Sensors and Actuators B: Chemical, 193, 320-325.

[67]   Kumar, R., & Yadav, B. C. (2016). Fabrication of polyaniline (PANI)—tungsten oxide (WO3) composite for humidity sensing application. Journal of Inorganic and Organometallic Polymers and Materials, 26(6), 1421-1427.

[68]   Jia, Y., Chen, L., Yu, H., Zhang, Y., & Dong, F. (2015). Graphene oxide/polystyrene composite nanofibers on quartz crystal microbalance electrode for the ammonia detection. RSC Advances, 5(51), 40620-40627.

[69]   Ionita, M., Crica, L. E., Vasile, E., Dinescu, S., Pandele, M. A., Costache, M., ... & Iovu, H. (2016). Effect of carboxylic acid functionalized graphene on physical-chemical and biological performances of polysulfone porous films. Polymer, 92, 1-12.

[70]   Ding, X., Li, J., Hu, W., Chen, X., & Xia, W. (2024). An ultra-sensitive QCM Humidity Sensor Based on GO/OH-GQDs. IEEE Sensors Journal.

[71]   Cabrini, A., Fisher, S. G., Iverson, E. T., Cerruti, P., De Nardo, L., Gentile, G., ... & Grunlan,

J. C. (2025). High gas barrier of clay/graphene oxide/chitosan multilayer nanocoatings at high humidity. Progress in Organic Coatings, 198, 108929.

[72]   Wang, L., Gao, J., & Xu, J. (2019). QCM formaldehyde sensing materials: Design and sensing mechanism. Sensors and Actuators B: Chemical, 293, 71-82.

[73]   Hou, C., Tai, G., Liu, Y., & Liu, X. (2022). Borophene gas sensor. Nano Research, 1-8.

[74]   Khan, M. I., Aziz, S. H., Majid, A., & Rizwan, M. (2021). Computational study of borophene/boron nitride (B/BN) interface as a promising gas sensor for industrial affiliated gasses. Physica E: Low-dimensional Systems and Nanostructures, 130, 114692.

[75]   Shen, J., Yang, Z., Wang, Y., Xu, L. C., Liu, R., & Liu, X. (2020). The gas sensing performance of borophene/MoS2 heterostructure. Applied Surface Science, 504, 144412.

[76]   Hou, C., Tai, G. A., Liu, B., Wu, Z., & Yin, Y. (2021). Borophene-graphene heterostructure: Preparation and ultrasensitive humidity sensing. Nano Research, 14(7), 2337-2344.

[77]   Hou, C., Tai, G., Liu, Y., Wu, Z., Wu, Z., & Liang, X. (2021). Ultrasensitive humidity sensing and the multifunctional applications of borophene–MoS 2 heterostructures. Journal of Materials Chemistry A, 9(22), 13100-13108.